Fall 2011

The Application of Melatonin and Platelet-Rich Plasma in the Development of a Bioactive Calcium Aluminate Bone Regenerative Scaffold

William Clafshenkel

THE APPLICATION OF MELATONIN AND PLATELET-RICH PLASMA IN THE DEVELOPMENT OF A BIOACTIVE CALCIUM ALUMINATE BONE REGENERATIVE SCAFFOLD

A Dissertation

Submitted to the Graduate School of Pharmaceutical Sciences

Duquesne University

In partial fulfillment of the requirements for

the degree of Doctor of Philosophy

By

William P. Clafshenkel

December 2011

THE APPLICATION OF MELATONIN AND PLATELET-RICH PLASMA IN THE DEVELOPMENT OF A BIOACTIVE CALCIUM ALUMINATE BONE REGENERATIVE SCAFFOLD

By

William P. Clafshenkel

Approved July 28, 2011

_____ Paula A. Witt-Enderby, Ph.D. Professor of Pharmacology-Toxicology Graduate School of Pharmaceutical Sciences Duquesne University Committee Chair	_____ Ellen S. Gawalt Associate Professor of Chemistry and Biochemistry Bayer School of Natural & Environmental Sciences Duquesne University
_____ David A. Johnson, Ph.D. Associate Professor of Pharmacology-Toxicology Graduate School of Pharmaceutical Sciences Duquesne University	_____ Jane E. Cavanaugh, Ph.D. Assistant Professor of Pharmacology Graduate School of Pharmaceutical Sciences Duquesne University
_____ James L. Rutkowski, Ph.D., D.M.D. Private Practice 35 South Second Avenue Clarion, PA	_____ James K. Drennen, III, Ph.D. Associate Dean, Research and Graduate Programs Graduate School of Pharmaceutical Sciences Duquesne University
_____ J. Douglas Bricker, Ph.D. Dean, Mylan School of Pharmacy and the Graduate School of Pharmaceutical Sciences Duquesne University	

ABSTRACT

THE APPLICATION OF MELATONIN AND PLATELET-RICH PLASMA IN THE DEVELOPMENT OF A BIOACTIVE CALCIUM ALUMINATE BONE REGENERATIVE SCAFFOLD

By

William P. Clafshenkel

July 2011

Dissertation supervised by Paula A. Witt-Enderby, Ph.D.

Over 500,000 bone graft procedures are conducted annually within the United States. Autografts contribute to donor site complications and disease transmission with allografts has been described. Many ceramics are only osteoconductive and are brittle, limiting their clinical use. Thus, the objective of this study was to create a bone substitute with osteoinductive properties similar to natural bone using the ceramic biomaterial calcium aluminate (CA). Calcium aluminate materials are durable and remain moldable for an extended period of time at room temperature. Further, the surfaces of CA scaffolds can be modified with biological agents through simple chemical means to locally deliver agents directly to sites of injury. In order to enhance local bone regenerating characteristics of CA scaffolds, melatonin and platelet-rich plasma (PRP)

were utilized for their known osteoinductive properties. Platelet-rich plasma enhances soft and hard tissue formation primarily through growth factor-mediated signaling pathways. Melatonin augments osteoblast differentiation and inhibits osteoclast-mediated bone resorption through receptor-dependent signaling and free radical scavenging activity, respectively. Thus, it was hypothesized that melatonin and/or PRP would provide osteoinductive properties to CA scaffolds to promote bone regeneration in a rodent model of critical-size calvaria defects. Modified CA scaffolds (CA-Mel) were produced by immobilizing melatonin to the CA surface through a covalent linkage. The biocompatibility of unmodified and modified CA scaffolds was initially tested *in vitro* and indicated that modified surfaces had a preference for the adhesion and proliferation of normal human osteoblasts versus NIH 3T3 fibroblasts. Moreover, the immobilization of melatonin to the CA surface may delay the differentiation of human adult mesenchymal stem cells (hAMSCs) and may have facilitated their migration across the CA surface. Two-month-old ovariectomized rats were randomized into implant groups receiving unmodified or modified scaffolds in the absence (CA and CA-Mel) or presence of PRP (CA+PRP and CA-Mel+PRP). Histological sections confirmed that both CA scaffold types were well-tolerated and provided evidence of tissue infiltration and scaffold biodegradation over time. Bone regeneration in animals was assessed by fluorochrome labeling at three and six months. While there was a lack of synergism between melatonin and PRP in the CA-Mel+PRP group, animals implanted with CA-Mel showed the greatest intensity and abundance of bone remodeling at both time points compared to all other groups. Radiographic data indicated a significant increase in the density of newly formed bone over time in all groups. The absence of a detectable

decrease in density suggests that the modest biodegradation of CA scaffolds is balanced with processes of bone formation. Finally, both unmodified and modified CA scaffolds continued to provide a supportive surface for bone formation out to six months. Overall, results from this study suggest that CA scaffolds modified with melatonin may enhance bone remodeling activity in calvarial defects through hAMSC differentiation and recruitment and by preferentially supporting the viability and function of mature osteoblasts. This novel bioactive ceramic scaffold has the potential to change the dogma of bone grafting in fields like dentistry and reconstructive surgery. Continued optimization of this therapy is warranted and the attachment of other osteoinductive biomolecules is being considered.

DEDICATION

This dissertation is dedicated to my parents, family, and in memoriam to my grandfather, William G. Clafshenkel.

ACKNOWLEDGEMENT

I thank my advisor, Dr. Paula Witt-Enderby, for encouraging me to obtain my Ph.D. and for suggesting this interesting project. I would also like to thank my committee members, Dr. Jane Cavanaugh, Dr. Ellen Gawalt, Dr. David Johnson, and Dr. James Rutkowski for their patience, encouragement, and guidance. It was great to work with all of you and I appreciate the opportunity to be part of such a diverse group of scientists. I am deeply indebted to the hard work of Christine Close and Denise Butler-Buccilli for their assistance with the animal surgeries and kind attention to the study animals.

I would like to acknowledge and thank the following people for their technical assistance during this project:

From the laboratory of Dr. Ellen Gawalt: Rachelle Palchesko, Jared Romeo, and Kristen Kruszewski for the preliminary data and assistance with the SEM photographs. I appreciate all of your time and help with my project.

From the Center for Metabolic Bone Disease, University of Alabama at Birmingham: Patricia L. Lott and her team for the histology work and assistance with all our technical questions.

Lastly, I thank all of the graduate students, faculty, and administrative staff of the Graduate School of Pharmaceutical Sciences for their support, advice, and friendship.

TABLE OF CONTENTS

LIST OF FIGURES

LIST OF ABBREVIATIONS

CA: Calcium aluminate; unmodified calcium aluminate scaffold

CA-Mel: Calcium aluminate scaffold modified by the covalent attachment of melatonin

hAMSC(s): Human adult mesenchymal stem cell(s)

OS- : Basal hAMSC medium lacking osteogenic supplements

OS+ : Basal hAMSC medium containing osteogenic supplements; used to induce hAMSC differentiation

PRP: Platelet-rich plasma

INTRODUCTION

Skeletal Development and Remodeling

Much of the appendicular skeleton is comprised of long bones such as the clavicles, humeri, radii, unlnae, femurs, tibiae, fibulae, and phalanges (1). Flat bones include the skull, mandible, scapulae, sternum, and ribs (1). Overall, the adult human skeleton is approximately 80% cortical (compact) bone and 20% trabecular (spongy) bone (1). Bone is a dynamic tissue that undergoes growth, modeling, and remodeling throughout the lifetime of an individual. Bone growth occurs through longitudinal and radial growth during childhood and adolescence (1). Bone modeling is the mechanism by which bone changes its overall shape in response to physiological influences or mechanical forces (1). Modeling leads to gradual adjustments of the skeleton to these forces. Bone remodeling is a process by which bone is renewed to maintain bone strength and mineral homeostasis (1).

Bone remodeling requires the recruitment and activity of several key cell types and follows a chronological progression through four sequential phases (Fig. 1). The first of these phases is activation (Fig. 1*A*). Given that osteoclast precursors are of hematopoietic origin, they are recruited from the circulation and fuse to the exposed bone surface via interactions between integrin receptors on their cell membrane and matrix peptides on the bone surface (1, 2). Once fused to the exposed bone surface, osteoclast precursors transition into mature osteoclasts. Mature osteoclasts are responsible for the removal of surface bone.

Osteoclast-mediated bone resorption follows the activation phase and can last two to four weeks during each remodeling cycle (1) (Fig. 1*B*). Osteoclast activity is regulated by specific biomolecules and cytokines including receptor activator of nuclear factor kappa B (NFκB) ligand (RANKL), osteoprotegrin (OPG), interleukin-1 (IL-1), IL-6, parathyroid hormone, vitamin D, and calcitonin (1) (Fig. 2). Many of these resorption activators increase the production of RANKL, which when bound to its receptor, RANK, on osteoclast progenitor cells, causes an increase in osteoclast production and function (3). Mature osteoclasts form an enclosed environment around the region to be remodeled via interaction with adhesion proteins such as integrins and vitronectin (3). Mobilization of bone mineral is aided by osteoclast secretion of hydrogen ions via H+-ATPase proton pumps and chloride channels to lower the pH of the resorbing environment and by direct digestion of the organic matrix (1). Osteoclasts also secrete proteases like cathepsin K and metalloproteinases that act to enzymatically break down collagen and other bone matrix proteins (3). The result of osteoclast activity is a resorption pit, a small burrow of resorbed bone beneath the sealed region.

Figure 1. Phase of Normal Bone Remodeling

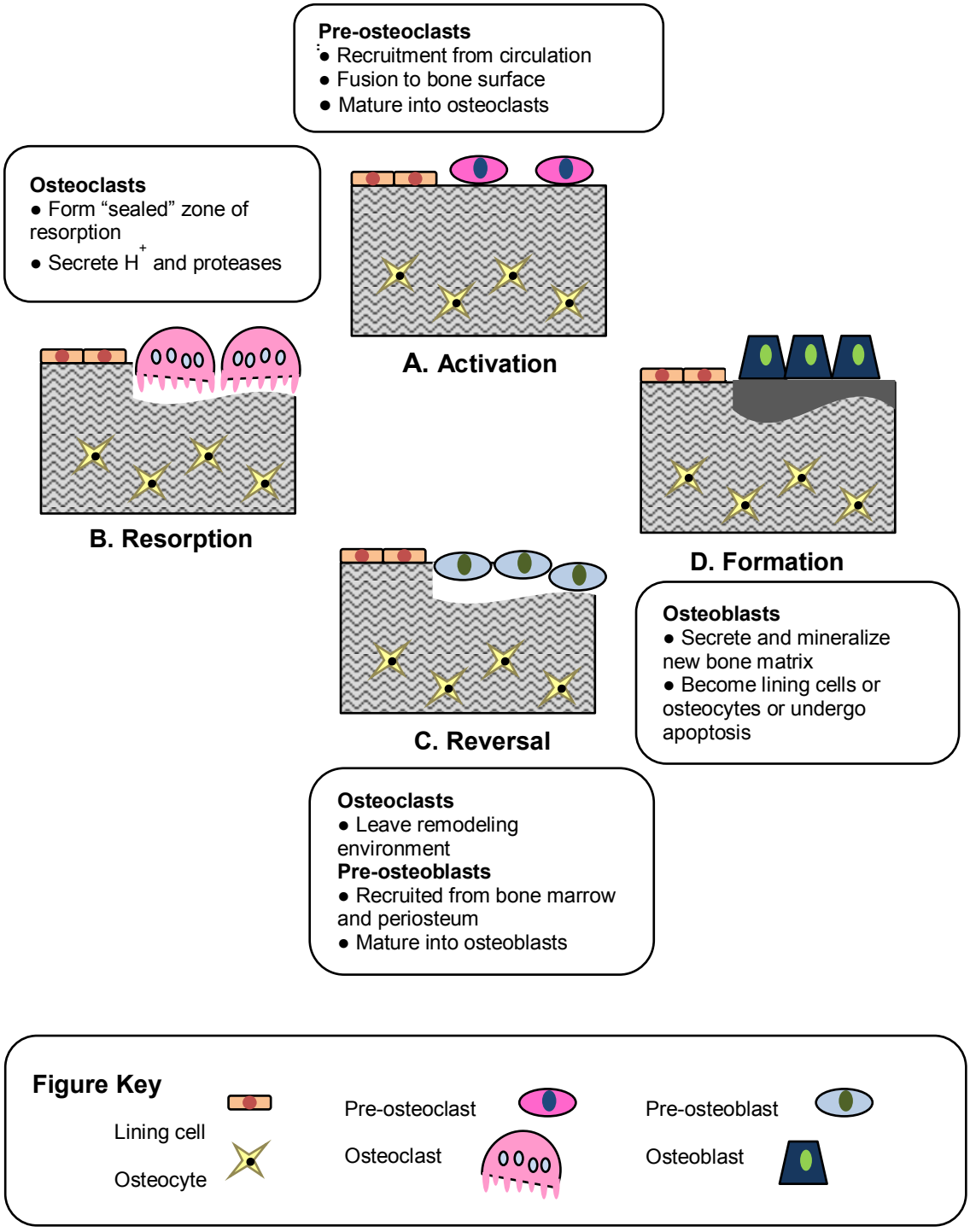

Figure created by William P. Clafshenkel.

The third phase is the reversal phase whereby bone resorption transitions to bone formation (Fig. 1*C*). Bone formation is dependent on the activity of bone-forming cells

called osteoblasts derived from mesenchymal stem cells residing in the bone marrow and periosteum (4, 5). Osteoblast activity in exchange for osteoclast activity is highly-coupled through signaling events that are poorly understood. Proposed signaling molecules that regulate the coupling of these signals include transforming growth factor-β (TGF- β), insulin growth factor-1 (IGF-1), IGF-2, bone morphogenetic proteins (BMPs), platelet-derived growth factor (PDGF), and fibroblast growth factor (FGF) (1) (Fig. 2). In fact, TGF-β and IGF-2 are the first and second most abundant mitogens in human bone extracellular matrix (6). TGF-β is a member of a family of polypeptide growth regulators that affect cell growth and differentiation during both developmental processes and tissue repair (6). It is present in the extracellular matrix as a latent component but is released and activated through increased bone resorption, where it is free to stimulate chondrogenesis (i.e., the development of hyaline cartilage) and osteogenesis (i.e., the development of new bone) (6). IGFs function to stimulate osteoblast proliferation and matrix synthesis (6). Moreover, osteoblasts synthesize osteoprotegrin (OPG), a known regulator of osteoclast activity and thus, bone resorption (7). In the absence of OPG, RANK ligand (RANKL) on the surface of osteoblasts is free to interact with RANK on the osteoclasts precursors and osteoclasts, thereby coupling osteoclast formation and activity with that of osteoblasts (7). However, this coupling event is blocked in the presence of OPG, which acts as a decoy receptor for RANKL. Blocking RANKL binding to RANK can result in the down-regulated transcription of osteoclastogenic genes in osteoclast precursors or the down-regulation of resorption activity of mature osteoclasts (7).

Figure 2. Signaling Events that Regulate and Couple Osteoblast and Osteoclast Activity

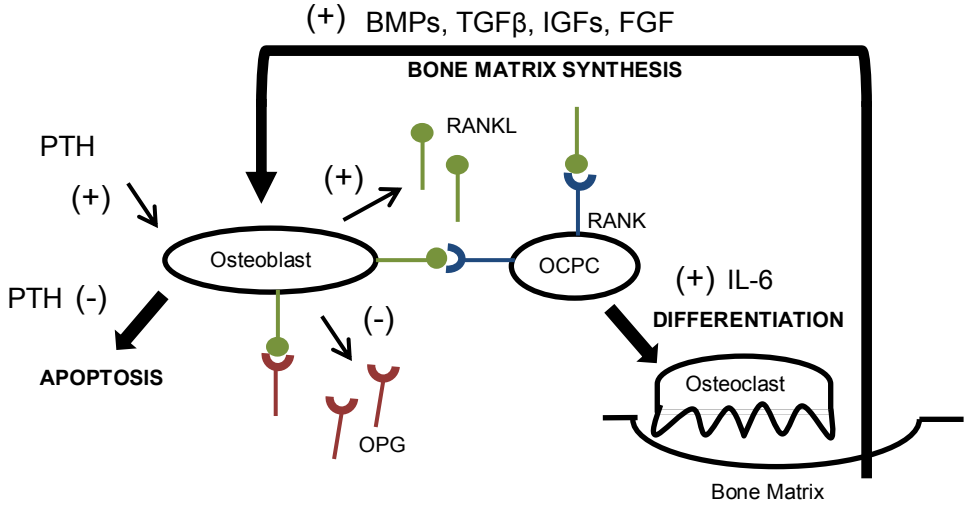

Figure 2. Osteoblast and osteoclast activities are highly regulated and coupled by hormones, cytokines, growth factors, and secreted proteins. Parathyroid hormone (PTH) stimulates bone remodeling by promoting the production of RANKL by osteoblasts. Additionally, PTH inhibits the apoptosis of osteoblasts and osteocytes. Receptor activator of NF-κB ligand (RANKL) is produced by osteoblasts and couples their interaction with osteoclast precursors (OCPC) to promote differentiation into mature osteoclasts. Osteoblasts also secrete osteoprotegrin (OPG), which acts as a decoy receptor for RANKL and reduces osteoclast formation and activity. Interleukin-6 (IL-6) is a positive regulator of OCPC differentiation and activity. Lastly, osteoclast-mediated bone resorption releases embedded growth factors from the bone matrix. These include bone morphogenetic proteins (BMPs), transforming growth factor-β (TGFβ), insulin-like growth factors (IGFs), and fibroblast growth factor (FGF). These growth factors promote the production of bone matrix by osteoblasts. Figure created by William P. Clafshenkel.

The final phase, bone formation, can last approximately four to six months (Fig. 1*D)*. Bone formation in the adult skeleton involves intramembranous bone formation and endochondral bone formation. The growth of long bones occurs by the conversion of cartilage into calcified bone, a process called endochondral ossification. During endochondral bone formation, mesenchymal stem cells differentiate into chondroblasts that synthesize a cartilage template that is later vascularized and replaced by mineralized bone (3). Intramembranous ossification differs from endochondral ossification in that there is no cartilage intermediate; mesenchymal stem cells differentiate directly into bone-forming osteoblasts (3). Intramembranous ossification is important for the

development of the cranial flat bones, the periosteal collar of long bones, and for fracture healing (3). During this time, osteoblast secrete new collagenous organic matrix that is subsequently mineralized through the concentration of calcium and phosphate (1). At the completion of the bone formation phase some osteoblasts will be embedded in the secreted bone matrix and become osteocytes, while others will become lining cells at the bone surface (1). Lining-cells have the capacity to redifferentiate into osteoblasts when exposed to parathyroid hormone or mechanical forces (1). Osteocytes form cell networks within the bone and can transduce mechanical stimuli from the periphery to the center of the bone (3).

Spectrum of Skeletal Disorders: Pathological, Congenital, and Acquired Bone Loss

Adult rates of bone remodeling (2-3%) are relatively low compared to those of childhood and adolescence, but are necessary to maintain the biomechanical strength of bone (1). Nonetheless, several factors can impact the rate of bone remodeling in the adult human. Some of these can lead to the bone disease called osteoporosis, a condition where bone remodeling is imbalanced. Specifically, the activity of osteoblasts is out-weighed by that of osteoclasts resulting in a net loss of bone during bone remodeling that can lead to reductions in bone strength and alterations to bone microarchitecture (2, 3). Risk factors for osteoporosis range from lifestyle habits, to disease states, to the use of certain medications. Physical conditions that increase a person's risk of developing osteoporosis include a low body weight, a small body frame, older age, a low bone mineral density, a low peak bone mass at maturity, surgically induced menopause, and estrogen deficiency (8, 9). Several disease states including diabetes type 1, adrenal insufficiency, inflammatory bowel disease, and others can increase osteoporosis risk (8,

9). Likewise, medications such as oral glucocorticoids can further increase the risk of developing osteoporosis (9). Lifestyle habits that contribute to osteoporosis and osteoporosis-related fractures include cigarette smoking, immobility, low physical activity, alcohol consumption, a diet low in calcium and vitamin D, and nightshift work (8-10). Osteoporosis is a global disease that affects many bones of the body including long bones, the spine, and bones of the jaw. The prevalence of osteoporosis-related fractures is predicted to increase from about 10 million to greater than 14 million by 2020 (11). Both men and women are susceptible to osteoporosis, although its prevalence among women is greater (11). Women 65 years and older account for approximately 74% of all fractures, while men the same age account for approximately 61% (estimates from 2005) (11).

Other skeletal disorders involving alterations to the normal rates of resorption and formation of bone and cartilage include osteoarthritis, rheumatoid arthritis, and bone disease associated with cancer. In osteoarthritis, articular cartilage is degraded giving way to hypertrophy of the subchondral bone (3). Rheumatoid arthritis is characterized by the destruction of articular cartilage and excessive resorption of the subchondral bone (3). Cancer metastases traveling through the blood stream can lead to the development of secondary tumors on bone surfaces. Focal cancer metastases on the bone can either cause abnormal bone formation (osteoblastic or osteosclerotic lesions) or bone breakdown (osteolytic lesion) (3). In both cases, the bone of the lesions is very weak and susceptible to fracture.

Bone abnormalities not only occur with lifestyle habits, aging, and disease states but can also occur with major trauma such as fractures or with congenital malformations.

Specifically, bone defects in the craniomaxillofacial skeleton remain a major and challenging health concern (12). These defects can occur as a result of congenital malformations or acquired injuries. For example, in 2001, approximately 38,000 children underwent surgery to repair birth defects, while approximately 24,000 underwent maxillofacial surgeries for injuries to the face and jaw (12). Wars in Iraq and Afghanistan have contributed to the largest incidence of head trauma since the Vietnam conflict (12). Moreover, large orthopedic defects, in which the natural regenerative capacity of the bone is exceeded, rely on the application of mechanically and biologically optimized biomaterials to facilitate healing (13).

Treatment Options for Bone Loss

The treatment of osteoporosis has long been investigated and many current therapies available on the market target bone changes associated with the progression of the disease. The majority of osteoporosis medications are antiresorptive agents aimed at mitigating bone loss by decreasing osteoclast activity. Antiresorptive agents include the bisphosphonates (alendronate [FOSAMAX], risedronate [ACTONEL], ibandronate [BONIVA], and zoledronic acid [RECLAST]), selective estrogen receptor modulators (SERMs) (raloxifene [EVISTA]), and more recently, a RANK ligand inhibitor (denosumab [PROLIA]) (14).

Bisphosphonates have been utilized for a wide spectrum of bone disorders including glucocorticoid-induced osteoporosis, Paget's disease, and the treatment of hypercalcemia related to bone malignancy (3). Although reportedly effective at slowing bone loss, clinicians report the incidence of osteonecrosis, or degradation, of the jaw

(ONJ) is increasing among menopausal patients utilizing oral bisphosphonates for the prevention and treatment of osteoporosis (15, 16). Based on cases reported in the literature, the incidence of ONJ induced by oral bisphosphonate therapy is estimated to be between 2.5% to 27.3% (17). Although the exact pathology is unknown, it is theorized that oral bisphosphonate-induced ONJ is attributed to the accumulation of bisphosphonates in areas of elevated bone remodeling, due to their high affinity for calcium, their limited metabolism, and their down-regulation of bone turnover (16, 17). Symptoms of ONJ include pain, swelling, exposed bone, and purulent secretions (17). ONJ further reduces the already limited quantity and quality of bone in the oral cavity of menopausal females, and can significantly prolong healing time after oral surgery. Consequently, the results of oral procedures sought to repair and/or replace jaw bone and missing teeth are often unsuccessful (18). Further, oral bisphosphonate use has the potential to increase the risk of low-energy subtrochanteric or diaphyseal femur fractures (19) and the accumulation of bone microdamage with treatment over time (20). This is most likely attributed to the continued catabolic nature of these antiresorptive agents on bone. From a structural point of view, the backbone of bisphosphonates is analogous to pyrophosphates (P-O-P), where a carbon atom replaces the oxygen atom. The functional differences between bisphosphonate species is related to side chain substitutions and the presence or absence of nitrogen (3, 21). Bisphosphonates embedded in the bone matrix enter into osteoclasts during bone resorption. Non-nitrogen-containing bisphosphonates are incorporated with adenosine monophosphate (AMP) to form non-hydrolyzable ATP analogs (21). These analogs are functionally inactive and their accumulation induces osteoclast apoptosis (21). Nitrogen-containing bisphosphonates inhibit farnesyl

pyrophosphate (FPP) synthase, the enzyme responsible for the generation of prenylated proteins that are required for osteoclast function and survival (21). It is thought that this inhibition induces osteoclast apoptosis via caspase activation pathways (21) (Fig. 3).

Figure 3. Mechanism of Action of Bisphosphonates on Osteoclasts

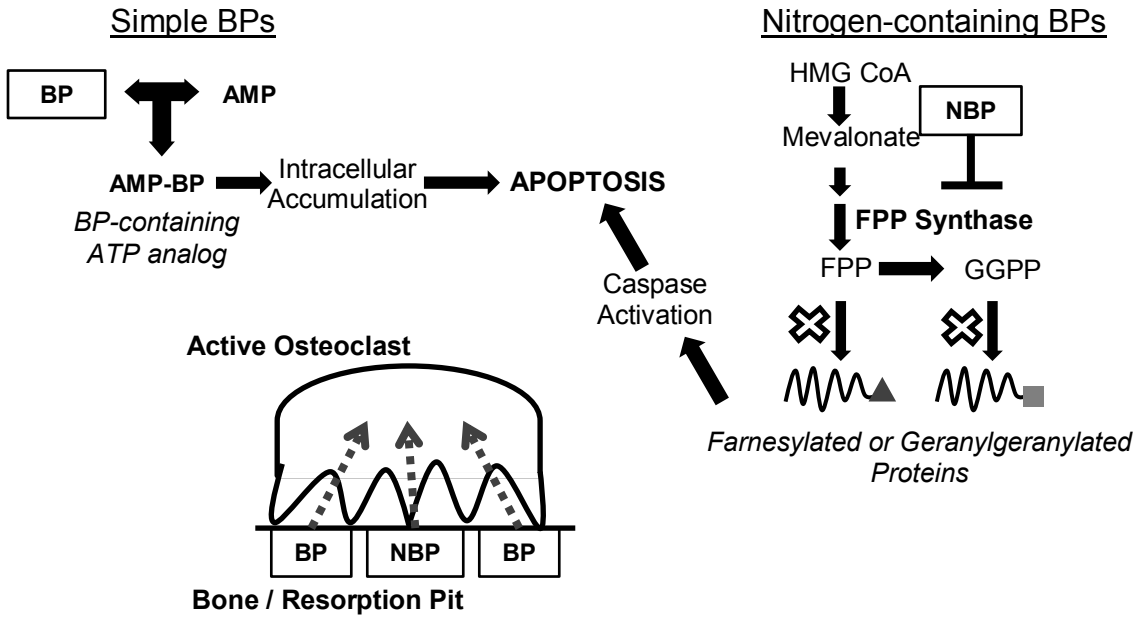

Figure 3. Simple (BP) and nitrogen-containing (NBP) bisphosphonates bound to bone mineral are internalized into osteoclasts during bone resorption. Simple bisphosphonates (e.g., etidrondate, DIDRONEL) are incorporated into non-hydrolyzable ATP analogs. The accumulation of such non-functional ATP species induces osteoclast apoptosis. Nitrogen-containing bisphosphonates (e.g., alendronate, FOSAMAX) inhibit farnesyl diphosphate (FPP) synthase disrupting the synthesis of FPP and geranylgeranyl diphosphate (GGPP) and their prenylated forms. NBP-induced apoptosis is thought to occur via the activation of caspase pathways. AMP = adenosine monophosphate. HMG CoA = 3-hydroxy-3-methyl-glutaryl Co-enzyme A; initial substrate for the mevalonate pathway. Figure created by William P. Clafshenkel.

Selective estrogen receptor modulators like raloxifene have been shown to reduce the incidence of vertebral fractures, although the increase in bone mineral density (BMD) is relatively modest (3). Likewise, SERMs are not without untoward effects. The activity of SERMs as agonists or antagonists is tissue specific, and while they maintain the beneficial effects of estrogen on bone, they can produce host flashes, vaginal dryness,

and increases the risk of thromboembolism (22, 23). Their mechanism of action is related to their unique ability to induce conformation changes in the estrogen receptor, which results in the recruitment of different combinations of co-activators or co-repressors (3). It is hypothesized that the availability of co-regulators represents the basis for their tissue-selective pharmacology (3).

Only the PTH analog, teriparatide [FORTEO] has been commercially developed for osteoporosis patients in an effort to rebuild new bone. Teriparatide has been shown to increase bone mass, increase bone density, and improve the microarchitecture of bone (14). It is thought that PTH accomplishes this by promoting the proliferation and differentiation of osteoblasts and osteocytes, while inhibiting their destruction by apoptosis (3). Mechanisms underlying PTH-induced osteoblast survival may include activation of cAMP response element binding protein (CREB)-mediated transcription of survival genes through G-coupled protein receptor pathways (24). Despite beneficial effects on the bone, the need for daily subcutaneous injections affects patient compliance (14) and its use is limited to a two-year duration (25). While medications can slow the progression of osteoporosis, many patients are still at increased risk for the development of fractures. Osteoporosis-related fractures contribute to a significant amount of economic expense through costly procedures, extended hospital stays, and prolonged rehabilitation.

The treatment of large bone defects remains a challenge as well. The current procedures for the restoration or replacement of bone for congenital or acquired bone defects often results in poor aesthetic and functional outcomes (12). Human bone morphogenetic protein 2 (BMP-2; [INFUSE]) has been used clinically for certain

interbody spinal fusions, open tibial fractures, and maxillofacial procedures (12, 26); however, instances of ectopic bone formation and uncontrolled bone growth have been described with higher doses (27). Interest is increasing in other recombinant forms of BMP family members, namely rhBMP-7 and rhBMP-4, albeit this research has been exclusive to animal models (27). Current research efforts seek to improve bone regeneration through the development of new surgical techniques or bone graft therapies.

Autologous, Allogenic, and Synthetic Bone Grafts

Bone restoration for osteoporosis-related fractures and bone replacement for larger bone defects have benefited from developments in bone grafting procedures. Over 500,000 bone grafting procedures are conducted annually within the United States, with 2.2 million occurring worldwide (28). Bone graft procedures have been used to repair bone defects in a variety of fields including orthopedics, neurosurgery, and dentistry. Ideally, bone grafts from either autogenic, allogenic, or synthetic sources would replicate the normal bone healing responses of autogenous bone by providing osteogenic, osteoinductive, and osteoconductive activity. An osteogenic graft would contain living cells that are capable of differentiating into bone (29). The osteoinductive, or stimulatory, effects of the graft material on local or transplanted cells would facilitate the differentiation of stem cells into osteoblasts or promote osteoblast activity (29). Lastly, osteoconductive properties of the graft material would provide a suitable surface for the apposition of newly formed bone (29, 30). The combination of osteoconductive and osteoinductive properties would allow the implanted graft to integrate into the newly formed bone, defined as osteointegration (31).

Although the bone autograft is considered to be the "gold standard" for bone graft procedures, its use has been associated with 8-20% of donor site complications including donor site hematoma, soft tissue breakdown, pain, and a lengthened hospital stay (28, 32). Moreover, the use of bone autografts in osteoporotic populations is usually contraindicated given a significant reduction in the quality and quantity of available bone (18). Although the prevalence of the bone allograft is slowly increasing, the risk of disease transmission has been described (28). Additionally, the chemical processing of bone allografts to remove cells and bioactive proteins in an effort to reduce immunogenicity weakens the mechanical integrity of the graft (28). The use of allografts is also limited to the volume of material readily available at most institutions (33).

There has been significant impetus in researching and developing an ideal synthetic bone substitute for a wide array of bone grafting procedures in an effort to circumvent the issues with bone autografts and allografts as described above. The research, development, and use of several biomaterials has spanned the better part of six generations and can be loosely divided into three evolutionary categories: bioinert materials, bioactive and biodegradable materials, and materials designed to stimulate specific host cellular responses through dynamic molecular signaling (34). Despite the conceptual transition of biomaterial development, many early forms are still widely used (34). Materials used for industrial applications provided the earliest forms of biomaterials because they were easily accessible. The only contingency governing their use was that they be inert so as to limit immune responses or foreign body reactions in the host (34). Biomaterials introduced in the 1940s included metal and metal alloy-based implants (stainless steel, cobalt-chrome alloys, titanium, and titanium alloys); porous

ceramics of alumina, zirconia, calcium; and polymers consisting of silicone rubber, acrylic resins, polyurethanes, polypropylene, and polymethylmethacrylate (34). Second generation biomaterials appeared between 1980 and 2000 and sought to enhance the biological response from the host environment as a means of facilitating tissue/surface bonding and bioabsorption (34). Bioactive materials that are still used clinically in fields like dentistry and orthopedic surgery included bioactive glasses, ceramics (calcium phosphate, β-tricalcium phosphate, and hydroxyapatite); bioactive ceramic-coated metals (calcium phosphate and hydroxyapatite-coated titanium and titanium alloys); and biodegradable polymers (polyglycolide, polyactide, polydioxanone, chitosan, hyaluronic acid, hydrogels) (34, 35). Hydroxyapatite-coated titanium implants, in particular, have been shown to help convert fibrous tissue to bone (36) and facilitate osteointegration (37). However, bioabsorbable implants have several advantages over traditional metallic implants including reduced stress shielding, elimination of surgeries to remove metallic components, and a reduction in hypersensitivity and osteolytic responses in the recipient (34). Indeed, hypersensitivity to metals and wear debris-induced osteolysis are still prevalent concerns (38-40). Approximately one million total joint replacements are completed world-wide each year (39). Many of the hip and knee prostheses are comprised of a polymer-based cup (e.g., ultra-high molecular weight polyethylene [UHMWP]) that articulates against a hard metal surface (39). Particulate debris from these implants is generated by either wear or corrosion and accumulates in the periprosthetic membrane and surrounding tissue where it is phagocytosed by macrophages (40). The macrophages release pro-inflammatory cytokines such as tumor necrosis factor-α (TNF-α) to recruit additional cells to the site in an attempt to evacuate

the particles (39, 40). Macrophage-secreted TNF-α is thought to initiate osteolysis by activating osteoclasts and bone resorption around the implant (39).

The most current conceptual transition of biomaterials has been to create implants that stimulate the host environment to facilitate healing and tissue regeneration. In fact, many commercially available products only provide for osteoconduction and osteointegration but exhibit no other properties of natural bone (27, 41). These materials are typically three-dimensional porous structures and can contain stem cells, growth factors, and/or peptide sequences as a means of promoting cell invasion, attachment, proliferation, and activation (34). Biomaterials have been combined with recombinant growth factors (42, 43), biomolecules (44, 45), and stem cells (46, 47) in an effort to achieve other natural bone properties. The repair and remodeling processes that will incorporate and potentially replace the grafted material are dependent on the specific interplay between local host cells and bioactive proteins at the surgical site.

Calcium-based Ceramics as a Synthetic Bone Graft Materials

Interest in implantable ceramic materials, including calcium aluminate and calcium phosphates stems from early research in the 1970s (48, 49). The three main calcium-based ceramics to be discussed are calcium hydroxyapatite ($Ca_{10}[PO_4]_6[OH]_2$), tricalcium phosphate ($Ca_3[PO_4]_2$), and calcium aluminate ($CaO \cdot Al_2O_3$).

Calcium hydroxyapatite is derived from coral exoskeleton that is treated by a hydrothermal exchange method to covert coral carbonate into pure hydroxyapatite (33). The process removes residual organic matter and leaves behind a unique macroscopic architecture similar to human cancellous (spongy) bone with pore sizes ranging from 500

– 600 μm (33). Hydroxyapatite implants have been utilized in several animal models of long bone, spinal, and mandibular defects where they generate a strong bone union with no fibrous tissue (33). Upon implantation in the canine tibia, porous hydroxyapatite demonstrates 50 percent greater strength than identical sites treated with cancellous bone grafts for six months; however, in its unimplanted state, it is significantly weaker than cancellous bone (33). The Food and Drug Administration (FDA) approved the use of porous hydroxyapatite in humans for the repair of metaphyseal and diaphyseal defects in long bones in 1982 (33).

Calcium phosphates, including tricalcium phosphate (TCP), have been extensively investigated for use in dental and orthopedic settings. The synthesis process begins with homogenization of the tricalcium phosphate powder with naphthalene. During compaction of the mixture, the naphthalene is removed by sublimation, leaving pores in the ceramic. The final step is a sintering process (>600^{o}C) that fixes the pore configuration and results in pore diameters ranging from 100 – 300 μm (33). Fluctuations in sintering temperatures can greatly affect microporosity and crystal size (35). Like hydroxyapatite, TCP has been tested in a variety of animal models which support its low toxicity, rapid bone ingrowth, and biodegradation into natural calcium and phosphate ions (33). The biodegradability of calcium phosphates is thought to occur, at least in part, by cellular engulfment of the graft material or dissolution in acidic microenvironments (35). However, the rate of biodegradation can be influenced by the implant environment and the stability of the surrounding bone (33). Tricalcium phosphates like β-TCP [Vitoss®, Cerasorb®] are used routinely for dental applications such as the repair of periodontal defects, augmentation of alveolar bone, sinus lifts, and

tooth replacement (35). In cases of defects in long bones or those created following curettage of bone malignancy, TCPs have demonstrated adequate regeneration of new bone and sufficient integration (31, 33). The use of TCP for spinal fusion has been tested in several models. TCP produced better results than hydroxyapatite or calcium carbonate in canines, improved fusion results over autologous bone in sheep, and was completely integrated into the vertebrae of baboons (31). Despite the advantages of calcium phosphate materials for bone regeneration, there is concern with the overall mechanical integrity of these ceramics. Calcium phosphate ceramics are brittle, lacking substantial mechanical strength, and require that the surrounding bone must be intact or rigidly stabilized to shield the implant from loading during integration (31, 33). The implants will fragment when subjected to shear forces (33). Although, β-TCP scaffolds implanted in 8 mm calvarial defects in rats showed signs of osteointegration and neovascularization after four weeks (50), substantial degradation prior to adequate bone fill may compromise the integrity of the biomaterial and the defect site.

The unique combination of alumina and calcium as a ceramic implant for dental applications was considered in the early 1970s. Acute toxicity testing revealed that calcium aluminate (CA) lacked cytotoxic effects (48). Subacute toxicity testing demonstrated that CA implanted in muscle pockets was well-tolerated and saline extracts of calcium aluminate injected intradermally were non-irritating (48). Later testing of CA in tibial and calvarial models was conducted by Uchida *et al*. Their studies revealed that although porous CA implants were well-tolerated, tissue ingrowth into implant pores was predominately acellular (i.e., fibers and extracellular matrix) even with larger pore sizes, longer periods of implantation, and the presence of bone marrow (49, 51). Interestingly,

signs of modest biodegradation of the CA implants were observed in calvarial defects (49). While early studies support the biocompatibility of CA, more robust bone ingrowth and integration are desired. Indeed, ceramic materials by nature are only osteoconductive (35, 37). Thus, alternative calcium-based implants with adequate mechanical properties to endure impact or weight-bearing forces while regenerating bone need to be considered for these locations in conjunction with stimulatory factors that will facilitate their integration.

Calcium aluminates are formed by the thermal treatment of an Al_2O_3 source and a CaO source. The chemical composition of calcium aluminates results from the ratio of Al_2O_3 to CaO and can produce a wide variety of chemical species. What is unique about this process is that calcium aluminates are prepared by mixing the reactants with a small amount of water resulting in a material that is moldable at room temperature for an extended period of time. Moreover, traditional heat treatments (>600^{o}C) used in the synthesis and strengthening of other ceramics (35) are not required for the manufacture of calcium aluminate scaffolds. Thus, there is a novel opportunity to functionalize CA surfaces with a variety of biological agents. These advantages were exploited to enhance the osteoinductive potential of CA scaffolds in the current study. To this end, two therapeutic agents were utilized for their reported effects on bone formation, melatonin and platelet-rich plasma.

Effects of Melatonin on Bone & Melatonin as an Osteoinductive Agent

Melatonin is a hormone synthesized and secreted into the systemic circulation from the pineal gland during periods of darkness (52). The biochemical conversion of

tryptophan to melatonin in pinealocytes has been well-described and is inhibited by light (52). Its endogenous release is controlled by specific master clock cells located in the suprachiasmatic nucleus (SCN) and it has been implicated in circadian entrainment of peripheral clocks (53, 54). Melatonin affects several physiological systems including those involved in sleep, immune defense, detoxification, reproduction, and bone maintenance either by receptor-dependent or receptor-independent actions (54). The endogenous levels of melatonin decline with age, the onset of menopause, inactivity or immobility, and exposure to artificial light at night (10, 54, 55).

Melatonin deficits have been theorized to be implicated in the etiology of bone diseases like osteoporosis and adolescent idiopathic scoliosis (56, 57). With age, bone marrow cell differentiation shifts towards an adipocyte lineage, reducing the formation of osteoblasts, increasing fat cell accumulation in the marrow, and contributing to osteoporosis risk (58). These alterations coincide with the decline in melatonin levels with age, implying that melatonin production and bone homeostasis are closely linked. Artificial light at night can suppress melatonin production and function. In a study of female nightshift workers exposed to light at night, women working nightshift had an increased risk of hip and wrist fractures over eight years of follow-up compared to cohorts that never worked nightshifts (10). Animal studies support these findings, as exposure to longer periods of light disrupted bone turnover in rats (59). Moreover, long-day conditions decreased the average circadian melatonin concentration and abolished the rhythmicity of the circadian peak (59). A separate study by the same authors found that pinealectomy induced biochemical markers of bone metabolism, while exogenous melatonin administration suppressed the same markers (60). These studies suggest that

lighting conditions can affect that normal pattern of melatonin production and secretion, and that melatonin production and secretion are an important mechanism regulating bone turnover activity in both animals and humans.

Persistent osteopenia, a condition where bone mineral density is lower than normal, is a hallmark of adolescent idiopathic scoliosis (AIS). Several human and animal studies have investigated the role melatonin may play in the etiology of AIS given its reputed effects on bone. The main hypothesis that melatonin deficiency is linked to AIS stems from studies in which pinealectomy of chickens and rats results in scoliosis that resembles the AIS pathology (57). Similar effects in fish suggest that gravity may not affect the response to pinealectomy with regard to the development of scoliosis (61). Surgically induced bipedalism in pinealectomized mice also results in scoliosis (62); however, the same is not true for non-human primates (57). Therefore, whether or not the results of experiments in lower animals can be extrapolated to humans remains to be determined. Nonetheless, genetic studies of AIS patients reveal that polymorphisms of the MT_2 receptor gene could predispose an individual to AIS (57), and that promoter polymorphisms of the MT1 receptor gene are likely not involved (63). Moreau and colleagues believe that the response to melatonin (i.e., inhibition of forskolin-induced cAMP accumulation in primary osteoblasts), not melatonin synthesis or the expression of melatonin receptors, could underlie AIS is humans (64). Indeed, their research has demonstrated an impaired melatonin signaling response in osteoblasts isolated from AIS patients (64) that could be the result of phosphorylation of serine residues affecting the activity of G inhibitory (G_i) proteins normally associated with melatonin receptors (65). Work by other authors suggests that the dysfunction in melatonin signaling in the

osteoblasts of AIS patients in due to abnormal MT_2 melatonin receptor expression (66). Work completed by Radio *et al*. (2006) and Sethi *et al*. (2010) support the notion that the MT_2 melatonin receptor may be important for regulating the activity of osteoblast (67, 68). These studies further support the connection between melatonin and bone physiology.

To date, there is only one clinical trial focused on the use of melatonin as a therapeutic intervention for the preservation of bone (Identifier# NCT01152580) (69), yet several studies have demonstrated that melatonin prevents bone deterioration in fish (61), chickens (70, 71), and mice (62). Melatonin is hypothesized to have three principle actions on bone metabolism including (1) the promotion of osteoblast differentiation and activity (52, 57, 67, 68, 72), (2) the suppression of osteoclast activity via its increase in osteoprotegrin and actions on receptor activator of NF-κB ligand (RANKL) (57, 73), and (3) potential scavenging of free-radicals generated by osteoclast-mediated bone resorption (57) (Fig. 4).

Figure 4. Proposed Mechanism of Melatonin on Bone Homeostasis

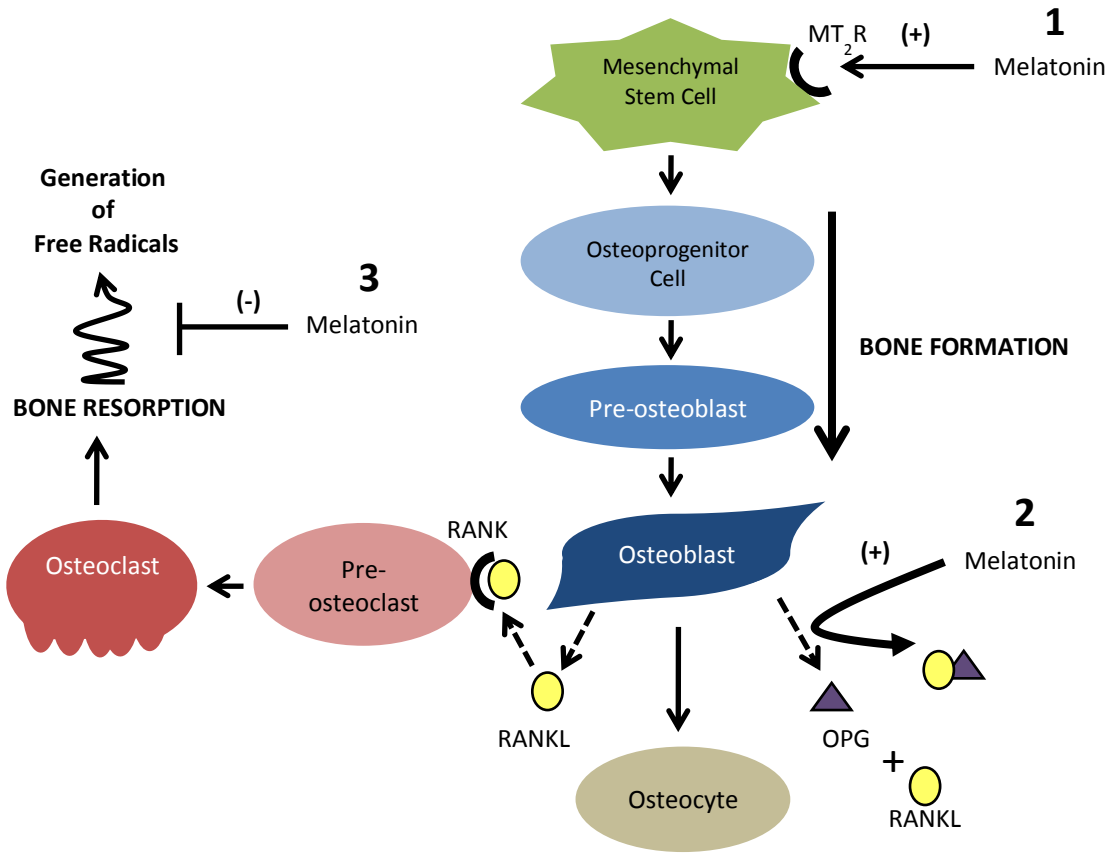

Figure. 4. Melatonin acts through many levels to modulate bone homeostasis. (*1*) Melatonin induces osteoblast differentiation through MT_2 receptors located on hAMSCs. (*2*) Melatonin induces the expression of osteoprotegrin (OPG) in osteoblasts, which acts as a decoy receptor for receptor activator of nuclear factor kappa B (NF-κB) ligand (RANKL). Complexes formed between OPG and RANKL prevent RANKL from binding to its receptor (RANK) on osteoclasts, thus diminishing the formation and activity of new osteoclasts. (*3*) As a free-radical scavenger, melatonin may prevent radical-induced destruction of osteoblasts and osteoclasts to prevent bone loss. Copyright 2011. From *Melatonin in the Promotion of Health* by Ronald Ross Watson (ed.). Reproduced by permission of Taylor and Francis Group, LLC, a division of Informa plc.

In pre-osteoblast cultures from rats and fully differentiated osteoblast-like cell lines, melatonin augments expression of the bone formation markers bone sialoprotein (BSP), alkaline phosphatase (ALP), osteopontin, and osteocalcin in a dose-dependent manner (72, 74). Also, melatonin promotes the proliferation of human bone cells and their synthesis of collagen type I, a major determinant of bone strength (75). Bone

marrow cells from both mice and humans contain high concentrations of melatonin and express the mRNA encoding the rate-limiting synthesis enzyme for melatonin production, *N*-acetyltransferase (76). Thus, the local production and secretion of melatonin in bone and its varied effects on bone remodeling may underlie its regulation of bone physiology. In fact, the modulatory effects of melatonin on both the anabolic and catabolic processes of bone remodeling has highlighted its potential use as an adjuvant therapy in osteoporotic populations (14, 54).

Likewise, several studies have supported the use of topically applied melatonin to facilitate the integration of bone implants. The topical application of 1.2 mg of lyophilized melatonin powder facilitated the osteointegration of titanium dental implants in Beagle dogs over a 2 – 8 week period (74, 77). Secondary four-week studies of platform implants in the mandibles of Beagle dogs demonstrated that 5 mg of lyophilized melatonin powder combined with collagenized porcine bone increased bone perimeter contact, bone density, and new bone formation in defects over collagenized porcine bone alone (78, 79). Moreover, melatonin accelerated the regeneration of cortical bone in tibial defects in rabbits when delivered as a 5 mg dose in resorbable Alveoprotect (a collagen fleece made from porcine dermis) (80). These studies substantiate claims that melatonin may have osteoinductive effects, both alone and when combine with supportive biomaterials, which accelerate the synthesis and mineralization of new bone.

Effects of Platelet-Rich Plasma on Soft and Hard Tissue Healing

Much of the biological stimuli for soft and hard tissue repair as well as angiogenesis originate from platelets activated at the site of injury (81). Platelets have

critical rolls in both soft and hard tissue healing including hemostasis, controlling inflammation, and the initiation of several growth factor-mediated signaling cascades (82). Platelets normally circulate in the blood as an inactivated, spheroid. Platelets are subsequently activated in response to tissue damage or vascular exposure (83). When activated, platelets undergo a process of degranulation in which several cytokines and growth factors are released into the surrounding environment from cytoplasmic α-granules (Fig. 5). The approximately 50 – 80 α-granules they contain hold over 30 bioactive proteins (82). The growth factors and cytokines released contribute to cell recruitment, proliferation, differentiation, and matrix synthesis (82).

Figure 5. Activation of Platelets and Platelet Degranulation

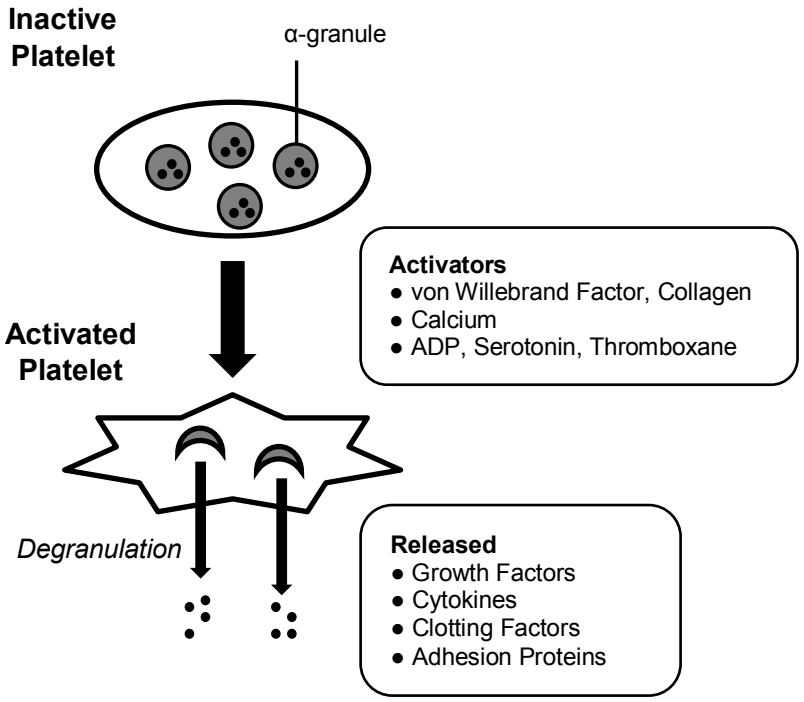

Figure 5. Platelets circulate as inactive spheroids. Activators such as von Willebrand factor, collagen, adenosine diphosphate (ADP), serotonin, or thromboxane induce a change in platelet morphology. Morphological changes in platelets promote the degranulation of α-granules, whereby growth factors, cytokines, clotting factors, and adhesion proteins are released into the microenvironment. Figure created by William P. Clafshenkel.

Platelet-rich plasma (PRP) has a 4 to 5-fold increase in platelet numbers above baseline, is a proven source of growth factors, and can be readily prepared from whole blood (81, 84, 85). Most individuals have a baseline blood platelet count of 200,000 ± 75,000/μL; therefore, a PRP platelet count of 1 million/μL has become the benchmark for "therapeutic PRP" (81). After clot formation, 95% of the growth factors concentrated in PRP are bioavailable after one hour (86). The seven main growth factors in PRP that likely contribute to the healing and remodeling of bone are vascular endothelial cell growth factor (VEGF), epidermal growth factor (EGF), platelet-derived growth factor (PDGF) αα, PDGF ββ, PDGF αβ, transforming growth factor (TGF)β-1, and TGFβ-2

(86). Many of these growth factors are significantly increased over baseline levels in whole blood, which while not appreciably affected by donor age or gender, can vary slightly with collection and activation methods (82, 87). PRP also contains three main adhesion proteins implicated in osteoconduction and extracellular matrix formation including fibrin, fibronectin, and vitronectin (81) as well as the full complement of clotting factors (83). The activity of these specific growth factors and adhesion proteins are summarized in Table 1 below. The infiltration of macrophages in response to PDGF becomes the primary source of growth factors and neovascularization after the platelets expire (81).

Table 1. Major Growth Factors and Adhesion Proteins Found in PRP

Growth Factor	Function	Mean PRP Concentration
• Epidermal Growth Factor	• Stimulates the proliferation of chondrocytes • Chemoattractant for fibroblasts and epithelial cells • Promotes angiogenesis • Influences the synthesis and turn-over of extracellular matrix	• 51 pmol/L
• Platelet-derived Growth Factor	• α and β isoforms are potent mitogens for fibroblasts, chondrocytes, and epithelial cells • Potent chemoattractant for hematopoietic and mesenchymal cells and fibroblasts • Activates TGF-β	• αβ: 117.5 ng/mL • ββ: 9.9 ng/mL
• Transforming Growth Factor-β	• Stimulates fibroblast chemotaxis and proliferation • Stimulates synthesis of extracellular matrix • Decreases dermal scarring • Antagonizes the biological activities of EGF, PDGF, FGFα and FGFβ	• β1: 169.9 ng/mL • β2: 0.4 ng/mL
• Vascular Endothelial Growth Factor	• Stimulates the proliferation of endothelial cells • Induces neovascularization	• 76 – 854 pg/mL
• Fibrin	• Fibrous protein formed by the conversion of fibrinogen by thrombin • Functions in blood coagulation, platelet activation, and protein polymerization	
• Fibronectin	• Extracellular matrix protein that binds other proteins including integrins, fibrin, collagen, and syndecans • Secreted by fibroblasts during matrix synthesis • Functions in cell adhesion, migration, and differentiation	
• Vitronectin	• Abundant glycoprotein of the extracellular matrix • Promotes hemostasis and cell migration, adhesion, and spreading	

Table 1. Table adapted from Alsousou J. *et al.* 2009. *J Bone Joint Surg [Br]*.

The use of PRP is wide-spread in the dental industry and in oral and maxillofacial surgery. It is routinely used in conjunction with dental implant procedures as well as in the treatment of diabetic ulcerations, slow healing wounds, soft tissue loss due to trauma,

and plastic surgery (88-91). It is hypothesized that the effects of PRP on bone formation and healing are due to its modulation of specific growth factors (81, 86, 92) or its effects on local cells (82). Osteoblasts, fibroblasts, endothelial cells, and adult mesenchymal stem cells have surface receptors for the growth factors found in PRP (86). *In vitro*, there is a dose-response relationship between platelet concentration and the proliferation of human adult mesenchymal stem cells and fibroblasts, and the production of type I collagen (82).

The promotion of bone regeneration with PRP has been investigated in several model systems both alone and in combination with other graft materials. The topical application of prepared PRP to human molar extraction site accelerated healing time (from 6 weeks in control sites to 2 weeks in PRP-treated sites) and augmented bone regeneration over a 12-week period (93). The application of thrombin-activated PRP to open femur fractures in Lewis rats increased bone formation and strength at 4 weeks compared to saline-treated controls (92). Bone regeneration in 10 mm circular calvarial defects was significantly enhanced in New Zealand rabbits after 4 weeks with the topical application of PRP (94).

Other studies have examined the bone-regenerating capacity of PRP when combined with autogenous bone, titanium implants, and commercially available bone substitutes. The combination of PRP with autogenous bone in maxillary sinus grafts in humans increased new bone formation over autogenous bone alone at three months (95). PRP potentiated the formation of new bone in critical-sized calvarial defects in mini-pigs when combined with autogenous bone; however, the effects of PRP were lost in the autogenous bone group after four weeks as detected by microradiographic assessment of

bone mineralization. Further, PRP did not appreciably affect bone regeneration when combined with commercially available biomaterials (Cerasorb®, β-tricalcium phosphate; Bio-Oss®, bovine sponginous bone block; or Colloss®, bovine collagen sponge) (96). The authors speculated that the short-lived mitogenic effects of PRP were likely responsible for the decrease in PRP response over time (96). Bone formation around laminar titanium implants in Wistar rats benefited from the application of PRP compared to untreated implants (97). PRP added to polycaprolactone-20% tricalcium phosphate composites fitted with titanium implants accelerated bone regeneration and increased bone volume at 6 and 9 months in mandibular defects of mongrel dogs (98). Interestingly, when PRP was combined with mesenchymal stem cells on fluorohydroxyapatite (FHA) scaffolds, bone formation in premolar extraction sites in mini-pigs was greater than FHA-treated sites or sites treated with autogenous bone after three months (99). Although a FHA-MSC group was not included as a means of comparison, the authors attributed the results of the FHA-MSC-PRP group to the ability of PRP to enhance MSC proliferation, thereby increasing the pool of progenitor cells capable of differentiating into osteoblasts (99). These findings suggest that the effect of PRP on mesenchymal stem cells, the host microenvironment, and its interaction with specific biomaterials may be important for bone formation in certain models.

Mesenchymal Stem Cells as a Model System for Studying Bone Formation Potential

Remodeling processes in the adult human that regenerate and repair damaged tissue require a constant supply of new cells, either local or circulating, that have retained the capacity to proliferate and differentiate into terminal lineages of many types (5).

Human bone marrow contains hematopoietic stem cells that provide eight distinct lineages comprising the hematopoietic system as well as stromal stem cells (i.e., mesenchymal stem cells, MSCs) (5). Mesenchymal stem cells can also originate from the periosteum and limited sources have been identified in muscle, fat, and synovium (4). Mesenchymal stem cells are a pluripotent population that can give rise to fibroblasts, osteoblasts, chondrocytes, tenocytes, myoblasts, and adipocytes (4). Mesenchymal stem cell differentiation into osteoblastic, chondroblastic, or fibroblastic lineages is directed by the local environment, including specific cytokines and cell-cell or cell-matrix interactions (5, 6). Osteoprogenitor cells derived from MSCs, are responsible for the expansion of osteoblast numbers via a transition through a pre-osteoblast stage whereby they become mature osteoblasts (6) (Fig. 6).

Figure 6. Transition of Mesenchymal Stem Cells into Mature Osteoblasts

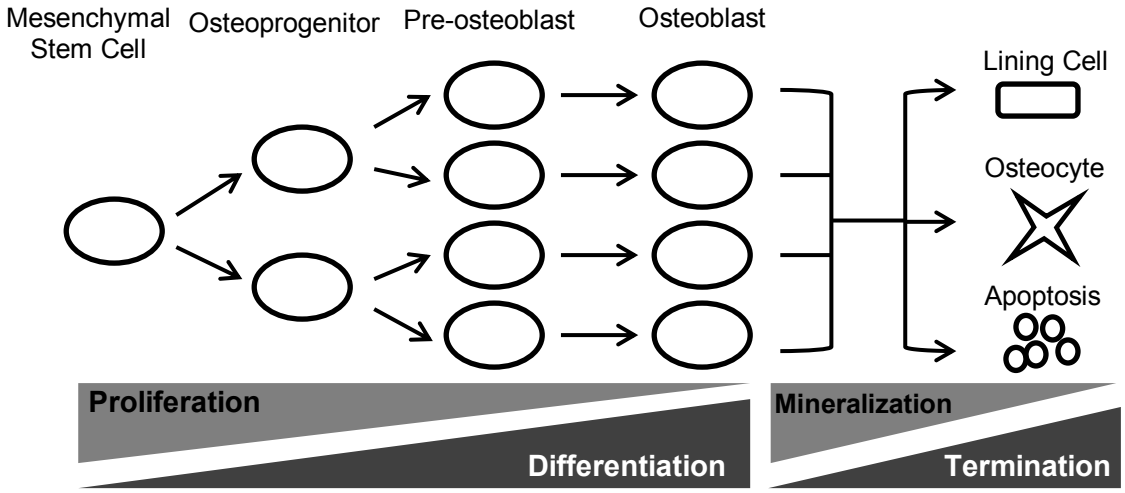

Figure 6. In the early stages of differentiation, mesenchymal stem cells proliferate into osteoprogenitor cells and pre-osteoblasts. Proliferation slows in latter stages of differentiation as pre-osteoblasts become mature osteoblasts. Following synthesis and mineralization of the bone matrix, osteoblasts are subject to one of three fates: lining cells, osteocytes, or apoptosis. Figure created by William P. Clafshenkel.

Mesenchymal stem cell number and activity is greatest in metaphyseal bone and areas of thick and vascular periosteum (e.g., long bones like the femur), which contributes to more robust healing at these locations (4). Although MSCs are still found in the bone marrow of older individuals, their numbers do decline with age (5) and osteoporosis (6), as does their potential for osteoblastic differentiation (100, 101). It is theorized that this reduction in the ability of MSCs to replace needed osteoblasts in the aged individual underlies the pathogenesis of osteoporosis (102).

Three criteria to identify MSCs have been proposed by the Mesenchymal and Tissue Stem Cell Committee of the International Society for Cellular Therapy including (1) the plastic adherence of isolated cells in culture, (2) the positive surface expression of CD105, CD73, and CD90, (3) the lack of surface expression of CD34, CD45, CD14 or CD11b, CD79a or CD19, and HLA-DR (100). MSCs can secrete a variety of angiogenic,

anti-apoptotic, and mitogenic factors such as vascular endothelial cell growth factor (VEGF), hepatocyte growth factor (HGF), angiopoietin-1, and insulin-like growth factor-1 (IGF-1) (100). Mesenchymal stem cells can reproducibly be induced into an osteoblastic lineage *in vitro*; however, this requires that they be exposed to optimal concentrations of dexamethasone, ascorbic acid, and β-glycerophosphate (103). Mesenchymal stem cells cultured under these conditions assume a cuboid morphology, have enhanced alkaline phosphatase activity, express osteoblastic cell surface antigens, modulate the synthesis of bone-forming genes, and produce mineralized nodules within 16 days (103). The average number of population doublings in cultured MSCs decreases with continued passaging; however, their osteogenic potential is conserved (103). Additionally, cryopreservation techniques do not affect the proliferation, differentiation, or osteogenic activity of cultured MSCs (103). It has been suggested that "young" MSCs (less than 10 passages) and more frequent media changes produce the best growth rates (103). Mesenchymal stem cells respond robustly to melatonin. Melatonin, via MT_2 melatonin receptors, increases the differentiation of MSCs into osteoblasts as shown by an increase in alkaline phosphatase activity and an increase in calcium deposition in culture (68). Additional work indicates that melatonin may regulate MSC differentiation and mineralization by inducing the expression of specific bone markers (68).

Statement of Problem & Study Objective

The treatment of bone loss, whether great or small, continues to be at the forefront of scientific research. The practice of tissue engineering combines several disciplines in an attempt to restore, rebuild, or replace pathological or traumatic bone loss. The costs

associated with treating bone loss continue to rise as more of the population reaches an elderly age. Complications with traditional methods of bone grafting or the utilization of commercially available bone substitutes warrants further research on biomaterials capable of replicating native bone tissue. To achieve this, unique biomaterials are being developed for the guided delivery of agents that stimulate the normal bone repair and restoration processes.

In this study, the biomaterial calcium aluminate (CA) was used to create synthetic scaffolds with the potential to deliver biomolecules, like melatonin, to bone defect sites through surface chemistry. Indeed, peptide attachment to the calcium aluminate surface can be accomplished through simple linker chemistry (50). Additionally, calcium aluminate meets many of the criteria for an ideal synthetic bone substitute including low toxicity and high mechanical strength (48, 104). Two therapeutic strategies were investigated in the current study, (1) the local delivery of melatonin by chemical attachment to the surface of the calcium aluminate scaffold and (2) the topical application of PRP at the bone defect site in conjunction with the developed scaffolds. Given the extensive effects of melatonin and PRP on bone formation and the characteristics of calcium aluminate as a synthetic bone substitute, it was hypothesized that the cooperative interaction between melatonin, PRP, and calcium aluminate would be a novel therapy to facilitate bone regeneration in a model of calvaria defects.

Hypothesis

Melatonin and/or platelet-rich plasma will provide osteoinductive properties to calcium aluminate scaffolds to enhance local bone regeneration.

Specific Aims

1. Assess the effects of unmodified (CA) and modified (CA-Melatonin) scaffolds on human adult mesenchymal stem cell (hAMSC) differentiation and morphology in the presence or absence of PRP.
2. Assess the effects of unmodified (CA) and modified (CA-Melatonin) scaffolds on bone formation and remodeling activity in the presence or absence of PRP in a rodent model of calvarial defects.

METHODS

1 Synthesis of Modified and Unmodified Calcium Aluminate Scaffolds

1.1 Casting Calcium Aluminate

Calcium aluminate disks were prepared as previously described (50) by a room temperature cast of different sized CA aggregates. Fifty percent -325 and 25 percent each of -30 + 60 and -60 sized aggregates were combined to form the CA scaffold. This mixture was chosen because of its durability and optimal pore size. The number -30 +60 means that the cement was passed through the mesh screen with 30 squares per inch and caught on the mesh screen with 60 squares per inch. If there is no + mesh number indicated, the cement was caught on a flat board. The larger the mesh numbers, the smaller the aggregate size (e.g., -325 is a fine powder-like cement). CA is a hydratable material that can be molded and shaped at room temperature for extended periods of time before setting. The CA aggregates were first dry mixed to ensure equal particle distribution. After dry mixing, double-distilled water was added to achieve a cement paste that was allowed to thicken over 20 minutes at room temperature. Upon thickening,

the cement was poured into a mold and allowed to set overnight at room temperature. Unmodified scaffolds were then sterilized by autoclaving at 121°C and 18 psi of steam for 60 minutes with fast exhaust (standard sterilization procedures for dry materials). Modified scaffolds were prepared with melatonin as described (Section 1.2). Seven millimeter diameter disks were used for *in vitro* assays. Six by six by one millimeter square scaffolds were implanted *in vivo*. The creation of unmodified and modified scaffolds for analyses was carried out in Dr. Gawalt's laboratory by Rachelle Palchesko and Jared Romeo.

1.2 Chemical Linkage of Melatonin to the CA Surface

Melatonin was attached to the CA surface (modified scaffold; CA-Mel) via a chemical linker through a two-step solution deposition process (105). This method provided for a prolonged attachment of melatonin to the CA surface versus other weak attachment methods like adsorption. First, the scaffolds were placed in a 2 mM 12-bromododecanoic acid in dry tetrahydrofuran (THF) solution for one hour at room temperature. The scaffolds were removed and placed in a 120°C oven for 24 hours. The scaffolds were then immersed in a 1 mg/mL solution of melatonin in methanol with 1% pyridine at 4°C for 24 hours and dried under vacuum for an additional 24 hours. A Thermo Nicolet Nexus 470 FT-IR Spectrophotometer equipped with diffuse reflectance was used to obtain the IR spectra of the substrates after each deposition step to confirm the attachment of melatonin to the CA surface. Modified scaffolds were then sterilized by autoclaving at 121°C and 18 psi of steam for 60 minutes with fast exhaust. Separate

diffuse reflectance infrared Fourier transform (DRIFT) spectroscopy analysis was used to confirm the attachment of melatonin after sterilization.

2 Cell Culturing & Cell-based Assessments

Culturing experiments for viability assessments (Section 2.1) were set up as follows: NIH 3T3 fibroblasts (from Swiss albino mice, Cat# CCL-92; ATCC, Manassas, VA) were cultured on unmodified or modified scaffolds at an initial seeding density of 10,000 cells/mL in DMEM plus 10% FBS in 48-well plates. Normal human osteoblasts (Nhost; Cat# CC-2538; Lonza, Walkersville, MD) were cultured on unmodified or modified scaffolds at an initial seeding density of 10,000 cells/mL in OGM medium in 48-well plates. Cells were incubated under 90% humidity at 37^{o}C and 5% CO_2.

For differentiation and morphology experiments (Section 2.2 and 2.3), multipotent human adult mesenchymal stem cells (hAMSCs; Cat# PT-2501; Lonza, Walkersville, MD) were cultured on unmodified or modified scaffolds at an initial seeding density of 20,000 hAMSCs/mL in chemically-defined basal medium (OS-; Lonza, Walkersville, MD) in 48-well plates. Human adult mesenchymal stem cells utilized in this study were collected from human bone marrow withdrawn from the posterior iliac crest of normal volunteers (106). The hAMSCs have been flow sorted by testing for the following antigens: CD105+, CD166+, CD29+, CD44+, CD14-, CD34-, and CD45- (106). Cells between 3-4 passages were used. After 24 hours, waste media was removed and the seeded scaffolds were transferred to individual wells of a sterile 24-well plate. Fresh osteogenic medium (OS+) was then added to each well. Waste media was replaced every 3 days up to 7 or 14 days. These time points have been shown to be

specific to heightened hAMSCs differentiation and alkaline phosphatase activity and occur before significant mineralization (67, 68, 103). Osteogenic medium was prepared by supplementing chemically-defined basal medium with 0.1 μM dexamethasone, 10 mM β-glycerophosphate, and 0.3 mM ascorbic acid. This medium is required to induce hAMSC differentiation towards an osteoblast phenotype (67, 68, 103). Ascorbic acid acts as a cofactor in the hydroxylation of proline and lysine residues for collagen formation and increases the synthesis of non-collagenous bone matrix proteins (107). The glycerophosphate is rapidly degraded to inorganic phosphate by alkaline phosphatase enzyme activity, whereby the inorganic phosphate is free to combine with calcium to form mineralized nodules (107). Glucocorticoids like dexamethasone are essential for the induction of osteoblast differentiation and production of a mineralized matrix (108). Dexamethasone reliably stimulates the development of many of the phenotypic features of human osteoblasts (109). Differentiation and matrix formation are regulated by the binding of dexamethasone to the glucocorticoid receptor-α (GRα), which in turn, modulates gene expression of osteocalcin, collagenIα1, and transforming growth factor-β1 via GC responsive elements (108). Cells were incubated under 90% humidity at 37^{o}C and 5% CO_2.

2.1 Live/Dead Assay

After 1, 4, and 7 days, the viability of the NIH 3T3 and Nhost cells on unmodified and modified scaffolds was determined using a Live/Dead® Viability/Cytotoxicity Assay Kit (Molecular Probes, Invitrogen, Carlsbad, CA). After removing waste media and washing twice with 1x PBS, cells were stained with a 2 μM calcein AM and 4 μM

ethidium homodimer (EthD-1) at 37°C for 30 minutes. Live cells are distinguished by the enzymatic conversion of the nonfluorescent cell-permeant calcein AM to intensely fluorescent calcein by ubiquitous intracellular esterase activity. Calcein has an excitation wavelength of 485 ± 10 nm and produces green fluorescence in live cells. Dead cells with damaged membranes allow the passage of EthD-1 into the nuclear compartment where it binds to nucleic acids. Binding to nucleic acids enhances EthD-1 fluorescence 40-fold. EthD-1 has an excitation wavelength of 530 ± 12.5 nm and produces red fluorescence in dead cells. Background fluorescence with this technique is minimal because both probes are virtually nonfluorescent before interacting with cells. Samples were viewed using a Zeiss Axioskop 2 under 10x magnification and five images per sample with an area of 0.6 mm^2 were taken using a Zeiss Axiocam. The number of live and dead cells per view was counted using Axiovision 4 software. The assessment of NIH3T3 fibroblast and normal human osteoblast adhesion and viability on calcium aluminate surfaces was carried out in Dr. Gawalt's laboratory by Rachelle Palchesko and Jared Romeo.

2.2 Preparation and Application of Platelet-Rich Plasma for *In Vitro* Studies

Platelet-rich plasma utilized for *in vitro* experiments was obtained from a human female subject with approval from the Duquesne University Institutional Review Board. Approximately 4 mL of blood was collected in a 4.5 mL BD Vacutainer™ tube containing 0.45 mL of the anticoagulant trisodium citrate (9:1) to prevent clotting (BD, Franklin Lakes, NJ). The whole blood was centrifuged and the PRP layer was collected as described in Section 3.3. The hAMSCs were plated and cultured as described in

Section 2 with the following modifications. Unmodified and modified CA scaffolds were seeded with hAMSCs in basal medium in 24-well plates. Twenty-four hours after initial seeding, waste medium was removed and hAMSCs were exposed to basal medium containing PRP. The harvested PRP (approximately 375 µL) was thoroughly mixed with 15 – 20 mL of warm, sterile basal medium before dispensing approximately 1 mL into each well. After 24 hours, waste media and clotted PRP were removed. The seeded scaffolds were washed twice with sterile 1x DPBS and then covered with osteogenic medium. Waste media was replaced every 3 days up to 7 or 14 days. As described in later sections, given the difficulties associated with these experiments and based on the in vivo results of PRP-treated groups, this arm of the *in vitro* aim was no longer pursued. Nonetheless, modifications to the experimental protocol will be addressed in future studies.

2.3 Alkaline Phosphatase Assay

Alkaline phosphatase activity was qualitatively assessed as a marker of osteoblast differentiation and activity (Alkaline Phosphatase Kit, Cat# 85L3R, Sigma-Aldrich, Inc., St Louis, MO). Human adult mesenchymal stem cells were cultured as described for 7 or 14 days. At each end point, scaffolds were washed twice with 1x PBS, then fixed for one minute with a 20% citrate/80% methanol solution. Scaffolds were washed twice with 1x PBS after fixing. Staining was completed with a diazonium salt/naphthol AS-MX phosphate alkaline solution. As a result of alkaline phosphatase activity, the substrate naphthol AS-MX phosphate is hydrolyzed to naphthol AS-MX, which immediately couples with the diazonium salt forming an insoluble, visible red pigment at sites of

phosphatase activity. A greater intensity of red staining indicates greater ALP activity. After 30-45 minutes of incubation at 37^{o}C, digital images were captured on a Nikon Steroscopic Zoom dissecting microscope equipped with an Olympus DP70 microscope digital camera. Scale bars were inserted digitally using NIH Image J.

2.4 Qualitative Alizarin Red S Staining

Calcium deposition occurs as bone matrix secreted from osteoblasts becomes mineralized and is a definitive sign of osteoblast differentiation and activity (1). In culture, mineralization by differentiated hAMSCs takes place between 14 and 21 days (68). Alizarin Red S, an anthraquinone derivative, chelates calcium ions in biological tissues and was used as a qualitative indicator of calcium deposition by hAMSCs on unmodified and modified CA surfaces. The hAMSCs were cultured as described above for 21 days in osteogenic media. For analysis, waste media was removed and scaffolds were fixed with 10% buffered formalin for 30 minutes at room temperature. The fixative was removed and replaced by 2% Alizarin Red S solution (pH 4.2; Sigma-Aldrich, Inc., St Louis, MO). After 10 minutes of incubation at room temperature, the stain was removed and the scaffolds were washed twice with nanopure water. Digital images were captured on a Nikon Steroscopic Zoom dissecting microscope equipped with an Olympus DP70 microscope digital camera. It should be noted that the nonspecific binding of Alizarin Red S to calcium made it difficult to distinguish calcium that had been deposited as a result of hAMSC mineralization activity from the calcium component of the CA scaffolds. In the future, fluorescent probes that specifically bind to the hydroxyapatite component of mineralized nodules, rather than calcium ions, will be used to circumvent

this issue. For the current study, ALP assays were used as an indication of mature osteoblasts activity.

2.5 Scanning Electron Microscopy

For scanning electron microscopy, hAMSCs were cultured as described. At the 7 and 14 day end points, scaffold were processed by a modified protocol (110). Briefly, media was removed and the seeded scaffolds were fixed in 2 % formaldehyde in 0.2 M phosphate buffer (pH 7.4) for 5 days at 4^{o}C. Individual scaffolds were then removed from the fixative, washed twice with 1x PBS, and immersed in 0.5 mL of 2 % osmium tetroxide (OsO_4; Sigma-Aldrich, Inc., St Louis, MO) for 1 hour at room temperature with gentle rocking. After 1 hour, the OsO_4 was removed and samples were washed 3 times with 1x PBS before being dehydrated through a graded ethanol series (in order: 25%, 50%, 70%, 95%, 100%). Following dehydration, scaffolds were transferred to hexamethyldisalizane (Sigma-Aldrich, Inc., St Louis, MO) for 10 minutes. Scaffolds were placed in clean glass scintillation vials and stored in a dessicator until imaging. Imaging was completed on a Hitachi S-3400N-II Variable Pressure scanning electron microscope under vacuum using Hitachi S-3400N software. Scale bars were inserted digitally using NIH Image J.

3 Calvarial Defect Model & Implantation

3.1 Pre-Surgical Preparation

Thirty three two-month-old ovariectomized female Sprague-Dawley rats (250-300 g; Hilltop Lab Animals Inc., Scottsdale, PA) were randomized and implanted with one of four scaffold types: calcium aluminate alone (CA; unmodified) or CA with chemically attached melatonin (modified; CA-Mel) in the absence or presence (CA + PRP, CA-Mel + PRP) of PRP. Animals were ovariectomized prior to transport to the Duquesne University Animal Facility and approximately 3 weeks prior to surgery to ensure estrogen levels had time to subside and create an imbalance in bone remodeling activity similar to a post-menopausal population (111). Estrogen has inherent effects on the bone remodeling process (112) and was thus considered a confounding variable for bone regeneration in this model. An ovariectomized model system is commonly used in research studies when mimicking post-menopausal bone loss is desired. Cancellous bone in the proximal tibia is progressively lost, being evident at two weeks and unequivocal at one month following ovariectomy (111). All surgical procedures were in accordance with Duquesne University IACUC Guidelines. Animals were anesthetized with sodium pentobarbital (10 mg/kg, IP; Nembutal®/Pentobarbital Sodium Injection USP, Butler Schein Animal Health, Dublin, OH) twenty minutes prior to the procedure and given 3% isoflurane by nosepiece to maintain anesthesia if necessary. The incision site was shaved and disinfected with iodopovidone solution. A full-thickness flap was initiated with a 1.2 cm incision through the skin and subcutaneous fascia at the most superior aspect of the frontal bone 3 to 4 mm posterior to the junction of the nasal and frontal bone and running posterior to the parietal bone. The periosteum was reflected bilaterally with

blunt dissection to expose the cranial bone. Calvarial defects were created in the exposed cranial bone as described below (Section 3.2).

3.2 Piezotome Surgical Protocol for Calvaria Osteotomy

Rodent models of critical-size calvarial bone defects have been widely used to study approaches designed to regenerate bone (13). In the current study, critical-size defects (6-mm x 6-mm) were created in the calvarial bone of ovariectomized Sprague-Dawley rats. This defect size will not heal spontaneously over the lifetime of the animal (13, 113). As larger rodents compared to mice, rats were chosen to improve the technical ease of generating cranial bone defects. Given the relatively sparse bone remodeling that occurs in calvarial bone (114), this site provides a suitable challenge to investigating the osteoconductive and osteoinductive nature of the designed therapies. While the defect size chosen was small enough to create two defects per animal, laterally performed craniotomies may impair local regeneration due to the close vicinity of adjacent defects (13). Thus, only a single defect was created in the skull of each animal.

Using a #4 round diamond bur in a slow speed electric handpiece, a 6-mm x 6-mm outline was made in the superior aspect of the frontal bone under constant irrigation with saline. Once the outline was thinned with the diamond bur, the final cuts were made with an ultrasonic Piezotome™ handpiece. The Piezotome™ allowed for cutting of the calvarial bone without affecting the underlying cerebral hemispheres or meninges. This methodology significantly reduced the risk of defect site morbidity and animal mortality in experimental groups while allowing for an easily reproducible defect. Likewise, in comparison studies with other available ultrasonic devices, the Piezotome™ has

demonstrated significantly better cutting performance and produced the smallest increase in operating temperature at the osseous surface (115). Care was taken not to damage the middle cerebral artery, superior cerebral veins, inferior cerebellar vein, and the superior sagittal sinus. Upon removal of the bone, an unmodified or modified calcium aluminate scaffold was placed into the osteotomy site. For groups receiving PRP, the scaffold was first covered with a few drops of the collected PRP in a sterile dish and the remainder of the PRP was added to the superior surface of the bone defect after placement of the implant. Incision closure was achieved with 3 surgical stables, as the dura and overlaying skin provide adequate support for implanted materials without the need for internal or external fixation (13).

Figure 7. Creation of Calvarial Bone Defects in Cadaver Rat Skull with Piezotome

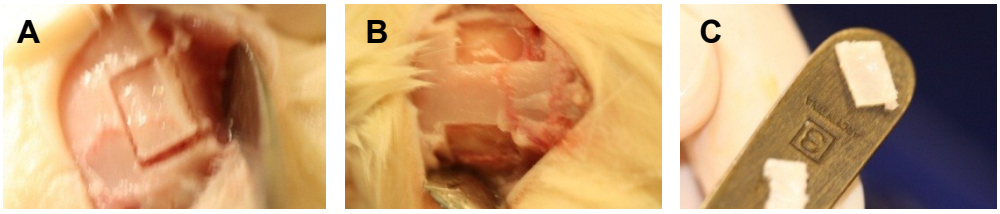

Figure 7. Creation of calvarial defects in cadaver rat skull using Piezotome. (*A*) The calvarial bone defect in skull is outlined using the Piezotome handpiece. (*B*) Double calvarial bone defect in cadaver rat skull with defect bone removed. Notice the meninges and soft tissue are intact and without damage. (*C*) Pieces of calvarial bone removed from the created defects. In the current study, only one defect was made in the calvarial bone per animal.

3.3 Preparation and Application of Platelet-Rich Plasma for *In Vivo* Studies

There are several commercially available products that mimic PRP and several different preparation techniques (116); however, this study utilized autologous PRP that was prepared with a relatively simple method to reduce platelet aggregation and optimize growth factor concentrations (85). Moreover, this preparation technique has been used previously to decrease the incidence of alveolar osteitis and enhance bone formation in

tooth extraction sites (93, 117). Platelet-rich plasma was prepared using blood collected from age-matched ovariectomized female Sprague-Dawley rats. Donor rats were deeply anesthetized with sodium pentobarbital (100 mg/kg, IP; Nembutal®/Pentobarbital Sodium Injection USP, Butler Schein Animal Health, Dublin, OH) until all withdrawal reflexes were absent. A 3 – 5 cm incision was made through the ventral body wall into the abdominal cavity starting from just below the diaphragm. After retraction of the skin layers and exposure of the abdominal aorta, a 21-gauge 1.5 inch latex-free needle affixed to a needle adapter was inserted in the direction of the heart. Approximately 4 mL of blood was collected in a 4.5 mL BD Vacutainer™ tube containing 0.45 mL of the anticoagulant trisodium citrate (9:1) to prevent clotting (BD, Franklin Lakes, NJ). Anticoagulant collection is necessary to prevent platelet degranulation and the release of vital growth factors. Trisodium citrate is used to bind free calcium ions in the blood to prevent coagulation (82). Micromolar concentrations of calcium and other activators including von Willebrand factor, collagen, and substances released from the platelets acting in autocrine or paracrine feedback loops will activate the PRP in the defect environment after application (118). The tubes were spun for 10 minutes in a room temperature table top centrifuge set at 1350 x *g*. Centrifugation times were based on previous studies which show a greater than 6-fold increase in platelet concentration after 10 minutes of centrifugation (85). The centrifugation speed of 1350 *g* is sufficient to create a buffy coat containing leukocytes, thus producing a leukocyte-rich preparation (85). The leukocytes concentrated by this method are vital to reductions in infection. For example, when PRP prepared by this method (i.e., containing the buffy coat) was applied to soft tissue wounds of 14 patients, it lead to a fewer number infections and shortened

their hospital stay (90). After centrifugation, the tubes were removed and allowed to set upright for 3minutes. Platelet-poor plasma was removed down to the top of the PRP level using a sterile syringe with a 21-gauge 1.5 inch latex-free needle. A separate, identically prepared syringe was used to aspirate approximately 375 µL of PRP. The prepared PRP was immediately applied to the surgical site and implant, as this is the most beneficial for growth factor concentration and platelet morphology (85).

3.4 Post-Surgical Follow-up

Antibiotic ointment was applied along the incision line immediately following surgery. Post-surgical recovery included a subcutaneous 3 mL saline bolus for fluid resuscitation and supplemental oxygen until the rats were responsive and able to exhibit righting reflex. Rats were housed individually in soft-bedded plastic cages with free access to food and water. Rats received a subcutaneous injection of Ketoprofen (10 mg/kg, SC; Butler Schein Animal Health, Dublin, OH) for analgesia, which was repeated as necessary every 12 hours for pain management. Follow-up inspections of the surgical site and records of body weight were continued on a regular basis until necropsy.

3.5 Double-Fluorochrome Labeling

Differences in bone remodeling between groups was assessed using a double-fluorochrome injection series. Bone remodeling is a process that involves organic matrix synthesis and mineralization of the organic material via osteoblast activity. The labeling technique utilized in this study is a relatively simple method which takes advantage of fluorescent bone markers (tetracycline antibiotic and calcein solution) to label and

demarcate the zone of osteoid tissue (unmineralized matrix) from mineralized bone. Fluorochromes like tetracycline and calcein are deposited in areas of the skeleton where new bone matrix is being synthesized and their deposition is consistent with the pattern of calcium deposition (119). Further, it has been suggested that the specific binding of fluorochromes to newly mineralized surfaces is due to the smaller size of the apatite crystals formed during the early stages of mineralization, compared with older mineralizing sites (13). Tetracycline antibiotic (Bio-Mycin 200/Oxytetracycline, Butler Schein Animal Health, Dublin, OH) and calcein (Sigma-Aldrich, Inc., St Louis, MO) solutions were prepared in sterile 0.9% saline. Tetracylcine (20 mg/kg, SC) was administered 10 days prior to necropsy. Calcein (20 mg/kg, SC) was administered 7 days after tetracycline and three days prior to necropsy. Animals were lightly sedated with 3% isoflurane and the skin on the back of the neck was tented. Injections were steadily administered with a 21-gauge 1.5 latex-free needle inserted into the skin fold. Rats were returned to their cage after injections and monitored until full recovery.

3.6 Animal Necropsy and Cranium Harvesting

Three rats per group were sacrificed at 3 months and 4-5 rats per group were sacrificed at 6 months for fluorescence, radiological, and histological assessments. These time points are consistent with the normal duration of bone remodeling in humans (1). At necropsy, all animals were euthanized according to Duquesne University IACUC protocols. Animals were first deeply sedated with 4 – 5% isoflurane. After the absence of reflexes was verified, the animals were placed securely in the decapitation apparatus and the head removed completely. Whole heads were immediately transferred to ice-cold

10% buffered formalin and stored at 4°C for 48 hours. After fixation, skin and muscle tissue were carefully trimmed and removed from the cranium. The skulls were cut transversely into superior and inferior halves and the brain carefully removed. The superior skull bone was stored in 70% ethanol until further processing could be completed.

4. Radiography and Histology

4.1 Radiograph Imaging and Processing

Prior to sectioning, superior aspect radiographs were taken of each skull to document radiographic density at the defect site. Radiographs of defect areas are routinely used to assess bone repair and the quality of bone that fills the defect site (13). Radiographs were digitally equilibrated to reduce variability between backgrounds (X-Ray Copy Service, North Huntington, PA). Radiographic intensity was quantified from the superior aspect of the implant surface and normalized to background intensity using NIH Image J software. Radiographs were quantified as follows:

1. Open image in NIH Image J
2. Image > Type > 16 bit
3. Analyze > Set Scale > 100 pixels = 1 arbitrary unit (AU)
4. Analyze > Set Measurement > Check: Integrated Density
5. Using the box tool, create a box size 0.5 x 0.5 AU over film background
6. Analyze > Measure (This value is background intensity)
7. Move the same box over the center of the scaffold using the arrow keys
8. Analyze > Measure (This value is the scaffold intensity)

9. For normalization, scaffold intensity was divided by the background intensity

4.2 General Histology and Fluorescence Microscopy

Sectioning, staining, and digital photographs of 3 month histology and 3 and 6 month fluorescence were completed at the Center of Metabolic Bone Disease, University of Alabama (P.F.L.). The area of interest, defined as a coronal section approximately centered inside the defect site, was brought to the surface through preliminary grinding. Afterwards, samples were cut to 100 μm (Exakt Diamond Saw, Exakt Technologies Inc., Oklahoma City, OK) and then ground to 20-30 μm sections (Exakt Grinding System, Exakt Technologies Inc., Oklahoma, OK). Ground sections were either stained for histology or left unstained for fluorescence microscopy. Stained sections were treated with a dibasic stain of 0.03 M methylene blue/ 0.018 M basic fuchsin to highlight cellular proteins (e.g., bone, collagen, and connective tissue) and DNA. This method is reported to provide vivid contrast between the cellular and connective tissue elements in tissue sections with results similar to a hematoxylin-and-eosin procedure (120). Methylene blue is a basic stain (i.e., positively charged) used to highlight the cell nucleus because it is attracted to the negative charge of nucleic acid chains (e.g., phosphate backbone in DNA). Unlike ethidium bromide, it is safer and will not intercalate into the DNA strand. Basic fuchsin is also a basic dye with a positive charge that is applied after excess methylene blue is washed away. Connective tissues, specifically collagen, are highlighted blue-purple, while cell cytoplasm develops a pink-to-purple coloration (120, 121). Digital images of stained 3 month histology and unstained 3 and 6 month

fluorescence were captured with an Olympus BX51 microscope equipped with a Q-Imaging camera with an Olympus MWBV2 Wideband Blue wavelength filter. Multiple digital photographs of stained and unstained sections were spliced together to create a montage of the complete skull section using Bioquant Image Analysis software. Digital images of stained 6 month histology were captured on an Olympus BX40 microscope using an Olympus DP70 camera and DP Controller software. This imaging was completed at Duquesne University and the images were not spliced together to create montages. Quantification of fluorescence within and surrounding the scaffold was completed using NIH Image J software as follows:

% Fluorescence and Number of Fluorescent Regions

1. Open image to be analyzed in NIH Image J
2. Process > Subtract background > Set pixels to 50.0 (default)
3. Image > Brightness/Contrast > Auto
4. Image > Color > Split Channels (Close all channels except for Green Channel)
5. Image > Adjust > Threshold > Check Dark Background
6. Set threshold to overlap actual fluorescence as closely as possible (red coloration)
7. Process > Smooth
8. Highlight around scaffold with Box tool
9. Analyze > Set Measurements > Check: Area, Area Fraction, Limit to Threshold, Display Label > OK (% Fluorescence)

10. Analyze > Analyze Particles > Check: Pixel Units and Summary; Size: 0-infinity; Show: Outlines > OK (No. of Fluorescent Regions)

Fluorescent Intensity

1. Follow above protocol to Process > Smooth
2. Highlight around scaffold with Box tool
3. Analyze > Set Measurements > Check: Integrated Density > OK
4. Analyze > Measure

5. Statistics

The statistical interaction between group means for each time point and treatment group was analyzed by a two-way ANOVA. The two-way ANOVA helps to determine if several population means are statistically different when evaluating two independent variables (e.g., treatment and time). A Bonferroni method was chosen for the *post-hoc* test given its fairly powerful nature and the planned (a priori) comparison of pairs of experimental groups. The effect of treatment groups at individual time points (i.e., main effect) was analyzed by a one-way ANOVA with a Bonferroni *post-hoc* test. Analyses were performed using GraphPad Prism 5.0® software. A p-value of less than 0.05 was considered significant.

RESULTS

Preliminary Data

The following data was collected by Rachelle Palchesko and Jared Romeo of Dr. Galwalt's laboratory. Analytical assessments were conducted to verify the reproducibility and accuracy of the chemical attachment of melatonin to the CA surface (Fig 8*A*). Calcium aluminates modified with a chemical linkage to the melatonin molecule were analyzed using Diffuse Reflectance Infrared Fourier Transform (DRIFT) spectroscopy. DRIFT analysis indicates that both 12-bromododecanoic acid (linker) and melatonin were attached in consecutive steps to the CA surface (Figs 8*B* and 8*C*, respectively). Functionality of this linkage was determined through other assessments.

Figure 8. Chemical Linkage of Melatonin to the Calcium Aluminate Surface is Accomplished Using Simple Linker Chemistry

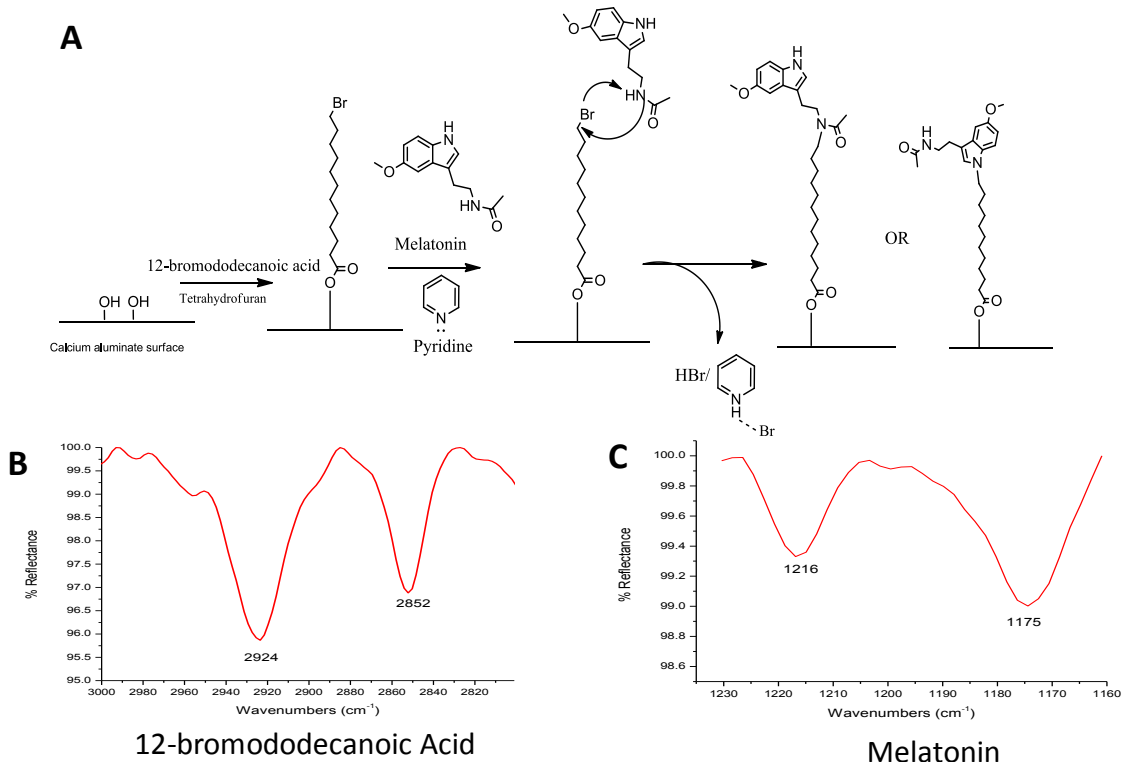

Figure. 8. Synthesis and confirmation of melatonin linkage on calcium aluminate surface. (*A*) Melatonin is attached to the calcium aluminate surface through a two-step deposition process using 2mM 12-bromododecanoic acid and 1 mg/mL melatonin/1% pyridine solutions. (*B*) Diffuse Reflectance Infrared Fourier Transform (DRIFT) spectroscopy produced peaks at 2918 cm^{-1} and 2850 cm^{-1} confirming the attachment of bromododecanoic acid to the calcium aluminate surface. (*C*) DRIFT spectroscopy produced peaks at 1215cm^{-1} and 1175cm^{-1} confirming the attachment of melatonin to the calcium aluminate surface.

Preliminary experiments were conducted *in vitro* to determine the viability of normal human osteoblasts (Nhosts) and NIH 3T3 fibroblasts on unmodified (CA) and modified (CA-Mel) scaffolds. The determination of cell viability by live/dead assay was conducted at day 1, 4, and 7 in culture (Fig. 9*A*). The number of viable fibroblasts was significantly reduced on CA-Mel scaffolds on days 4 and 7 ($p < 0.001$, Fig. 9*C*, *D*) suggesting that the presence of surface melatonin molecules affects fibroblast viability. The number of viable osteoblasts was significantly increased on CA-Mel scaffolds for all time points (Fig. 9*B-D*; $p < 0.001$). Moreover, viable osteoblasts were significantly

greater at all time points when compared to viable fibroblasts on modified scaffolds (Fig. 9*B-D*; $p < 0.001$), with the greatest difference at day 7 (Fig. 9*D*; $p < 0.001$). These findings suggest a preference of normal human osteoblasts for viability on the scaffolds where melatonin had been attached. Further, viability of osteoblasts on both scaffold types supports the biocompatibility of calcium aluminate with this mature cell type.

Figure 9. Normal Human Osteoblast and NIH 3T3 Fibroblast Viability is Differentially Affected by CA Scaffold Surface

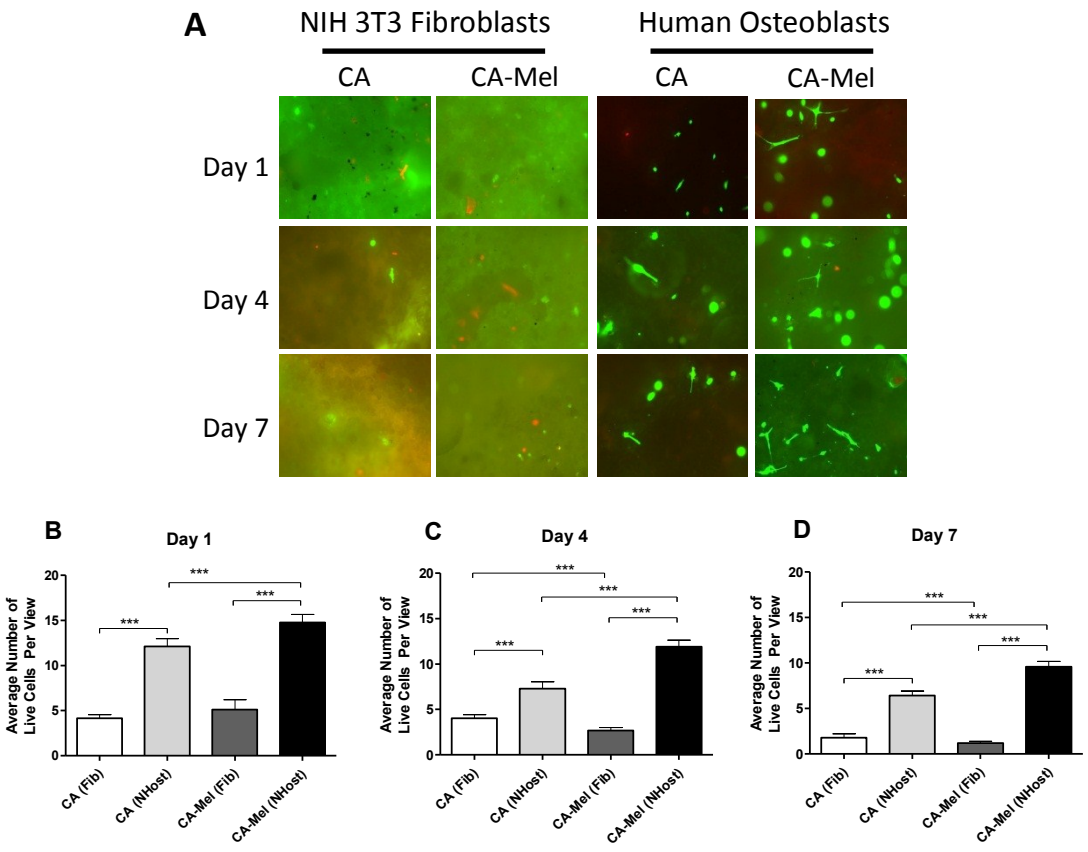

Figure 9. Calcium aluminate scaffolds functionalized with melatonin demonstrate a preference for normal human osteoblast adherence and proliferation over 7 days in culture when compared to unmodified (CA) and modified (CA-Mel) scaffolds seeded with NIH 3T3 fibroblasts and unmodified scaffolds seeded with normal human osteoblasts. (*A*) Cell viability on scaffold surfaces was assessed by live/dead fluorescence at the time points indicated and representative photos are shown. Green fluorescence indicates live cells, red fluorescence indicates dead cells. Magnification = 10x. (*B-D*) Live cells were averaged from 5 separate fields of view for each scaffold type at 1, 4, and 7 days in culture. Unmodified and modified CA surfaces demonstrate a preference for Nhost versus NIH 3T3 fibroblast viability at all time points ($p < 0.001$) with the greatest preference seen on surfaces modified with melatonin ($p < 0.001$ for all time points). Modified scaffolds significantly reduce NIH 3T3 fibroblast viability over unmodified scaffolds at days 4 and 7 (*C* and *D*, respectively; $p < 0.001$ for both). Viability of NIH 3T3 fibroblasts on unmodified or modified CA surfaces is not significantly different on day 1 *(B)*. Group averages were statistically analyzed using a One-way ANOVA with a Bonferroni *post-hoc* test. n = 9 scaffolds per group for each time point. Photographs and quantified data courtesy of Rachelle Palchesko and Jared Romeo.

Specific Aim One

Assess the effects of unmodified (CA) and modified (CA-Melatonin) scaffolds on human adult mesenchymal stem cell (hAMSC) differentiation and morphology in the presence and absence of PRP.

The ability of unmodified and modified scaffolds to induce osteogenic differentiation of hAMSCs was examined at 7 and 14 days by assessing alkaline phosphatase activity, a known marker of osteoblast differentiation and activity, in osteogenic medium (OS+). Osteogenic medium provides as stimulus to hAMSCs that favors differentiation versus proliferation. The exposure of hAMSCs to osteogenic medium slows their proliferation and promotes their differentiation into an osteoblast lineage as exemplified in Fig. 6. These time points have been shown to be specific to heightened hAMSCs differentiation and alkaline phosphatase activity (67, 68, 72). Alkaline phosphatase (ALP) staining after 7 and 14 days in osteogenic medium appears more abundant on unmodified CA scaffolds compared to scaffolds modified with melatonin (Fig. 10*B*). However, the presence of ALP staining in the CA-Mel group suggests melatonin remains functionally active when attached to the CA surface and may delay the differentiation of hAMSCs into an osteoblast lineage. The linkage to the nitrogen in the indole ring leaves both side arms of the molecule free from constraints. As such, the methoxy and N-acetyl groups may freely interact with receptors in hAMSCs to induce their differentiation. Although not fully investigated in this study, the application of specific inhibitors could be considered in the future to determine receptor-dependent activity. Indeed, ALP activity appears to increase with an increased duration of exposure

to melatonin in osteogenic medium (Fig. 10*B*). Interestingly, hAMSCs cultured on the unmodified CA surface underwent differentiation in basal (OS-) medium lacking osteogenic supplements (Fig. 10*A*). This could suggest that the CA material alone has inherent capabilities of stimulating differentiation that may further enhance differentiation over that of modified CA groups when in the presence of osteogenic medium.

Figure 10. Human Adult Mesenchymal Stem Cell Differentiation is Supported on Both Unmodified and Modified CA Surfaces

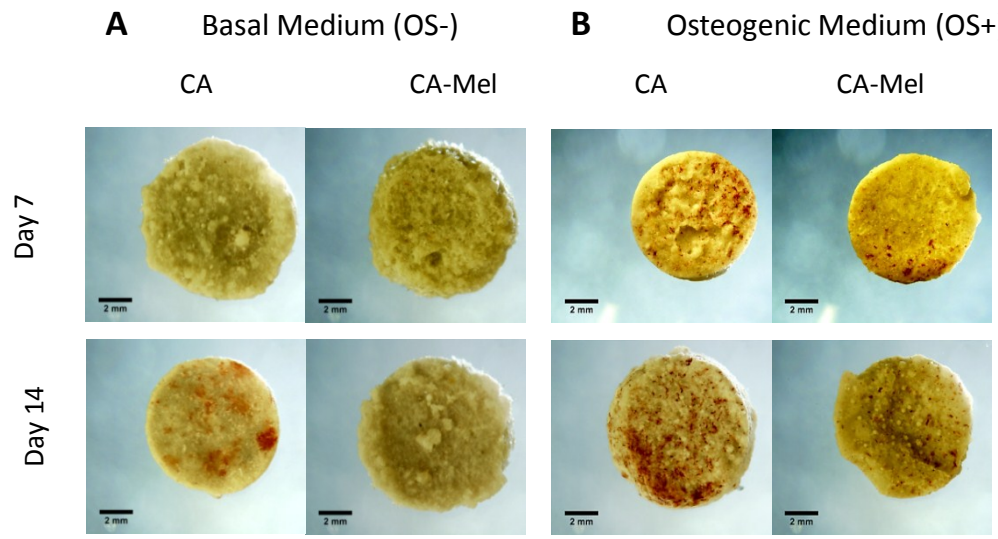

Figure 10. Human adult mesenchymal stem cell differentiation occurs on both unmodified and modified CA surfaces. The effect of CA scaffolds on hAMSC differentiation into osteoblasts was assessed qualitatively by the presence of alkaline phosphatase after 7 and 14 day incubation in (*A*) basal (OS-) and (*B*) osteogenic (OS+) media. (*A*) Alkaline phosphatase activity, as indicated by red staining, was not observed for CA-Mel groups in basal media, suggesting osteogenic supplements facilitate melatonin-induced hAMSCs differentiation. (*B*) Alkaline phosphatase activity increases from day 7 to day 14 on both unmodified and modified scaffolds. Images recorded at 10x; scale bars measure 2 mm.

Scanning electron microscopy was utilized to investigate hAMSC morphology and migration on unmodified and modified CA surfaces (Fig. 11). The hAMSCs cultured on unmodified surfaces are elongated and plate-like, a sign of intracellular cytoskeletal rearrangement associated with adhesion and differentiation into an osteoblast lineage (122). The majority of hAMSCs cultured on CA surfaces modified with melatonin exhibited a rounded morphology, although occasional elongated cells were also present (Additional pictures in Appendix). Whether or not the rounded morphology of hAMSCs cultured on modified surfaces affects processes of differentiation remains to be determined. Exposure to melatonin by this delivery method may delay the differentiation of hAMSCs into mature osteoblasts when cultured on modified surfaces.

CA surfaces without the presence of hAMSCs were not analyzed in the current study but may benefit future comparisons and aid in distinguishing extracellular matrix material from cellular components. Nonetheless, these *in vitro* studies could highlight important effects of culture conditions (i.e., 2-dimensional versus 3-dimensional) and melatonin delivery methods (i.e., exogenous administration versus immobilization) on hAMSCs differentiation when cultured on CA scaffolds. Physical (e.g., clotting) and chemical (e.g., signaling responses) barriers created by the addition of PRP limited the experimental analysis that could be conducted for PRP-treated groups in culture. These limitations will be addressed in later sections. Optimization of culture methods for experimental groups containing PRP are warranted for future investigation.

Figure 11. Morphological Assessment of hAMSCs Cultured on Unmodified and Modified CA Surfaces

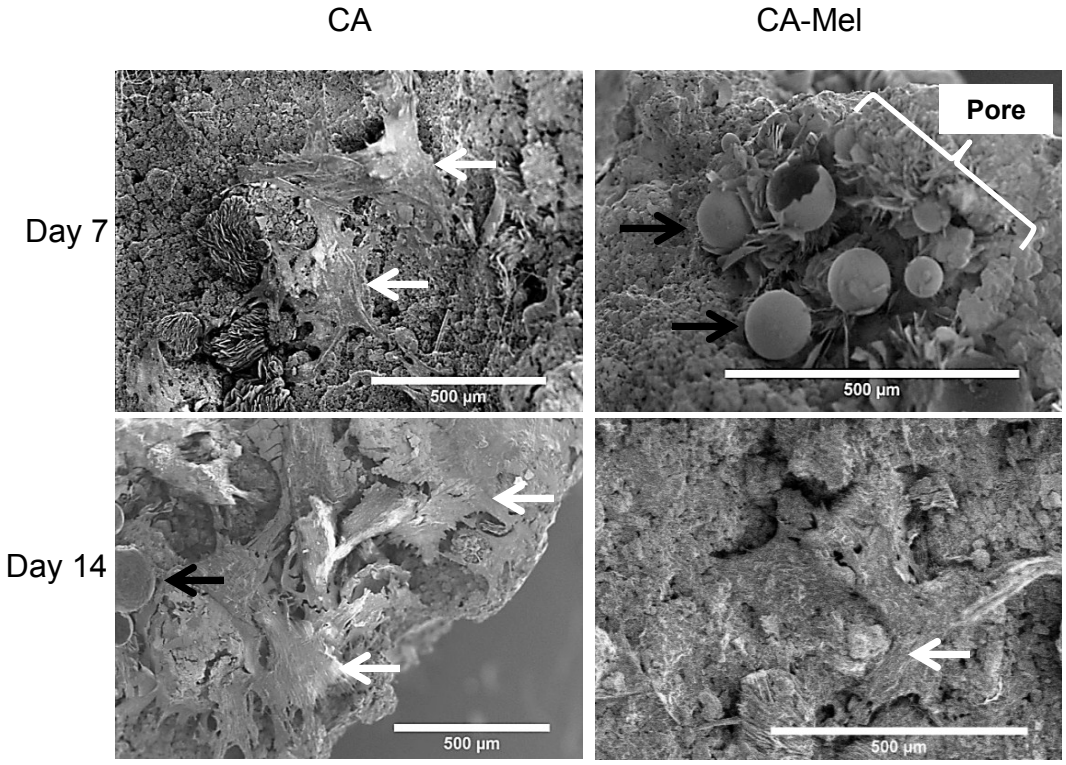

Figure 11. Modified CA surfaces affect hAMSC morphology. hAMSCs grown on CA surfaces modified with melatonin exhibit a rounded morphology that may indicate a more migratory nature at both 7 and 14 days in culture (black arrows). hAMSCs grown on unmodified CA surfaces exhibit an elongated, flattened morphology associated with cytoskeletal reorganization for adhesion and differentiation at both 7 and 14 days in culture (white arrows). Imaging was completed on a Hitachi S-3400N-II Variable Pressure scanning electron microscope under vacuum. Representative images are shown. Scale bars measure 500 µm.

Specific Aim Two

Assess the effects of unmodified (CA) and modified (CA-Melatonin) scaffolds on bone formation and remodeling activity in the presence or absence of PRP in a rodent model of calvarial defects.

Bone removal in the calvaria defect model was the most critical aspect of this procedure as the morbidity and mortality rate is usually high with this step. No animals

suffered neurologic symptoms following partial frontal bone removal and animal mortality associated with the surgical procedure was approximately 10% (of 33 animals). Animal recovery was uneventful with no signs of local infection, lingering algesia, or abnormal body weight fluctuations. The use of the Piezotome™ for bone removal likely contributed to reduced group mortality and defect morbidity. Histology and radiology of the defect site revealed that some of the implants had shifted away from the original defect site during healing in a few animals. These animals were not excluded from the following assessments given the close proximity of the implant to the original osteotomy site and the importance of gathering information about the osteoinductive nature of the biomaterial.

Before sectioning, radiographs of each skull were recorded to determine qualitative and quantitative changes in bone and/or scaffold density at the implant site. Radiograph films were digitally equilibrated to reduce the variability of background correction (Fig. 12*A*). There was no significant difference in the radiographic intensity between treatment groups at 3 or 6 months (Fig. 12*B*). However, the overall radiographic intensity of all groups increased significantly with time between the 3 month (1.26 ± 0.03) and 6 month (1.36 ± 0.04) time points ($p = 0.0359$) as would be expected with normal healing. Radiographs may have been a limited assessment of bone formation in experimental groups given that they only detect superficial changes on the most superior aspects of the scaffold surface. Thus, histological and fluorescence assessments of calvarial bone sections were used to gain a more detailed look at bone remodeling activity and bone formation between groups.

Figure 12. Radiographic Intensity of the Superior Aspect of Unmodified and Modified CA Surfaces is Significantly Increased Over Six Months

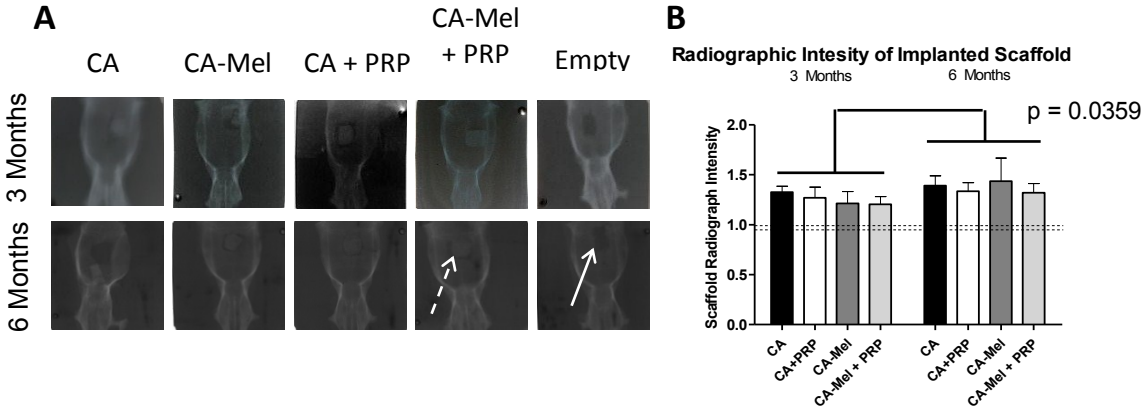

Figure 12. Radiographic intensity at calvarial defect sites is significantly increased between three and six months. (*A*) Representative superior skull radiographs for three and six month time points. Included is a radiograph of an empty defect site to illustrate that these defects will not spontaneously heal by six months. (*B)* Radiographs were digitally equilibrated to reduce background variability and quantification of radiographic intensity was normalized to background intensity. The effect of time on group means was statistically significant (3 mo: 1.26 ± 0.03 versus 6 mo: 1.36 ± 0.04; $p = 0.0359$); however, treatment and the interaction between treatment and time were non-significant. Bars represent mean ± SEM. Black dashed line represents the range of radiographic intensity for empty defect sites. Solid white arrow indicates empty defect site. Dashed white arrow indicates CA scaffold seated in defect site. Groups were compared via a Two-way ANOVA with Bonferroni *post hoc* test. n = 3 - 5.

Unstained histological sections from each experimental group were visualized with fluorescence microscopy to assess the incorporation of the injected fluorochromes as an indication of active bone remodeling. Qualitative assessments suggest that the CA-Mel group may have a higher degree of bone remodeling activity when compared to the other treatment groups (Fig. 13*A*). To support qualitative observations, the percentage of scaffold fluorescence, fluorescent intensity, and the number of fluorescent regions were quantified from double-labeled sections (Fig. 13*B-D*). The degree of scaffold fluorescence was significantly greater for the CA-Mel group at three months compared to the CA or CA + PRP groups ($p < 0.05$ for both; Fig. 13*B*). Likewise, a significantly greater percentage of scaffold fluorescence was noted for the CA-Mel group at six

months compared to all other groups ($p < 0.01$; Fig. 13*B*). Fluorescent intensity was significantly greater for the CA-Mel group at three months when compared to the CA + PRP group ($p < 0.05$) and at six months when compared to all other groups ($p < 0.05$ for CA and CA-Mel +PRP; $p < 0.01$ for CA + PRP; Fig. 13*C*). The number of fluorescent regions was found to be significantly greater for the CA-Mel group at six months when compared to other experimental groups ($p < 0.01$ for CA and CA + PRP; $p < 0.001$ for CA-Mel + PRP; Fig. 13*D*). This suggests that the CA-Mel implant may significantly impact the degree, intensity, and abundance of osteoid tissue mineralization and bone formation in this model. Analysis of scaffold fluorescent intensity for the unmodified group (CA) in the absence of PRP at three and six months by an unpaired t-test revealed a significant decrease at six months ($p = 0.0155$). Further, increased sites of internal mineralization suggest melatonin may facilitate migration of cells into the scaffold interior. The time between three and six month assessments did not significantly impact the effect of any treatment. It may be that the peak of melatonin activity is reached at early time points and maintained at a plateau level or that the time interval between three and six months is not long enough to detect a significant change. The addition of PRP did not significantly improve these parameters alone or in conjunction with melatonin suggesting the temporal regulation of chemical cues for proliferation and differentiation may need to be adequately separated in order to see a synergistic effect in the combination group.

Figure 13. Scaffolds Modified with Melatonin Augment Bone Remodeling Activity In Vivo

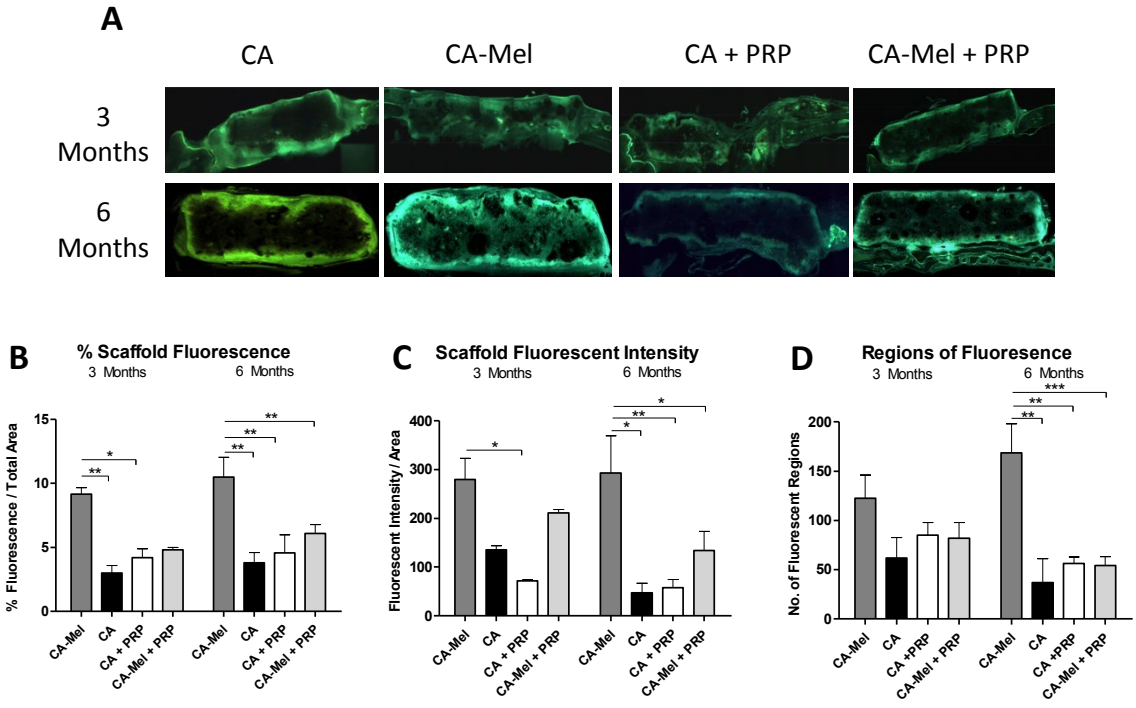

Figure 13. The effect of unmodified (CA) and modified (CA-Mel) scaffolds on bone remodeling activity in calvarial defects in ovariectomized Sprague-Dawley rats was assessed by fluorochrome incorporation (*A*) and quantifiable characteristics from fluorescent photomicrographs (*B-D*). Double-fluorochrome labeling at three and six months is more robust in the CA-Mel group. These observations are confirmed by quantification, showing that CA-Mel scaffolds have a greater degree (*B*), intensity (*C*), and abundance of bone remodeling activity when compared to other experimental groups. Time and the interaction between time and treatment were not statistically different. Bars represent means ± SEM. * indicates significance, $p < 0.05$; ** indicates significance, $p < 0.01$; *** indicates significance, $p < 0.001$ by two-way ANOVA with Bonferroni *post hoc* test. Three and six month photomicrograph montages prepared from 4x magnification. n = 3 - 5.

A methylene blue/basic fuchsin stain was used to examine general histology of the defect site and the implant circumference for signs of tissue ingrowth and osteoid synthesis along the scaffold surface. This method is reported to provide vivid contrast between the cellular and connective tissue elements in tissue sections with results similar to a hematoxylin-and-eosin procedure (120). Methylene blue is positively charged, basic dye used to highlight the cell nucleus because it is attracted to the negative charge of nucleic acid chains (e.g., phosphate backbone in DNA). Basic fuchsin, also a positively

charged, basic dye, highlights connective tissues. Connective tissues, specifically collagen, are highlighted blue-purple, while cell cytoplasm develops a pink-to-purple coloration (120, 121). Review of the stained sections at the three month time point indicates that the implanted scaffolds provide a favorable surface for the growth and incorporation of cells and connective tissues (Fig. 14*A*). In some cases, implanted scaffolds shifted away from the defect site and were located over intact bone (Fig. 14*A*; CA and CA+PRP at 6 months). Interestingly, early histological assessments provide evidence of the degradation of the calcium aluminate scaffold along the implant border (Fig. 14*A*). Regions of interest from experimental groups were noted and viewed under higher magnification. Defect sites implanted with CA-Mel with and without PRP showed signs of scaffold integration, tissue infiltration into scaffold pores, and osteoid synthesis along the scaffold surface (Fig. 14*B*). Many of the cells that were present around the implanted scaffolds at 3 months had subsequently been replaced by bone matrix tissues (e.g., parallel bands of collagen or lamellar bone attachments) (Fig. 14*B*), indicative of the normal bone repair process. Thus, the cells noted in the 3 month photomicrographs may be cell types associated with the early stages of bone remodeling such as osteoprogenitor cells or those associated with osteoid synthesis and mineralization such as osteoblasts, as other cell types such as fibroblasts would not contribute to bone remodeling. This is further supported by the preference of the calcium aluminate material for osteoblasts versus fibroblasts noted in the preliminary studies (Fig. 9) and the qualitative and quantitative results from the double-labeled sections (Fig. 13*A-D*). Signs of tissue infiltration or attachments from the defect border were not noted in the unmodified group with or without PRP (CA+ PRP and CA, respectively). Instead,

open space filled with fine connective tissue was observed (Fig. 14*B*). Furthermore, because the fluorescence around and through the scaffolds overlaps the cells and proteins depicted by the histological stain and the quantification of fluorescence was averaged from 3 – 5 animals per group, the fluorescence noted in the photomicrographs is not a result of artifacts from the staining or visualization procedures.

Figure 14. Unmodified and Modified Scaffolds are Osteoconductive and Biocompatible

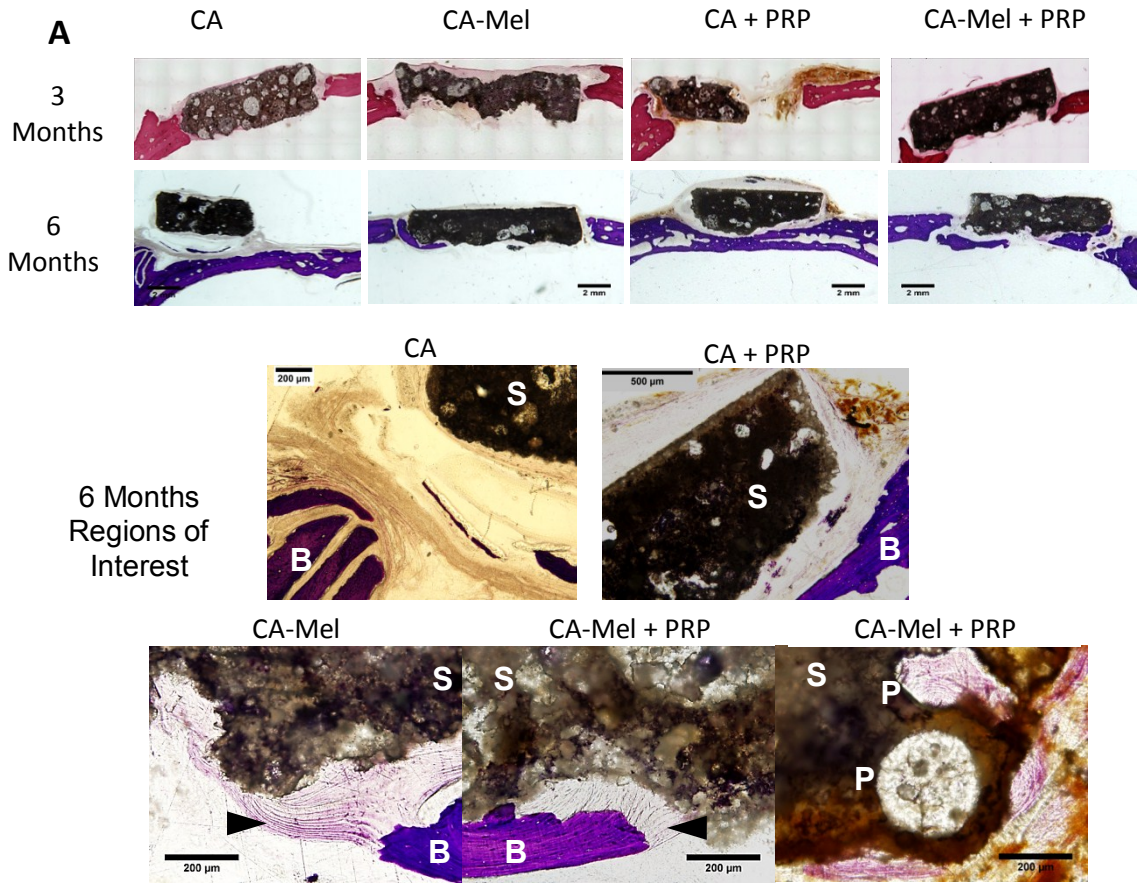

Figure 14. Histological evidence of the biocompatibility and potential biodegradation of the calcium aluminate material in experimental groups. (*A)* Early (3 month) and late (6 month) histological sections stained for cellular proteins (e.g., bone, collagen, and connective tissue; pink/purple) and DNA (e.g. cell nucleus; blue/dark purple) indicate that implanted scaffolds provide a favorable surface for the growth and incorporation of cells and connective tissues. (*B)* Regions of interest from select experimental groups at six months were viewed under higher magnification. Defects sites implanted with CA-Mel with and without PRP showed signs of scaffold integration, tissue infiltration into scaffold pores, and osteoid synthesis along the scaffold surface. Three month photomicrograph montages prepared from 4x magnification. Six month photomicrographs captured at 10x; scale bars measure 2 mm. Regions of interest for 6 month photomicrographs captured at 200x; scale bars measure 200 µm. S = Scaffold, B = bone at defect edge, P = scaffold pore, arrow = lamellar attachments. n = 3 – 5.

Overall, melatonin was successfully linked to CA surfaces using simple chemical methods carried out at room temperature. Both unmodified and modified CA scaffolds were found to be biocompatible in *in vitro* and *in vivo* environments. Scaffolds modified

with melatonin demonstrated a preference for the adhesion and proliferation of normal human osteoblast but may delay the differentiation of hAMSCs. These results may have contributed to the enhanced bone remodeling activity in calvarial defects of animals implanted with modified CA scaffolds. The application of PRP confounded *in vitro* analyses and had negligible impact on bone remodeling *in vivo*, both alone and when combined with melatonin. Radiographic intensity of the defect site increased over time for all experimental groups. Although signs of biodegradation were observed, both unmodified and modified CA scaffolds provided osteoconductive surfaces out to six months. Mechanisms regulating the recruitment, attachment, and activity of hAMSCs and mature osteoblasts may underlie the effects of melatonin on bone formation when immobilized on CA surfaces.

DISCUSSION

1. Study Summary

Bone possesses inherent capabilities of regeneration in response to adult development and traumatic injury. The process of bone regeneration involves the orchestration on several spatially and temporally regulated events mediated by specific signaling cascades and cell-cell interactions. In the majority of cases, the new bone will have largely restored its native mechanical and physiological properties and be relatively indistinguishable from adjacent uninjured bone (123). Nonetheless, there are cases where total bone regeneration is impaired either by exceeding the normal regenerative capacity of the bone (e.g., large bone defects created by trauma, tumor resection, or skeletal

abnormalities), or in cases where the normal regenerative capacity is compromised (e.g., osteoporosis) (123).

Despite a wide variety of methods for treating impaired bone regeneration, current tissue engineering strategies aim to regenerate native bone tissue without the disadvantages associated traditional autogenic or allogenic bone grafts. While the limitations associated with traditional bone grafting methods have driven the development of synthetic substitutes, no synthetic bone material currently available exceeds or matches the biological or mechanical properties of native bone tissue (123). Thus, there is significant impetus to recapitulate the biological and mechanical properties of human bone tissue in a cost-effective and safe manner through the development of bioactive bone substitutes that contain growth factors and/or osteoprogenitor cells for guided bone regeneration. The goal of the current study was to optimize the bone regenerating properties of calcium aluminate (CA) scaffolds by exploiting their potential as carriers of therapeutic agents that could locally direct and facilitate new bone formation. Histological, radiological, and mechanistic analyses were utilized to evaluate the osteoconductive and osteoinductive properties of unmodified (CA) and modified (CA-Mel) scaffolds in the presence or absence of growth factor-rich platelet-rich plasma (PRP) as well as their biocompatibility with a variety of cell types common to the bone remodeling process. Specifically, a rodent model of calvarial defects was employed to investigate the effect of locally delivered melatonin and/or PRP in combination with the CA biomaterial on new bone formation.

This study reports an effective way of attaching melatonin to customizable CA scaffolds using simple linker chemistry carried out at room temperature (Fig. 8). Post-

operative healing in experimental groups was uneventful, with the implanted materials producing no signs of inflammation, infection, or inducing detectable behavioral changes. The biocompatibility of the CA material was additionally supported by histology (Fig. 14) and external *in vitro* testing (Figs. 9 and 10). The chemical linkage of melatonin to CA significantly increased the degree, intensity, and abundance of bone remodeling activity in critical-size calvarial defects in ovariectomized rats (Fig 13). These findings may be attributed to the preference modified (CA-Mel) scaffolds demonstrated for the proliferation and adhesion of normal human osteoblasts (Nhosts) (Fig. 9) and their support of human adult mesenchymal stem cell (hAMCS) differentiation (Fig. 10). Modified scaffolds may delay hAMSC differentiation, which increases with the duration of culture in the presence of osteogenic medium (Fig. 10) and may promote a more migratory phenotype in surface hAMSCs (Fig. 11). The inclusion of PRP upon implantation appears to have negligible effects or to attenuate melatonin-induced effects on bone remodeling activity *in vivo* (Fig. 13). Radiographic data regarding the density of newly formed bone shows a significant increase over time in all groups (Fig. 12). The absence of a detectable decrease in density suggests that the apparent biodegradation of CA scaffolds (Fig. 14) is balanced with processes of bone formation (Fig. 13). Likewise, both unmodified and modified CA scaffolds continue to provide an osteoconductive surface out to six months (Fig. 14). Taken together, *in vivo* and *in vitro* results suggest CA scaffolds modified with melatonin may enhance bone remodeling activity in calvarial defects through hAMSC differentiation and recruitment, and a preferential effect on the viability and function of mature osteoblasts.

2. Calcium Aluminate Synthesis & Modification

Stainless steel, titanium, cobalt-chromium, nickel, and their alloys are all examples of metallic implants. The rigid nature of metallic biomaterial enhances their strength characteristics making them better suited for the repair and reconstruction of high impact regions. However, their rigid physical structure prevents the customization of the implant to suit defect size and volume. Moreover, the inertness of metallic implants limits the chemical bonding between the bone/implant interface due to the passive oxide layer that forms on their surface (124). This oxidized layer is resistant to further chemical reactions, confounding the ability to attach organic molecules (125). Chemical attachment to titanium surfaces through common silanization methods are hydrolytically unstable, leaving little protection of the bound molecules from aqueous reactions (126). Recent engineering approaches have sought to enhance the proliferation and adhesion of osteoblasts and bone formation by creating different roughness patterns and surfaces for chemical attachment (126-128).

The nature of calcium-based ceramics is much less rigid than metallic devices, and thus, allows them to be molded to fit distinct defect shapes and sizes. Their crystalline structure provides some control over porosity during synthesis which benefits osteointegration (129). While high heat treatments can reinforce the crystalline structure and give strength to the material, it limits their functionalization (130). Moreover, many calcium-based ceramics remain brittle and require stabilization when used in regions of high impact (31, 33).

Physical analyses of the CA material conducted in other laboratories found that normal sterilization procedures (121^{o}C and 18psi of steam for 60 minutes) did not affect

the porosity of the material and interestingly, enhanced mechanical integrity (105). In this study, scaffolds of calcium aluminate were prepared by mixing the reactants with a small amount of water. There were several advantages to this process including (i) the CA material remains moldable for an extended period of time, (ii) porosity can be controlled, and (iii) the resulting cast will develop and exhibit high mechanical strength at room temperature (105). Structure formation at room temperature is especially important for functionalization of biological agents to the scaffold surface. Thus, there are several attractive properties of calcium aluminate with regard to its synthesis and mechanical properties that support its potential use as a bone substitute material.

Ceramic materials, by nature, are only osteoconductive (37); however, the inclusion of osteoinductive factors can be used to promote the differentiation of stem cells into osteoblasts or augment osteoblast activity (29). Bone ingrowth into CA scaffolds in calvarial defects at four weeks was reported to be negligible (50) and was not typical of calvarial defect sites at six months (49). Thus, a chemical method to link biological molecules to the CA surface to locally stimulate osteoinduction was investigated here.

Locally delivered agents provide several advantages such as reducing systemic side effects and producing a higher concentration of drug at the target site (130). Methods of local delivery can include adsorption or covalent immobilization. Adsorption is the non-specific physical interaction between a biomolecule and a biomaterial surface (131). While this method is simpler, less disruptive to the biomolecule, and cheaper, it is often a weak association that can be disturbed by temperature, pH, and other factors

(131). Covalent techniques can be used to more permanently affix the biomolecule to the biomaterial surface (131). Chemical methods in this study use the free end of organic linkers covalently bound to the CA surface as a reactive location for the attachment of other chemical and biological entities (131). The covalent immobilization of biomolecules to biomaterial surfaces addresses many of the challenges associated with the exogenous delivery of growth factors including the control of growth factor diffusion and dosage (132, 133). Biomolecule immobilization is relevant to physiological models as immobilized growth factors occur naturally, either sequestered in the extracellular matrix or directly bound to cell surface binding moieties or intermediary molecules (132).

Other previously collected data suggest that the organic acid linkers of the CA surface are not disrupted by chemical (i.e., solvent rinses) or mechanical (i.e., sonication) means (134). Diffuse reflectance infrared Fourier transform (DRIFT) spectroscopy was used to verify the attachment of both the organic linker and melatonin molecule during a two-step chemical deposition process (Fig. 8*A*). DRIFT analysis confirmed the attachment of melatonin to the organic linker by spectral peaks representative of chemical moieties associated with each substrate (Figs. 8*B* and *C*, respectively). Thus, the chemical methods described in this study can be used to attach biomolecules to the CA surface with the intent to locally deliver them to specific target sites. As discussed in later sections, the functionality of CA-melatonin linkages was also confirmed.

3. *In Vitro* Biocompatibility of Unmodified & Modified Calcium Aluminate Scaffolds

3.1 Effect of Unmodified & Modified Calcium Aluminate Scaffolds on Normal Human Osteoblast & NIH 3T3 Fibroblast Viability

Preliminary aims of the study examined the effect of unmodified and modified CA surfaces on the mature, non-transformed cell types, normal human osteoblasts (Nhosts) and NIH 3T3 fibroblasts. Osteoblasts are the main bone forming cells of the body and function to mineralize the bone matrix to impart strength (1). Fibroblasts are common cells of connective tissues and function to synthesize extracellular matrix and collagen (135). As such, they have critical roles in wound healing (135). Unmodified CA aluminate surfaces supported the viability and proliferation of both cell types, confirming results from acute toxicity testing revealing that CA lacks cytotoxic effects (48). Interestingly, CA surfaces modified with melatonin enhanced the proliferation and viability of Nhosts (Fig. 9). These findings are supported by work conducted by Nakade *et al.* demonstrating that exogenous melatonin at doses between 50 and 100 μM enhanced the proliferation of normal human bone (HOB-M) cells and human osteoblastic (SV-HFO) cells (75). Conversely, melatonin appeared to reduce the proliferation and viability of NIH 3T3 fibroblasts over time (Fig 9). Hypertrophic scar tissue is formed by the abnormal proliferation of fibroblasts and excessive deposition of extracellular matrix (136). Melatonin receptors are expressed at greater levels in fibroblasts from human hypertrophic scars than normal human dermis (137). In studies of NIH 3T3 fibroblasts transfected with human MT1 or human MT2 receptors, melatonin pretreatment reduced proliferation and transformation (138). A reduction in fibroblast proliferation would be

especially important in wound healing as the accumulation of fibrous connective tissue can limit bone union (139). Taken together, these results suggest that the presence of melatonin can preferentially affect cell viability. Thus, chemical modification of CA surfaces with melatonin may be a valuable tool in directing cellular fate in bone regeneration models. Likewise, these results suggest that the chemical attachment of melatonin to the CA surface does not render the molecule biologically inactive.

3.2 Effects of Unmodified & Modified Calcium Aluminate Scaffolds on Human Adult Mesenchymal Stem Cell Viability, Differentiation, & Morphology

Based on the viability studies supporting the preferential functionality of the melatonin linkage, it was assumed that melatonin-induced effects on the differentiation of hAMSCs would also be apparent. The pluripotent nature of mesenchymal stem cells (MSCs) allows them to differentiate into several different lineages. The chemical cues that drive mesenchymal stem cells toward an osteoblast phenotype can be replicated *in vitro* by supplementing basal medium with dexamethasone, β-glycerophosphate, and ascorbic acid (67, 68, 72). The differentiation of hAMSCs is further enhanced by the exogenous administration of 50 nM melatonin (67, 68, 72). The most appropriate treatment method for enhanced differentiation and calcium deposition was reported to be the continuous administration of 50 nM melatonin every other day for a period of 21 days (68). However, the effect of immobilized melatonin on hAMSCs differentiation has not been reported. Thus, unmodified and modified CA scaffolds were seeded with hAMSCs to determine the functionality of the melatonin linkage compared to control surfaces and

to evaluate the specific time point(s) where hAMSCs transition into bone-forming osteoblasts by this delivery method.

The effect of unmodified and modified CA surfaces on the differentiation of hAMSCs into an osteoblast lineage was qualitatively assessed by ALP staining (Fig. 10). An increase in the exposure of hAMSCs to surfaces modified with melatonin resulted in increased differentiation in the presence of osteogenic medium suggesting that the presence of melatonin does not negatively affect, but may delay, this process (Fig. 10*B*). It has been hypothesized that melatonin-induced differentiation occurs when unique protein scaffolds containing extracellular signal-regulated kinase 1/2 (ERK1/2), the melatonin receptor (MT_2), and β-arrestin are localized to the cytosol (68). These complexes control the translocation patterns of ERK 1/2, a known modulator of cell fate, to facilitate cellular differentiation versus proliferation (cytosolic localization versus nuclear localization, respectively) (140). Moreover, ERK 1/2 is localized to the cytosol when melatonin-induced ALP activity is highest (68), which supports the notion that localization of ERK 1/2 in the cytosol promotes differentiation rather than proliferation. These same mechanisms may have been occurring in this study, although not fully investigated. In the future, culturing experiments on unmodified and modified CA surfaces should incorporate the use of non-specific and specific melatonin receptor antagonists (i.e., luzindole and 4-PPDOT, respectively) to confirm the above mechanisms regulating differentiation of hAMSCs by melatonin.

Interestingly, hAMSCs cultured on the unmodified CA surface underwent differentiation in basal (OS-) medium lacking osteogenic supplements (Fig. 10*A*). These findings may suggest that the chemical and physical characteristics of unmodified CA

scaffolds may have played a role in promoting hAMSC differentiation. Evidence for this phenomenon comes from a study designed by Castro-Raucci *et al*., in which a novel calcium aluminate cement was compared against the gold standard dental cement, mineral trioxide aggregate (MTA) with regard to osteogenic proliferation and differentiation (141). Osteogenic cells harvested from the calvarial bone of newborn rats demonstrated significant viability, proliferation, and differentiation on CA compared to MTA (141). Likewise, although many calcium-based ceramics are not considered osteoinductive, some calcium phosphate materials have produced ectopic bone formation in the absence of osteogenic signals (35). It is suggested that the release of calcium ions enhances the adhesion of osteogenic cells and osteoclasts (37). Early studies demonstrate CA can release free calcium ions in the local area of the implant (142). Additionally, the physical properties of a biomaterial can regulate tissue morphogenesis in a lineage specific manner (143). For example, harder surfaces that mimic the mineralized bone matrix favor mesenchymal stem cell differentiation into osteoblasts (143). Nanoscale topography (i.e., nanoscopic physical characteristics) of biomaterial surfaces can increase mesenchymal stem cell sensitivity to soluble signals and significantly enhance their differentiation into osteoblasts (144). Pre-osteoblast cells from mouse calvarial bone (MC3T3-E1) exhibited an increase in focal adhesion complexes and thick F-actin fiber development, events consistent with differentiation, on "textured" nanoparticle-modified surfaces compared to smooth glass surfaces (144). Evidence for this in the current study may stem from hAMSCs differentiation that occurred on porous unmodified CA surfaces in the absence of medium-based osteogenic signals. Osteogenic media is a requirement for melatonin-induced increases in hAMSC differentiation (67) and is likely the reason

why CA-Mel did not induce differentiation of hAMSC in basal media in the current study. The inherent capability of unmodified CA scaffolds to promote hAMSC differentiation requires further study.

Morphological assessment of unmodified and modified CA surfaces reveals two distinct hAMSC morphologies (Fig. 11). Although both surfaces contained rounded and flattened hAMSCs, the rounded phenotype was more commonly observed on the modified CA surface. A flattened morphology is typical of adhesion and differentiation processes while rounded morphology is a sign of contact inhibition that may indicate cellular migration (122). The immobilization of melatonin molecules to the synthetic surface through the described chemical modification may drive the migration of hAMSCs, in particular, to regions of melatonin localization.

It has been reported that immobilized growth factors may also promote the migration of cells across chemical gradients. Bioprinting is a technology that uses a modified printing device to deposit biological materials in two- or three-dimensional patterns. Recent studies involving the use of bioprinting have been designed to investigate how cells react to spatial patterns of immobilized growth factors. A study by Miller *et al*. found that mesenchymal stem cells will migrate across a fibrin meshwork (i.e., bioprinting substrate) in response to heparin-bound epidermal growth factor-like growth factor (HB-EGF) (132). Interestingly, the mesenchymal stem cells were equally guided away from the cell source regardless of whether the immobilized growth factor concentration was equivalent across the bioprinting substrate or if the concentration followed a low-to-high concentration pattern (132). These results could indicate that

simple uniform distributions of growth factors immobilized on extracellular matrix material may be just as effective in directing cell migration as more complex patterns with concentration gradients (132). In another study, recombinant VEGF-165 was immobilized onto collagen sponge scaffolds using 1-ethyl-3-[3-dimethylaminopropyl]carbodiimide hydrochloride (EDC) chemistry. The immobilized VEGF-165 patch was used to drive the migration and proliferation of endothelial cells as a means of promoting myocardial repair. The resulting greater angiogenic responses from VEGF-165 patches contributed to improved cell survival and tissue formation (145). The persistence of the immobilized growth factor pattern over time likely contributes to a constant stimulus for cellular migration and proliferation in these studies.

Although the migration studies discussed above occurred on patterned, smooth, planar surfaces, melatonin is known to have chemoattractant effects (146) and may have similar effects on cell behavior in our model system. Thus, the chemical immobilization of melatonin may stimulate cell migration and interaction between cell surface receptors on hAMSCs and the immobilized molecule. While the distribution of melatonin molecules is hypothesized to be equally distributed over the surface of the treated CA (147), the concentration of molecules may be dependent on specific attachment points which, in turn, may be dependent on specific topographic characteristics of the CA surface. Those hAMSCs seeded in areas with adequate access to melatonin may have undergone differentiation, while those established in areas of reduced melatonin access would benefit from migration towards adequate concentrations. The motile nature of the cultured hAMSCs on modified CA surfaces may be evident by their rounded morphology, a sign of migration (122) (Fig. 11). Consequently, the time points for

observing the differentiation effects of melatonin on hAMSCs may be altered as these cells first migrate across the CA surface before adhering and undergoing differentiation. If these observations are supported in future studies, the time points for melatonin-induced differentiation, as detected by ALP induction, may proceed at time points that follow hAMSC migration. It is also worth mentioning that initial inflammatory responses *in vivo* after implantation may have facilitated the migration of both immature (i.e., MSC) and mature (i.e., osteoblast) cells via chemotactic factors released from immune cells such as macrophages including interferon-gamma (INF-γ), tumor necrosis factor-alpha (TNF-α), and interleukins. Additional SEM analysis is required to fully investigate the migration patterns of hAMSCs on both unmodified and modified surfaces.

4. *In Vivo* Biocompatibility of Unmodified & Modified Calcium Aluminate Scaffolds

The host response to biomaterials can vary widely based on the characteristics of the host, material, and surgical procedure (124). In terms of biomaterials, biocompatibility is difficult to define, but is loosely defined as "the ability to perform with an appropriate host response in a specific situation" (124). This definition of biocompatibility supersedes the traditional concept of biomaterial inertness, as many newly developed biomaterials favor specific host responses (e.g., increased bone-forming activity, vascularization, etc.) in order to optimize the performance of the device. Indeed, it is now recognized that no biomaterial is completely inert in the human body, even the most stable metallic implants (124). Thus, it was important to ensure that any benefit to utilizing CA biomaterials for bone regeneration were outweighed by toxicity associated

with its components. Signs of inflammation, infection, or behavioral changes in animals (e.g., reluctance to be handled, avoidance or aggressive behavior, changes in eating habits) were not observed and all animals gained weight at a normal rate.

4.1 Osteoconductive Properties of Unmodified & Modified Calcium Aluminate Scaffolds

The biocompatibility of the biomaterial in the host environment can directly impact its osteoconductive nature. Osteoconductive properties of a biomaterial allow it to serve as a suitable surface for cellular events, interactions, and the apposition of new bone (29, 30, 153). Histopathological analysis was employed to examine the osteoconductive nature of implanted unmodified and modified CA scaffolds in a calvarial defect model including signs of cell migration and tissue infiltration. All experimental groups support the growth and expansion of cells and tissues derived from the defect site and the surrounding bone (Fig. 14*A*). Moreover, histological staining identified the presence of immature connective tissues (i.e., osteoid) around the outer circumference of the scaffold and lining scaffold pores (Fig. 14*B*).

Porosity is a hallmark of both trabecular and cortical bone. The morphology of trabecular bone is 50-90% porous with pore sizes on the order of 1 mm in diameter (154). Cortical bone is a relatively solid structure, but a series of Haversain canals results in a porosity of 3-12% (154). Porosity of both native bone and scaffold biomaterials supports the migration and proliferation of mesenchymal stem cells, osteoblasts, and osteoclasts as well as the development of vasculature and new bone (130). Tissue infiltration further aids the fixation of the implant in the local environment (124). The average pore size of

the CA material utilized in this study is reported to be 100 μm (105, 147), which is sufficient for cell migration and bone ingrowth (31). After seeding cells on calcium aluminate surfaces with a pore size of 100 μm, Bose *et al*. found that some of the CA material contained monolayers of human osteoblasts (155). Further, calcium aluminate cylindrical pellets with larger pore sizes (100 – 150 μm and 150 – 200 μm) had substantial bone ingrowth in canine femoral defects compared to smaller pore sizes (75 – 100 μm) that contained unmineralized osteoid tissue (154). Thus, the histological results described in the current study confirm that CA materials with adequate porosity support the infiltration of cells and tissues and that the size and interconnectivity of scaffold pores plays an important role in these findings.

4.2 Osteoinductive Properties of Unmodified & Modified Calcium Aluminate Scaffolds

The goal of this study was to create a synthetic bone substitute with regenerating properties similar to natural bone including developing its osteoinductive properties to facilitate osteointegration. While early *in vitro* studies and *in vivo* histology provide evidence that both unmodified and modified CA surfaces are biocompatible with a variety of cell types and support the development of connective tissues after implantation, the enhancement of bone formation through osteoinductive modifications were also considered and analyzed. To this end, the osteoinductive influence of modified CA scaffolds in the presence or absence of growth factor-rich PRP was investigated in a rodent model of critical-size calvarial defects based on the reported osteoinductive properties of melatonin and PRP. Calvarial defects provide little bone peripherally

around the implant and lack significant impact or weight-bearing forces that will contribute to spontaneous bone regeneration. Thus, a calvarial defect model provides a substantial challenge to the osteoconductive and osteoinductive properties of the implanted material, as the major contribution to bone regeneration must come from the scaffold, not the host bone (44, 156) .

Studies of bone marrow from rats and humans indicate that melatonin is synthesized and stored locally in the bone tissue where it is twice as high as nighttime levels in peripheral blood (76, 157). These findings suggest that local synthesis and storage of melatonin in bone may be important for bone repair. Although, the topical application of melatonin facilitated the osteointegration of dental implants in Beagle dogs (74, 77-79) and rabbits (80), its delivery via a surface linkage to CA scaffolds has not been tested in an appropriate model of bone repair. As mentioned before, DRIFT analysis confirms that molecules of melatonin can be attached to the CA surface utilizing simple linker chemistry (Fig. 8) and thus, can be delivered directly to the defect site to stimulate host cell activity.

PRP was added to both unmodified and modified scaffolds during implantation to further potentiate the osteoinductive effects on the host microenvironment. PRP enhances the proliferation of mesenchymal stem cells *in vitro* (158-160) and has been defined as an osteopromotive substance (4). Recombinant growth factor therapy, although reportedly beneficial (26, 43, 45, 161), cannot replicate the complex milieu of growth factor signaling that occurs with healing and bone development. Moreover, the clinical use of recombinant human bone morphogenetic protein-2 (rhBMP-2) and rhBMP-7 have shown signs of uncontrolled bone growth (27). Mesenchymal stem cells

are receptive to growth factor signals produced in the host tissue and are necessary to initiate the beginnings of bone healing (162); however, obtaining sufficient numbers can prove challenging. While MSCs can be expanded in culture in preparation for implantation, continued passaging of MSCs or the use of MSCs from aged donors can lead to a loss of mitogenic and osteogenic potential (101-103). This is most likely attributed to an increase in cell senescence and/or apoptosis (101, 103). Thus, the benefits of including autologous PRP in the implant procedure was two-fold: (i) robust enhancement of host progenitor cell numbers at the defect site without the need for extensive subculturing of stem cells and (ii) replication of the complex signaling events associated with healing and bone regeneration.

Evidence of bone regeneration after incorporation of these therapies was initially investigated by radiological assessment of the defect site (Fig. 12). There was no radiographic evidence that functionalization of CA with melatonin or the addition of PRP enhanced defect site intensity more than the unmodified CA group; however, there was an overall increase in radiographic intensity over time for all groups from three months to six months (Fig. 12*B*). Initial histology of experiment groups provided some evidence of scaffold degradation, although the overall integrity of the defect site was not compromised out to six months (Fig. 14*A*). Taken together, these results suggest that the degradation of CA scaffolds may be adequately balanced by bone formation. Indeed, a decrease in radiographic intensity would likely indicate a rapid degradation of the biomaterial without appropriate bone fill. Moreover, unbalanced rates of degradation and bone tissue formation could compromise the integrity of the defect site.

Just as the porosity of a biomaterial can dictate the extent of cellular migration and tissue infiltration, porosity also exposes the biomaterial to the *in vivo* environment and likely facilitates its degradation (124). The process of biodegradation and the degree to which an implant is resorbed can have a large influence on the materials bone bonding properties (124). Biodegradation of many of the bioactive ceramics occurs through either solution-mediated or cellular-mediated processes. For example, calcium phosphate materials like hydroxyapatite and β-TCP undergo simple dissolution to release free calcium and phosphate ions (124). Likewise, the biodegradation of these materials can also be attributed to phagocytosis by mesenchymal stem cells or giant cells (124). Indeed, the various phases of CA (due to variations in Ca:Al ratios) can provide a method for controlling the rate of ceramic dissolution (142, 155). It is possible that similar biodegradation processes were occurring at the implant site during the current study, as signs of particulate accumulation in the surrounding connective tissue are absent. Further investigation of this phenomenon is warranted in future studies. Additionally, while radiological techniques are routinely used to measure bone-defect repair, x-ray computed microtomography enables 3D construction of the internal structure of small radio-opaque objects (13). Thus, this technology may have valuable applications for the investigation of qualitative and quantitative aspects of bone formation on and within CA scaffolds.

Radiographic analysis provided a limited analysis of bone formation and changes in scaffold density at the implant site. Therefore, the presence and difference in bone remodeling capabilities between experimental groups was assessed qualitatively and quantitatively using a double fluorochrome labeling series. Fluorochromes, like

oxytetracycline and calcein, are fluorescent labels with calcium affinity. The incorporation of different fluorochrome injections at two different time points allows the pattern and rate of calcium precipitation during mineralization to be visualized with the aid of different wavelength filters.

Bone remodeling activity was significantly enhanced in defect sites treated with modified scaffolds (Fig. 13). Specifically, the presence of melatonin on CA scaffolds increased the degree, intensity, and abundance of bone remodeling activity at three and six month time points compared to other experimental groups (Fig. 13*B-D*). These findings suggest that modified scaffolds may significantly impact the mineralization of osteoid tissue that adheres to the CA surface and further promote bone formation *in vivo*. Increased bone remodeling activity may be a result of the effect of melatonin on osteoblast differentiation and activity (57, 67, 68) including increasing the transcription of genes implicated in remodeling processes such as *Runx-2, Bmp-2,* and *osteocalcin* (68, 72, 74) and increasing collagen type I synthesis (75). Based on the *in vitro* studies and histology, the presence of melatonin on the scaffold surface does not appear to interfere with the differentiation of hAMSCs into osteoblast or the migration of cells and the infiltration of tissue from the defect border. On the contrary, it may actually enhance these phenomena as a chemoattractant molecule (146).

More abundant sites of remodeling in the CA-Mel group support histological findings and suggest cell migration to deeper aspects of the scaffold may have been aided by an optimal pore size and interconnectivity (Fig. 13*A*). Specifically, these results suggest that cell types associated with bone remodeling were capable of reaching and functioning at interior portions of the CA biomaterial. Bone remodeling within a porous

biomaterial is critical for the integration of the implant into the environment. Bone remodeling located exclusively around the periphery of a porous implant would not facilitate its fixation in the bone environment nor aid in the transmission of load-bearing forces (124).

Despite the possibility of CA-induced hAMSC differentiation noted *in vitro*, these results may not have translated to the *in vivo* model system or, conversely, may not be adequate enough to stimulate all aspects of the bone remodeling process. Although the average pore size of the unmodified CA material utilized in this study is sufficient for cell migration and bone ingrowth (31), negligible bone matrix infiltration and bone remodeling activity were observed (Figs. 13 and 14). Thus, efforts to enhance the stimulatory effects of the implants on the host microenvironment may be required for successful bone formation *in vivo* in calvarial defects as indicated by the benefits of CA-Mel groups.

Although CA-Mel implants significantly impacted bone remodeling in calvarial defects, a non-significant effect of time was obtained (Fig. 14). In the future, *in vivo* time points should be adjusted to determine the onset and duration of action of melatonin on modified CA scaffolds. For example, if melatonin activity reaches a peak and is maintained over time, time points prior to 3 months may be necessary to analyze this effect. Conversely, if melatonin activity gradually increases over time, extended time between each time point may be required to detect significant changes, such as 3, 8, and 13 month time points. These future modifications could determine whether the effects of melatonin are early, exhibit only modest increases over 3 month periods, or are maintained after a specific "window" of peak activity. Other collected data suggest that

the organic acid modifiers (linkers) of the CA surface cannot be removed by chemical (i.e., solvent rinses) or mechanical (i.e., sonication) means (134); however, future studies should examine the stability of the immobilized melatonin over time by analyzing the release of melatonin from the CA surface in culture. Evidence for melatonin release and the pattern of its dissolution could be examined in exhausted cell media or simulated body fluid by radioimmunoassay or HPLC methods. The lack of two distinct labels on fluorescent micrographs may be due to the close proximity of the tetracycline and calcein injections. As the injection series was based on a protocol for double labeling long bones, it may need to be modified to include an increased time span between label injections in future studies when working with calvarial defect models. Nonetheless, visual evidence of fluorochrome incorporation supports bone remodeling activity is occurring. Further, given that fluorescence around and through the scaffolds overlaps the cells and proteins depicted by the histological stain, the quantified fluorescence is a reliable predication of bone remodeling activity for the experimental groups.

Theoretically, the growth factors contained in PRP could have synergistic effects on osteoprogenitor cell and osteoblast proliferation to improve bone formation and integration (163). Despite containing over 30 biomolecules, many implicated in initiating a variety of responses associated with bone healing (86), the inclusion of PRP in this model of calvarial defects showed either negligible or inhibitory effects on bone remodeling when used alone or in combination with melatonin, respectively for the time points analyzed (Fig. 13). Specifically, combinations of PRP with CA-Mel scaffolds reduced bone remodeling to control levels.

Our findings seem consistent with other studies that have demonstrated that the effects of PRP are transient and take place within a short period of time. This is most likely attributed to the fact that the robust release of growth factors lasts for only the lifespan of the platelets. Although age and gender do not appear to affect platelet numbers or growth factor levels in PRP harvested from humans (164), variability of PRP effects in animal models may be species-related or suggest differences in growth factor signal responsiveness. Indeed, some report no effect of PRP on bone formation when combined with stem cells, autogenous bone, or biomaterials (44, 84, 165, 166). Interestingly, PRP produced greater effects on bone regeneration when applied to metallic surfaces versus ceramic surfaces (163), suggesting that the chemistry of the implant surface may affect the osteopromotive effects of PRP. Additionally, the rapid coagulation of PRP over the CA implants may have occluded scaffold pores making it difficult for host cells to migrate onto the scaffold surface and/or limiting bone ingrowth. Although evidence of connective tissue infiltration was observed in histological sections or PRP-treated implants, the conflict created between the proliferative signals of PRP and the differentiation signals of melatonin may have delayed or attenuated the progression of bone remodeling**.** While PRP enhances the proliferation of stem cells (118, 159, 167), it either decreases (159) or does not affect (118, 160) their differentiation. Thus, differentiation responses may be postponed to later time points and may correspondingly delay osteoid mineralization. These physical and chemical barriers associated with PRP application may explain the lack synergism between PRP and melatonin *in vivo*. Interestingly, the combination of melatonin with fibroblast growth factor-2 enhanced bone formation and facilitated osteointegration (168). This suggest that the

differentiation signal may need to be the stronger of the two for adequate bone regeneration. The effects of PRP on hAMSC differentiation and calcium deposition requires closer examination of specific time points based on the results reported here. The temporal regulation of growth factor signals at the site of implantation may be of key importance and warrants further study.

Although some report the exogenous activation of PRP prior to its application (94, 116), its activation can occur spontaneously under microenvironmental cues and is required for the release of growth factors (85, 159). PRP prepared in this study was not activated with either bovine thrombin or calcium chloride. Previous studies have shown that growth factor levels through this preparation technique are similar to activated PRP preparations (118). Activation with bovine thrombin and calcium chloride has been shown to adversely affect growth factor levels (169) and may compromise bone healing (170). Moreover, the use of bovine thrombin in humans can induce a robust immune response, including the development of cross-reactive antibodies (171). Thus, it is believed that microenvironmental cues were sufficient to activate PRP in the current study without the need for activation by exogenous additives that may have compromised bone formation.

FUTURE DIRECTIONS

The application of PRP to *in vitro* models needs to be further refined for future studies. In the current study, the presence of residual cell types for extended periods of time in culture and coagulation of PRP over scaffold surfaces complicated the analysis of

PRP-treated groups. In the future, methods to further purify and concentrate the platelet population should be considered. For example, differential centrifugation techniques using a Histopaque®/Percoll™ gradient could be used to separate platelets and peripheral blood mononuclear cells (i.e., monocytes, lymphocytes, and macrophages) from erythrocytes or to specifically concentrate the platelet population. Likewise, the concentration of PRP may have significant implications on the cellular response to the therapy. High concentrations (>10%) suppressed, while low concentrations (1 – 5%) stimulated, the viability and proliferation of alveolar bone cells (172). Moreover, researchers have suggested that the concentration of platelets in PRP required for a desired biological effect in human subjects may vary between individuals (172). The "therapeutic" target range for platelet concentration has been set at 5 times baseline levels, approximately 1 million platelets/μL (81). Future studies should determine the concentration of platelets needed to elicit regenerative responses in the models tested and verify adequate concentrations of platelets are achieved prior to application. Platelet concentration can be determined using manual or automated counting procedures. The removal of clotted PRP from scaffold wells may have inadvertently disrupted or removed the layer of hAMSCs. To circumvent this issue, culture plate membrane inserts could be considered as a means of physically separating clotted PRP from the hAMSC layer while still allowing the diffusion of growth factors (e.g., Minicell Cell Culture Inserts, Millipore, Billerica, MA).

The main inorganic portion of bone is hydroxyapatite ($Ca_{10}(PO_4)_6(OH)_2$). *In vitro* mineralization can be assessed using histochemical stains such as von Kossa or Alizarin

Red S. Von Kossa stain reacts with the anionic portion of phosphates, carbonates, and other salts (173) while Alizarin Red chelates with the calcium portion (174). Thus, neither method is specific to the hydroxyapatite molecule. As such, the use of Alizarin Red S in initial mineralization assessments was confounded by the calcium component of CA scaffolds. Specifically, nonspecific binding made it difficult to differentiate between the calcium component of the CA material and that of calcium deposits as a result of mineralization. Moreover, the Von Kossa method is not quantifiable. In future experiments, the assessment of *in vitro* mineralization may benefit from the use of OsteoImage Mineralization Assay kits (Lonza, Walkersville, MD). These kits are designed with a fluorescent probe that specifically binds the hydroxyapatite molecule in mineralized nodules. Mineralization by this method can be assessed qualitatively using fluorescence microscopy or quantitatively by plate reader methods.

Although *in vitro* assays contribute to the comprehension of biological mechanisms, they are limited in their capacity to fully replicate the complex milieu of the *in vivo* microenvironment. In order to achieve the clinical translation of bone tissue engineering strategies, models should mimic the clinical and biological environment and allow the success and functional performance of the regeneration to be assessed by qualitative and quantitative methods (13). In an attempt to further define molecular mechanisms of melatonin and PRP combinations in culture while replicating the host microenvironment, co- and tri-culture experiments should be considered. Experiments could be devised to examine the effect of osteoinductive components on the dynamic relationship between osteoblasts, osteoclasts, and hAMSCs. Additionally, bioreactors

can be utilized to provide biophysical stimulation, improve nutrient transfer, and enhance functional assembly of cells cultured on scaffold materials (175). Interstitial flow through a scaffold material can be replicated with a perfusion bioreactor and has been shown to induce osteoblastic differentiation as well as extracellular matrix and calcium deposition (175, 176). These culture conditions and devices could be valuable tools for further studying the mechanisms of cell-scaffold interactions while approximating a physiological environment.

Platelet-rich plasma is a growth factor-rich substance that promotes mitogenic responses *in vitro* and *in vivo*. The additive or synergistic effect between PRP and melatonin in the current study may be dependent on an appropriate separation of proliferative and differentiative responses. Indeed, the temporal and spatial regulation of growth factor release and activity is a common attribute of biological repair mechanisms (81, 82). Future cell culture models should consider defining an appropriate "window" between PRP application and melatonin exposure to optimize hAMSCs response for the greatest differentiation and most robust calcium deposition. As platelets typically expire within 5 -7 days (81), the development of a slow-release melatonin component to CA scaffolds may sufficiently separate hAMSC exposure to the influences of PRP and melatonin. While the immobilization of melatonin to the CA surface resulted in significant osteoinductive improvements, there is little control over when cells and tissues of the microenvironment are exposed to the molecule. Alternate drug delivery systems could be designed to release agents at a specific rate over a specific period of time at the desired location (130). Because the synthesis of CA scaffolds does not require high heat

treatments to impart mechanical strength, the thermal degradation of the melatonin component may be avoided.

The creation of an optimal grafting material typically centers around three biological prerequisites for fracture healing: (i) suitable osteoconductive surfaces, (ii) osteoinductive stimulation by growth factors, and (iii) viability and availability of osteogenic cells (153). Although not considered in the current study, the influence of osteogenic components on bone regeneration should be considered in future models. For example, hAMSCs could be seeded and cultured on CA scaffolds prior to implantation in defect models. This modification would be of substantial value given the reported effects of modified scaffolds on hAMSCs and bone remodeling reported here and the effects of exogenous melatonin administration on the differentiation of hAMSCs reported elsewhere (67, 68). Porous hydroxyapatite and β-tricalcium phosphate scaffolds seeded with allogenic MSCs demonstrated regenerative capacity comparable to autogenous cancellous bone in large femoral defects in dogs (4). Additionally, the development of tissue engineered temporomandibular joint constructs for craniofacial applications has benefited greatly from the incorporation of MSCs (177). Finally, encouraging results have been reported from clinical trials utilizing MSCs for the treatment of osteogenesis imperfect and metachromatic leukodystrophy (5).

The quality and quantity of bone formation in osseous defects can be influenced by the species of animal used, age of the animal, stability of the defect, anatomic location, type of bone, and the presence or absence of periosteum (114). Given the

challenges associated with regenerating bone in the calvarial model and in light of the beneficial effects of modified scaffolds on bone remodeling reported here, equally or more significant effects may be seen in models where impact forces facilitate bone remodeling activity (e.g., femoral or tibial defects) and should be considered in the future. These models could provide vital information regarding the utility of unmodified and modified CA scaffolds for long bone injuries.

Finally, physical forces have been investigated in fracture healing and include pulsed electromagnetic fields (PEMF) and pulsed ultrasound (low-intensity pulsed ultrasound; LIPUS) (178, 179). Numerous authors have reported that these adjuvant techniques have a positive effect on bone healing, specifically with regard to vertebral and long bone injuries (179). A systematic review of the published clinical data on both techniques revealed that LIPUS speeds acute fracture healing and promotes healing in nonunion fractures (179). Application of physical forces to fresh fractures showed an acceleration of healing by 30% and a 71% reduction in nonunion with 12 weeks after the initiation of therapy (178). It is hypothesized that the strain-generated electrical potentials may be a regulator signal for cellular processes of bone regeneration (178). These methods may further enhance the bone forming potential of bioactive CA therapies.

CONCLUSION

The use of autogenous bone for grafting procedures is still a relevant clinical practice given its naturally inherent bone regenerating capacity and histocompatability. Nonetheless, donor site morbidities are prevalent concerns and the average cost of a routine iliac crest bone graft harvest is estimated at $4200 including anesthesia and hospital stay (180). Significant advances in the field of tissue engineering and regenerative medicine have provoked scientists to evaluate the clinical utility of cheaper, less invasive methods of bone grafting utilizing synthetic materials. Mimicry of native bone physiology and mechanical properties, however, is a substantial challenge to these endeavors.

The objective of this study was to create a bone regenerative substitute that more accurately displays the bone regenerating properties of natural bone (e.g., osteoconduction and osteoinduction). The use of calcium aluminates for bone replacement provides for an unlimited quantity and consistent quality of the graft material while removing the need for autologous donor sites. It is a moldable, durable material that may withstand the forces of weight-bearing or high-impact activity while limiting the potential for implant site infection or material rejection. The unique combination of CA scaffolds with melatonin has created a novel bioactive biomaterial with both osteoconductive and osteoinductive potential. Slow degradation of the calcium aluminate over time would best allow for the infiltration and integration of new bone matrix and mature bone formation. Given the challenges associated with regenerating bone in this model, equally or more significant effects should be seen in models where impact forces facilitate bone remodeling activity. The use of this novel bioactive synthetic scaffold has

the potential to change the dogma of bone grafting in several fields including dentistry and reconstructive surgeries. The clinical use of this technology has the potential to significantly reduce the cost and complications associated with bone graft procedures, reduce the time patients spend in recovery, and reduce or eliminate the need for revisional surgeries. Continued research and optimization of this therapy is warranted and the attachment of other biomolecules that facilitate cell adhesion and combat infection have been considered (50, 105).

REFERENCES

1. Clarke B. Normal bone anatomy and physiology. Clin J Am Soc Nephrol [Internet]. 2008 Nov;3 Suppl 3:S131-9.

2. Teitelbaum SL. Osteoclasts: What do they do and how do they do it? Am J Pathol [Internet]. 2007 Feb;170(2):427-35.

3. Goltzman D. Discoveries, drugs and skeletal disorders. Nat Rev Drug Discov [Internet]. 2002 Oct;1(10):784-96.

4. Kraus KH, Kirker-Head C. Mesenchymal stem cells and bone regeneration. Vet Surg [Internet]. 2006 Apr;35(3):232-42.

5. Vaananen HK. Mesenchymal stem cells. Ann Med [Internet]. 2005;37(7):469-79.

6. Long MW. Osteogenesis and bone-marrow-derived cells. Blood Cells Mol Dis [Internet]. 2001 May-Jun;27(3):677-90.

7. Kearns AE, Khosla S, Kostenuik PJ. Receptor activator of nuclear factor kappaB ligand and osteoprotegerin regulation of bone remodeling in health and disease. Endocr Rev [Internet]. 2008 Apr;29(2):155-92.

8. Kalu DN. Evolution of the pathogenesis of postmenopausal bone loss. Bone [Internet]. 1995 Oct;17(4 Suppl):135S-44S.

9. Nochowitz B, Siegert S, Wasik M. An update on osteoporosis. Am J Ther [Internet]. 2009 Sep-Oct;16(5):437-45.

10. Feskanich D, Hankinson SE, Schernhammer ES. Nightshift work and fracture risk: The nurses' health study. Osteoporos Int [Internet]. 2009 Apr;20(4):537-42.

11. Burge R, Dawson-Hughes B, Solomon DH, Wong JB, King A, Tosteson A. Incidence and economic burden of osteoporosis-related fractures in the united states, 2005-2025. J Bone Miner Res [Internet]. 2007 Mar;22(3):465-75.

12. Szpalski C, Barr J, Wetterau M, Saadeh PB, Warren SM. Cranial bone defects: Current and future strategies. Neurosurg Focus [Internet]. 2010 Dec;29(6):E8.

13. Gomes PS, Fernandes MH. Rodent models in bone-related research: The relevance of calvarial defects in the assessment of bone regeneration strategies. Lab Anim [Internet]. 2011 Jan;45(1):14-24.

14. Witt-Enderby PA, Clafshenkel WP, Kotlarczyk MP, Sethi S. Melatonin in Bone Health.In: Watson RR, editor. Melatonin in the Promotion of Health. 2nd ed. CRC Press; 2011;

15. Ruggiero SL, Mehrotra B, Rosenberg TJ, Engroff SL. Osteonecrosis of the jaws associated with the use of bisphosphonates: A review of 63 cases. J Oral Maxillofac Surg [Internet]. 2004 May;62(5):527-34.

16. Torres J, Tamimi F, Garcia I, Cebrian JL, Lopez-Cabarcos E, Lopez A. Management of atrophic maxilla in severe osteoporosis treated with bisphosphonates: A case report. Oral Surg Oral Med Oral Pathol Oral Radiol Endod [Internet]. 2008 Nov;106(5):668-72.

17. Yarom N, Yahalom R, Shoshani Y, Hamed W, Regev E, Elad S. Osteonecrosis of the jaw induced by orally administered bisphosphonates: Incidence, clinical features, predisposing factors and treatment outcome. Osteoporos Int [Internet]. 2007 Oct;18(10):1363-70.

18. Friedlander AH. The physiology, medical management and oral implications of menopause. J Am Dent Assoc [Internet]. 2002 Jan;133(1):73-81.

19. Kim SY, Schneeweiss S, Katz JN, Levin R, Solomon DH. Oral bisphosphonates and risk of subtrochanteric or diaphyseal femur fractures in a population-based cohort. J Bone Miner Res [Internet]. 2011 May;26(5):993-1001.

20. Stepan JJ, Burr DB, Pavo I, Sipos A, Michalska D, Li J, Fahrleitner-Pammer A, Petto H, Westmore M, Michalsky D, Sato M, Dobnig H. Low bone mineral density is associated with bone microdamage accumulation in postmenopausal women with osteoporosis. Bone [Internet]. 2007 Sep;41(3):378-85.

21. Russell RG, Watts NB, Ebetino FH, Rogers MJ. Mechanisms of action of bisphosphonates: Similarities and differences and their potential influence on clinical efficacy. Osteoporos Int [Internet]. 2008 Jun;19(6):733-59.

22. Gennari L, Merlotti D, Nuti R. Selective estrogen receptor modulator (SERM) for the treatment of osteoporosis in postmenopausal women: Focus on lasofoxifene. Clin Interv Aging [Internet]. 2010 Feb 2;5:19-29.

23. Shifren JL, Schiff I. Role of hormone therapy in the management of menopause. Obstet Gynecol [Internet]. 2010 Apr;115(4):839-55.

24. Manolagas SC. Birth and death of bone cells: Basic regulatory mechanisms and implications for the pathogenesis and treatment of osteoporosis. Endocr Rev [Internet]. 2000 Apr;21(2):115-37.

25. Bilezikian JP. Combination anabolic and antiresorptive therapy for osteoporosis: Opening the anabolic window. Curr Osteoporos Rep [Internet]. 2008 Mar;6(1):24-30.

26. McKay WF, Peckham SM, Badura JM. A comprehensive clinical review of recombinant human bone morphogenetic protein-2 (INFUSE bone graft). Int Orthop [Internet]. 2007 Dec;31(6):729-34.

27. Kotoulas HK, Sakellariou VI, Sofianos IP. Bone morphogenetic proteins. background and clinical practice in reconstructive surgery of hip and knee. EEXOT. 2005;60(2):119-126.

28. Giannoudis PV, Dinopoulos H, Tsiridis E. Bone substitutes: An update. Injury [Internet]. 2005 Nov;36 Suppl 3:S20-7.

29. Bauer TW, Muschler GF. Bone graft materials. an overview of the basic science. Clin Orthop Relat Res [Internet]. 2000 Feb;(371)(371):10-27.

30. Albrektsson T, Johansson C. Osteoinduction, osteoconduction and osseointegration. Eur Spine J [Internet]. 2001 Oct;10 Suppl 2:S96-101.

31. Damron TA. Use of 3D beta-tricalcium phosphate (vitoss) scaffolds in repairing bone defects. Nanomedicine (Lond) [Internet]. 2007 Dec;2(6):763-75.

32. Watson JT. Overview of biologics. J Orthop Trauma [Internet]. 2005 Nov-Dec;19(10 Suppl):S14-6.

33. Bucholz RW, Carlton A, Holmes RE. Hydroxyapatite and tricalcium phosphate bone graft substitutes. Orthop Clin North Am [Internet]. 1987 Apr;18(2):323-34.

34. Navarro M, Michiardi A, Castano O, Planell JA. Biomaterials in orthopaedics. J R Soc Interface [Internet]. 2008 Oct 6;5(27):1137-58.

35. LeGeros RZ. Calcium phosphate-based osteoinductive materials. Chem Rev [Internet]. 2008 Nov;108(11):4742-53.

36. Soballe K, Hansen ES, Brockstedt-Rasmussen H, Bunger C. Hydroxyapatite coating converts fibrous tissue to bone around loaded implants. J Bone Joint Surg Br [Internet]. 1993 Mar;75(2):270-8.

37. Blokhuis TJ, Termaat MF, den Boer FC, Patka P, Bakker FC, Haarman HJ. Properties of calcium phosphate ceramics in relation to their in vivo behavior. J Trauma [Internet]. 2000 Jan;48(1):179-86.

38. Hallab NJ, Cunningham BW, Jacobs JJ. Spinal implant debris-induced osteolysis. Spine (Phila Pa 1976) [Internet]. 2003 Oct 15;28(20):S125-38.

39. Ingham E, Fisher J. The role of macrophages in osteolysis of total joint replacement. Biomaterials [Internet]. 2005 Apr;26(11):1271-86.

40. Ingham E, Fisher J. Biological reactions to wear debris in total joint replacement. Proc Inst Mech Eng H [Internet]. 2000;214(1):21-37.

41. De Long WG,Jr, Einhorn TA, Koval K, McKee M, Smith W, Sanders R, Watson T. Bone grafts and bone graft substitutes in orthopaedic trauma surgery. A critical analysis. J Bone Joint Surg Am [Internet]. 2007 Mar;89(3):649-58.

42. Kim SJ, Shin HS, Shin SW. Effect of bone block graft with rhBMP-2 on vertical bone augmentation. Int J Oral Maxillofac Surg [Internet]. 2010 Sep;39(9):883-8.

43. Burastero G, Scarfi S, Ferraris C, Fresia C, Sessarego N, Fruscione F, Monetti F, Scarfo F, Schupbach P, Podesta M, Grappiolo G, Zocchi E. The association of human mesenchymal stem cells with BMP-7 improves bone regeneration of critical-size segmental bone defects in athymic rats. Bone [Internet]. 2010 Jul;47(1):117-26.

44. Khojasteh A, Eslaminejad MB, Nazarian H. Mesenchymal stem cells enhance bone regeneration in rat calvarial critical size defects more than platelete-rich plasma. Oral Surg Oral Med Oral Pathol Oral Radiol Endod [Internet]. 2008 Sep;106(3):356,62; discussion 363.

45. Wernike E, Montjovent MO, Liu Y, Wismeijer D, Hunziker EB, Siebenrock KA, Hofstetter W, Klenke FM. VEGF incorporated into calcium phosphate ceramics promotes vascularisation and bone formation in vivo. Eur Cell Mater [Internet]. 2010 Feb 22;19:30-40.

46. Kang SW, Lee JS, Park MS, Park JH, Kim BS. Enhancement of in vivo bone regeneration efficacy of human mesenchymal stem cells. J Microbiol Biotechnol [Internet]. 2008 May;18(5):975-82.

47. Kikuiri T, Kim I, Yamaza T, Akiyama K, Zhang Q, Li Y, Chen C, Chen W, Wang S, Le AD, Shi S. Cell-based immunotherapy with mesenchymal stem cells cures bisphosphonate-related osteonecrosis of the jaw-like disease in mice. J Bone Miner Res [Internet]. 2010 Jul;25(7):1668-79.

48. Autian J, Hamner JE,3rd. A toxicity profile for calcium aluminate. J Dent Res [Internet]. 1972 May-Jun;51(3):880.

49. Uchida A, Nade SM, McCartney ER, Ching W. The use of ceramics for bone replacement. A comparative study of three different porous ceramics. J Bone Joint Surg Br [Internet]. 1984 Mar;66(2):269-75.

50. Miljkovic ND, Cooper GM, Hott SL, Disalle BF, Gawalt ES, Smith DM, McGowan K, Marra KG. Calcium aluminate, RGD-modified calcium aluminate, and beta-tricalcium phosphate implants in a calvarial defect. J Craniofac Surg [Internet]. 2009 Sep;20(5):1538-43.

51. Uchida A, Nade S, McCartney E, Ching W. Bone ingrowth into three different porous ceramics implanted into the tibia of rats and rabbits. J Orthop Res [Internet]. 1985;3(1):65-77.

52. Cutando A, Gomez-Moreno G, Arana C, Acuna-Castroviejo D, Reiter RJ. Melatonin: Potential functions in the oral cavity. J Periodontol [Internet]. 2007 Jun;78(6):1094-102.

53. Dubocovich ML, Delagrange P, Krause DN, Sugden D, Cardinali DP, Olcese J. International union of basic and clinical pharmacology. LXXV. nomenclature, classification, and pharmacology of G protein-coupled melatonin receptors. Pharmacol Rev [Internet]. 2010 Sep;62(3):343-80.

54. Witt-Enderby PA, Radio NM, Doctor JS, Davis VL. Therapeutic treatments potentially mediated by melatonin receptors: Potential clinical uses in the prevention of osteoporosis, cancer and as an adjuvant therapy. J Pineal Res [Internet]. 2006 Nov;41(4):297-305.

55. Sandyk R, Anastasiadis PG, Anninos PA, Tsagas N. Is postmenopausal osteoporosis related to pineal gland functions? Int J Neurosci [Internet]. 1992 Feb;62(3-4):215-25.

56. Girardo M, Bettini N, Dema E, Cervellati S. The role of melatonin in the pathogenesis of adolescent idiopathic scoliosis (AIS). Eur Spine J [Internet]. 2011 May;20 Suppl 1:S68-74.

57. Sanchez-Barcelo EJ, Mediavilla MD, Tan DX, Reiter RJ. Scientific basis for the potential use of melatonin in bone diseases: Osteoporosis and adolescent idiopathic scoliosis. J Osteoporos [Internet]. 2010 Jun 1;2010:830231.

58. Reiter RJ, Tan DX, Manchester LC, Pilar Terron M, Flores LJ, Koppisepi S. Medical implications of melatonin: Receptor-mediated and receptor-independent actions. Adv Med Sci [Internet]. 2007;52:11-28.

59. Ostrowska Z, Kos-Kudla B, Marek B, Kajdaniuk D. Influence of lighting conditions on daily rhythm of bone metabolism in rats and possible involvement of melatonin and other hormones in this process. Endocr Regul [Internet]. 2003 Sep;37(3):163-74.

60. Ostrowska Z, Kos-Kudla B, Nowak M, Swietochowska E, Marek B, Gorski J, Kajdaniuk D, Wolkowska K. The relationship between bone metabolism, melatonin and other hormones in sham-operated and pinealectomized rats. Endocr Regul [Internet]. 2003 Dec;37(4):211-24.

61. Fjelldal PG, Grotmol S, Kryvi H, Gjerdet NR, Taranger GL, Hansen T, Porter MJ, Totland GK. Pinealectomy induces malformation of the spine and reduces the mechanical strength of the vertebrae in atlantic salmon, salmo salar. J Pineal Res [Internet]. 2004 Mar;36(2):132-9.

62. Oyama J, Murai I, Kanazawa K, Machida M. Bipedal ambulation induces experimental scoliosis in C57BL/6J mice with reduced plasma and pineal melatonin levels. J Pineal Res [Internet]. 2006 Apr;40(3):219-24.

63. Qiu XS, Tang NL, Yeung HY, Cheng JC, Qiu Y. Lack of association between the promoter polymorphism of the MTNR1A gene and adolescent idiopathic scoliosis. Spine (Phila Pa 1976) [Internet]. 2008 Sep 15;33(20):2204-7.

64. Moreau A, Wang DS, Forget S, Azeddine B, Angeloni D, Fraschini F, Labelle H, Poitras B, Rivard CH, Grimard G. Melatonin signaling dysfunction in adolescent idiopathic scoliosis. Spine (Phila Pa 1976) [Internet]. 2004 Aug 15;29(16):1772-81.

65. Azeddine B, Letellier K, Wang da S, Moldovan F, Moreau A. Molecular determinants of melatonin signaling dysfunction in adolescent idiopathic scoliosis. Clin Orthop Relat Res [Internet]. 2007 Sep;462:45-52.

66. Man GC, Wong JH, Wang WW, Sun GQ, Yeung BH, Ng TB, Lee SK, Ng BK, Qiu Y, Cheng JC. Abnormal melatonin receptor 1B expression in osteoblasts from girls with adolescent idiopathic scoliosis. J Pineal Res [Internet]. 2011 May;50(4):395-402.

67. Radio NM, Doctor JS, Witt-Enderby PA. Melatonin enhances alkaline phosphatase activity in differentiating human adult mesenchymal stem cells grown in osteogenic medium via MT2 melatonin receptors and the MEK/ERK (1/2) signaling cascade. J Pineal Res [Internet]. 2006 May;40(4):332-42.

68. Sethi S, Radio NM, Kotlarczyk MP, Chen CT, Wei YH, Jockers R, Witt-Enderby PA. Determination of the minimal melatonin exposure required to induce osteoblast differentiation from human mesenchymal stem cells and these effects on downstream signaling pathways. J Pineal Res [Internet]. 2010 Oct;49(3):222-38.

69. Witt-Enderby PA. Melatonin osteoporosis prevention study (MOPS). Duquesne University. Identifier# NCT01152580. [Internet].

70. Inoh H, Kawakami N, Matsuyama Y, Aoki T, Kanemura T, Natsume N, Iwata H. Correlation between the age of pinealectomy and the development of scoliosis in chickens. Spine (Phila Pa 1976) [Internet]. 2001 May 1;26(9):1014-21.

71. Turgut M, Kaplan S, Turgut AT, Aslan H, Guvenc T, Cullu E, Erdogan S. Morphological, stereological and radiological changes in pinealectomized chicken cervical vertebrae. J Pineal Res [Internet]. 2005 Nov;39(4):392-9.

72. Roth JA, Kim BG, Lin WL, Cho MI. Melatonin promotes osteoblast differentiation and bone formation. J Biol Chem [Internet]. 1999 Jul 30;274(31):22041-7.

73. Suzuki N, Hattori A. Melatonin suppresses osteoclastic and osteoblastic activities in the scales of goldfish. J Pineal Res [Internet]. 2002 Nov;33(4):253-8.

74. Cutando A, Gomez-Moreno G, Arana C, Munoz F, Lopez-Pena M, Stephenson J, Reiter RJ. Melatonin stimulates osteointegration of dental implants. J Pineal Res [Internet]. 2008 Sep;45(2):174-9.

75. Nakade O, Koyama H, Ariji H, Yajima A, Kaku T. Melatonin stimulates proliferation and type I collagen synthesis in human bone cells in vitro. J Pineal Res [Internet]. 1999 Sep;27(2):106-10.

76. Conti A, Conconi S, Hertens E, Skwarlo-Sonta K, Markowska M, Maestroni JM. Evidence for melatonin synthesis in mouse and human bone marrow cells. J Pineal Res [Internet]. 2000 May;28(4):193-202.

77. Guardia J, Gomez-Moreno G, Ferrera MJ, Cutando A. Evaluation of effects of topic melatonin on implant surface at 5 and 8 weeks in beagle dogs. Clin Implant Dent Relat Res [Internet]. 2009 Aug 3

78. Calvo-Guirado JL, Gomez-Moreno G, Barone A, Cutando A, Alcaraz-Banos M, Chiva F, Lopez-Mari L, Guardia J. Melatonin plus porcine bone on discrete calcium deposit implant surface stimulates osteointegration in dental implants. J Pineal Res [Internet]. 2009 Sep;47(2):164-72.

79. Calvo-Guirado JL, Gomez-Moreno G, Lopez-Mari L, Guardia J, Marinez-Gonzalez JM, Barone A, Tresguerres IF, Paredes SD, Fuentes-Breto L. Actions of melatonin mixed with collagenized porcine bone versus porcine bone only on osteointegration of dental implants. J Pineal Res [Internet]. 2010 Apr;48(3):194-203.

80. Calvo-Guirado JL, Ramirez-Fernandez MP, Gomez-Moreno G, Mate-Sanchez JE, Delgado-Ruiz R, Guardia J, Lopez-Mari L, Barone A, Ortiz-Ruiz AJ, Martinez-Gonzalez JM, Bravo LA. Melatonin stimulates the growth of new bone around implants in the tibia of rabbits. J Pineal Res [Internet]. 2010 Nov;49(4):356-63.

81. Marx RE, Carlson ER, Eichstaedt RM, Schimmele SR, Strauss JE, Georgeff KR. Platelet-rich plasma: Growth factor enhancement for bone grafts. Oral Surg Oral Med Oral Pathol Oral Radiol Endod [Internet]. 1998 Jun;85(6):638-46.

82. Eppley BL, Pietrzak WS, Blanton M. Platelet-rich plasma: A review of biology and applications in plastic surgery. Plast Reconstr Surg [Internet]. 2006 Nov;118(6):147e-59e.

83. Mehta S, Watson JT. Platelet rich concentrate: Basic science and current clinical applications. J Orthop Trauma [Internet]. 2008 Jul;22(6):432-8.

84. Dori F, Huszar T, Nikolidakis D, Arweiler NB, Gera I, Sculean A. Effect of platelet-rich plasma on the healing of intra-bony defects treated with a natural bone mineral and a collagen membrane. J Clin Periodontol [Internet]. 2007 Mar;34(3):254-61.

85. Rutkowski JL, Thomas JM, Bering CL, Speicher JL, Radio NM, Smith DM, Johnson DA. Analysis of a rapid, simple, and inexpensive technique used to obtain platelet-rich plasma for use in clinical practice. J Oral Implantol [Internet]. 2008;34(1):25-33.

86. Marx RE. Platelet-rich plasma: Evidence to support its use. J Oral Maxillofac Surg [Internet]. 2004 Apr;62(4):489-96.

87. Eppley BL, Woodell JE, Higgins J. Platelet quantification and growth factor analysis from platelet-rich plasma: Implications for wound healing. Plast Reconstr Surg [Internet]. 2004 Nov;114(6):1502-8.

88. Anitua E. The use of plasma-rich growth factors (PRGF) in oral surgery. Pract Proced Aesthet Dent [Internet]. 2001 Aug;13(6):487,93; quiz 487-93.

89. Rozman P, Bolta Z. Use of platelet growth factors in treating wounds and soft-tissue injuries. Acta Dermatovenerol Alp Panonica Adriat [Internet]. 2007 Dec;16(4):156-65.

90. Valbonesi M, Giannini G, Migliori F, Dalla Costa R, Galli A. The role of autologous fibrin-platelet glue in plastic surgery: A preliminary report. Int J Artif Organs [Internet]. 2002 Apr;25(4):334-8.

91. Margolis DJ, Kantor J, Santanna J, Strom BL, Berlin JA. Effectiveness of platelet releasate for the treatment of diabetic neuropathic foot ulcers. Diabetes Care [Internet]. 2001 Mar;24(3):483-8.

92. Simman R, Hoffmann A, Bohinc RJ, Peterson WC, Russ AJ. Role of platelet-rich plasma in acceleration of bone fracture healing. Ann Plast Surg [Internet]. 2008 Sep;61(3):337-44.

93. Rutkowski JL, Johnson DA, Radio NM, Fennell JW. Platelet rich plasma to facilitate wound healing following tooth extraction. J Oral Implantol [Internet]. 2010;36(1):11-23.

94. Torres J, Tresguerres I, Tamimi F, Clemente C, Niembro E, Blanco L. Influence of platelet-rich plasma on bone regeneration: A histomorphometric study in rabbit calvaria. Int J Oral Maxillofac Implants [Internet]. 2007 Jul-Aug;22(4):563-8.

95. Thor A, Franke-Stenport V, Johansson CB, Rasmusson L. Early bone formation in human bone grafts treated with platelet-rich plasma: Preliminary histomorphometric results. Int J Oral Maxillofac Surg [Internet]. 2007 Dec;36(12):1164-71.

96. Wiltfang J, Kloss FR, Kessler P, Nkenke E, Schultze-Mosgau S, Zimmermann R, Schlegel KA. Effects of platelet-rich plasma on bone healing in combination with autogenous bone and bone substitutes in critical-size defects. an animal experiment. Clin Oral Implants Res [Internet]. 2004 Apr;15(2):187-93.

97. Fontana S, Olmedo DG, Linares JA, Guglielmotti MB, Crosa ME. Effect of platelet-rich plasma on the peri-implant bone response: An experimental study. Implant Dent [Internet]. 2004 Mar;13(1):73-8.

98. Rai B, Ho KH, Lei Y, Si-Hoe KM, Jeremy Teo CM, Yacob KB, Chen F, Ng FC, Teoh SH. Polycaprolactone-20% tricalcium phosphate scaffolds in combination with platelet-rich plasma for the treatment of critical-sized defects of the mandible: A pilot study. J Oral Maxillofac Surg [Internet]. 2007 Nov;65(11):2195-205.

99. Pieri F, Lucarelli E, Corinaldesi G, Fini M, Aldini NN, Giardino R, Donati D, Marchetti C. Effect of mesenchymal stem cells and platelet-rich plasma on the healing of standardized bone defects in the alveolar ridge: A comparative histomorphometric study in minipigs. J Oral Maxillofac Surg [Internet]. 2009 Feb;67(2):265-72.

100. Zou Z, Zhang Y, Hao L, Wang F, Liu D, Su Y, Sun H. More insight into mesenchymal stem cells and their effects inside the body. Expert Opin Biol Ther [Internet]. 2010 Feb;10(2):215-30.

101. Zhou S, Greenberger JS, Epperly MW, Goff JP, Adler C, Leboff MS, Glowacki J. Age-related intrinsic changes in human bone-marrow-derived mesenchymal stem cells and their differentiation to osteoblasts. Aging Cell [Internet]. 2008 Jun;7(3):335-43.

102. Dalle Carbonare L, Valenti MT, Zanatta M, Donatelli L, Lo Cascio V. Circulating mesenchymal stem cells with abnormal osteogenic differentiation in patients with osteoporosis. Arthritis Rheum [Internet]. 2009 Nov;60(11):3356-65.

103. Bruder SP, Jaiswal N, Haynesworth SE. Growth kinetics, self-renewal, and the osteogenic potential of purified human mesenchymal stem cells during extensive subcultivation and following cryopreservation. J Cell Biochem [Internet]. 1997 Feb;64(2):278-94.

104. Franz A, Konradsson K, Konig F, Van Dijken JW, Schedle A. Cytotoxicity of a calcium aluminate cement in comparison with other dental cements and resin-based materials. Acta Odontol Scand [Internet]. 2006 Feb;64(1):1-8.

105. Palchesko RN. Optimization of calcium aluminate for use as a bone scaffold material through physical and chemical surface modification. (Dissertation)]. Bayer School of Natural and Environmental Sciences, Duquesne University; 2011

106. Lonza W, Inc. Poietics® hMSC human mesenchymal stem cells & media technical sheet. 2010

107. Jaiswal N, Haynesworth SE, Caplan AI, Bruder SP. Osteogenic differentiation of purified, culture-expanded human mesenchymal stem cells in vitro. J Cell Biochem [Internet]. 1997 Feb;64(2):295-312.

108. Eijken M, Koedam M, van Driel M, Buurman CJ, Pols HA, van Leeuwen JP. The essential role of glucocorticoids for proper human osteoblast differentiation and matrix mineralization. Mol Cell Endocrinol [Internet]. 2006 Mar 27;248(1-2):87-93.

109. Jorgensen NR, Henriksen Z, Sorensen OH, Civitelli R. Dexamethasone, BMP-2, and 1,25-dihydroxyvitamin D enhance a more differentiated osteoblast phenotype: Validation of an in vitro model for human bone marrow-derived primary osteoblasts. Steroids [Internet]. 2004 Apr;69(4):219-26.

110. Passey S, Pellegrin S, Mellor H. Scanning electron microscopy of cell surface morphology. Curr Protoc Cell Biol [Internet]. 2007 Dec;Chapter 4:Unit4.17.

111. Kalu DN. The ovariectomized rat model of postmenopausal bone loss. Bone Miner [Internet]. 1991 Dec;15(3):175-91.

112. Riggs BL, Khosla S, Melton LJ,3rd. Sex steroids and the construction and conservation of the adult skeleton. Endocr Rev [Internet]. 2002 Jun;23(3):279-302.

113. Cuevas P, de Paz V, Cuevas B, Marin-Martinez J, Picon-Molina M, Fernandez-Pereira A, Gimenez-Gallego G. Osteopromotion for cranioplasty: An experimental study in rats using acidic fibroblast growth factor. Surg Neurol [Internet]. 1997 Mar;47(3):242-6.

114. Bosch C, Melsen B, Vargervik K. Importance of the critical-size bone defect in testing bone-regenerating materials. J Craniofac Surg [Internet]. 1998 Jul;9(4):310-6.

115. Harder S, Wolfart S, Mehl C, Kern M. Performance of ultrasonic devices for bone surgery and associated intraosseous temperature development. Int J Oral Maxillofac Implants [Internet]. 2009 May-Jun;24(3):484-90.

116. Roukis TS, Zgonis T, Tiernan B. Autologous platelet-rich plasma for wound and osseous healing: A review of the literature and commercially available products. Adv Ther [Internet]. 2006 Mar-Apr;23(2):218-37.

117. Rutkowski JL, Fennell JW, Kern JC, Madison DE, Johnson DA. Inhibition of alveolar osteitis in mandibular tooth extraction sites using platelet-rich plasma. J Oral Implantol [Internet]. 2007;33(3):116-21.

118. Rutkowski JL. Mechanistic and clinical studies of platelet rich plasma: a simple clinical method for enhancing bone and soft tissue healing. (Dissertation).]. Graduate School of Pharmaceutical Sciences, Duquesne University; 2008

119. FROST HM, VILLANUEVA AR, ROTH H, STANISAVLJEVIC S. Tetracycline bone labeling. J New Drugs [Internet]. 1961 Sep-Oct;1:206-16.

120. di Sant'Agnese PA, De Mesy Jensen KL. Dibasic staining of large epoxy tissue sections and applications to surgical pathology. Am J Clin Pathol [Internet]. 1984 Jan;81(1):25-9.

121. Huber JD, Parker F, Odland GF. A basic fuchsin and alkalinized methylene blue rapid stain for epoxy-embedded tissue. Stain Technol [Internet]. 1968 Mar;43(2):83-7.

122. Oh S, Brammer KS, Li YS, Teng D, Engler AJ, Chien S, Jin S. Stem cell fate dictated solely by altered nanotube dimension. Proc Natl Acad Sci U S A [Internet]. 2009 Feb 17;106(7):2130-5.

123. Dimitriou R, Jones E, McGonagle D, Giannoudis PV. Bone regeneration: Current concepts and future directions. BMC Med [Internet]. 2011 May 31;9(1):66.

124. Black J, Hastings G, editors. Handbook of biomaterial properties. New York: Chapman & Hall; 1998 (.

125. Gawalt ES, Avaltroni MJ, Koch N, Schwartz J. Self-assembly and bonding of alkanephosphonic acids on the native oxide surface of titanium. Langmuir. 2001;17:5736.

126. Schwartz J, Avaltroni MJ, Danahy MP, Silverman BM, Hanson EL, Schwarzbauer JE, Midwood KS, Gawalt ES. Cell attachment and spreading on metal implant materials. Mat Sci Eng C. 2003;23:395.

127. Borsari V, Giavaresi G, Fini M, Torricelli P, Salito A, Chiesa R, Chiusoli L, Volpert A, Rimondini L, Giardino R. Physical characterization of different-roughness titanium surfaces, with and without hydroxyapatite coating, and their effect on human osteoblast-like cells. J Biomed Mater Res B Appl Biomater [Internet]. 2005 Nov;75(2):359-68.

128. Yang GL, He FM, Song E, Hu JA, Wang XX, Zhao SF. In vivo comparison of bone formation on titanium implant surfaces coated with biomimetically deposited calcium phosphate or electrochemically deposited hydroxyapatite. Int J Oral Maxillofac Implants [Internet]. 2010 Jul-Aug;25(4):669-80.

129. Hulbert SF, Young FA, Mathews RS, Klawitter JJ, Talbert CD, Stelling FH. Potential of ceramic materials as permanently implantable skeletal prostheses. J Biomed Mater Res [Internet]. 1970 Sep;4(3):433-56.

130. Mourino V, Boccaccini AR. Bone tissue engineering therapeutics: Controlled drug delivery in three-dimensional scaffolds. J R Soc Interface [Internet]. 2010 Feb 6;7(43):209-27.

131. Goel MK. Immobilized enzymes. [Internet]. Tory, NY: Department of Chemical and Biological Engineering, Rensselaer Polytechnic Institute

132. Miller ED, Li K, Kanade T, Weiss LE, Walker LM, Campbell PG. Spatially directed guidance of stem cell population migration by immobilized patterns of growth factors. Biomaterials [Internet]. 2011 Apr;32(11):2775-85.

133. Masters KS. Covalent growth factor immobilization strategies for tissue repair and regeneration. Macromol Biosci [Internet]. 2011 Apr 20

134. McGowan K, Gawalt ES, inventorsFunctionalized artificial bone and joint compositions and methods of use and manufacture. (United States Patent Application Publication).

135. Shamis Y, Hewitt KJ, Carlson MW, Margvelashvilli M, Dong S, Kuo CK, Daheron L, Egles C, Garlick JA. Fibroblasts derived from human embryonic stem cells direct development and repair of 3D human skin equivalents. Stem Cell Res Ther [Internet]. 2011 Feb 21;2(1):10.

136. Cao C, Li S, Dai X, Chen Y, Feng Z, Zhao Y, Wu J. Genistein inhibits proliferation and functions of hypertrophic scar fibroblasts. Burns [Internet]. 2009 Feb;35(1):89-97.

137. Zhang JC, Xie YF, Liu SJ, Dai LB, Li JP. The expression of melatonin receptor in human hypertrophic scar. Zhonghua Zheng Xing Wai Ke Za Zhi [Internet]. 2010 May;26(3):203-7.

138. Jones MP, Melan MA, Witt-Enderby PA. Melatonin decreases cell proliferation and transformation in a melatonin receptor-dependent manner. Cancer Lett [Internet]. 2000 Apr 14;151(2):133-43.

139. Diegelmann RF, Evans MC. Wound healing: An overview of acute, fibrotic and delayed healing. Front Biosci [Internet]. 2004 Jan 1;9:283-9.

140. Luttrell LM, Roudabush FL, Choy EW, Miller WE, Field ME, Pierce KL, Lefkowitz RJ. Activation and targeting of extracellular signal-regulated kinases by beta-arrestin scaffolds. Proc Natl Acad Sci U S A [Internet]. 2001 Feb 27;98(5):2449-54.

141. Castro-Raucci LM, Oliveira IR, Teixeira LN, Rosa AL, Oliveira PT, Jacobovitz M. Effects of a novel calcium aluminate cement on the early events of the progressionof osteogenic cell cultures. Braz Dent J [Internet]. 2011;22(2):99-104.

142. Graves GA, Noyes FR, Villanueva AR. The influence of compositional variations on bone ingrowth of implanted porous calcium aluminate ceramics. J Biomed Mater Res [Internet]. 1975 Jul;9(4):17-22.

143. Shastri VP. In vivo engineering of tissues: Biological considerations, challenges, strategies, and future directions. Adv Mater [Internet]. 2009 Sep 4;21(32-33):3246-54.

144. Lipski AM, Pino CJ, Haselton FR, Chen IW, Shastri VP. The effect of silica nanoparticle-modified surfaces on cell morphology, cytoskeletal organization and function. Biomaterials [Internet]. 2008 Oct;29(28):3836-46.

145. Miyagi Y, Chiu LL, Cimini M, Weisel RD, Radisic M, Li RK. Biodegradable collagen patch with covalently immobilized VEGF for myocardial repair. Biomaterials [Internet]. 2011 Feb;32(5):1280-90.

146. Pena C, Rincon J, Pedreanez A, Viera N, Mosquera J. Chemotactic effect of melatonin on leukocytes. J Pineal Res [Internet]. 2007 Oct;43(3):263-9.

147. Gawalt ES. Controlling interactions on surfaces. Presented at Duquesne University: Sept 2009

148. Gupta VB, Anitha S, Hegde ML, Zecca L, Garruto RM, Ravid R, Shankar SK, Stein R, Shanmugavelu P, Jagannatha Rao KS. Aluminium in alzheimer's disease: Are we still at a crossroad? Cell Mol Life Sci [Internet]. 2005 Jan;62(2):143-58.

149. Ribes D, Colomina MT, Vicens P, Domingo JL. Impaired spatial learning and unaltered neurogenesis in a transgenic model of alzheimer's disease after oral aluminum exposure. Curr Alzheimer Res [Internet]. 2010 Aug;7(5):401-8.

150. Garcia T, Ribes D, Colomina MT, Cabre M, Domingo JL, Gomez M. Evaluation of the protective role of melatonin on the behavioral effects of aluminum in a mouse model of alzheimer's disease. Toxicology [Internet]. 2009 Nov 9;265(1-2):49-55.

151. Colomina MT, Roig JL, Sanchez DJ, Domingo JL. Influence of age on aluminum-induced neurobehavioral effects and morphological changes in rat brain. Neurotoxicology [Internet]. 2002 Dec;23(6):775-81.

152. Valdes TI, Kreutzer D, Moussy F. The chick chorioallantoic membrane as a novel in vivo model for the testing of biomaterials. J Biomed Mater Res [Internet]. 2002 Nov;62(2):273-82.

153. Giannoudis PV, Einhorn TA, Marsh D. Fracture healing: The diamond concept. Injury [Internet]. 2007 Sep;38 Suppl 4:S3-6.

154. Karageorgiou V, Kaplan D. Porosity of 3D biomaterial scaffolds and osteogenesis. Biomaterials [Internet]. 2005 Sep;26(27):5474-91.

155. Bose S, Darsell J, Hosick HL, Yang L, Sarkar DK, Bandyopadhyay A. Processing and characterization of porous alumina scaffolds. J Mater Sci Mater Med [Internet]. 2002 Jan;13(1):23-8.

156. Volkov AV, Alekseeva IS, Kulakov AA, Gol'dshtein DV, Shustrov SA, Shuraev AI, Arutyunyan IV, Bukharova TB, Rzhaninova AA, Bol'shakova GB, Grigor'yan AS.

Regeneration of skull bones in adult rabbits after implantation of commercial osteoinductive materials and transplantation of a tissue-engineering construct. Bull Exp Biol Med [Internet]. 2010 Oct;149(4):505-10.

157. Tan DX, Manchester LC, Reiter RJ, Qi WB, Zhang M, Weintraub ST, Cabrera J, Sainz RM, Mayo JC. Identification of highly elevated levels of melatonin in bone marrow: Its origin and significance. Biochim Biophys Acta [Internet]. 1999 Oct 18;1472(1-2):206-14.

158. Duan J, Kuang W, Tan J, Li H, Zhang Y, Hirotaka K, Tadashi K. Differential effects of platelet rich plasma and washed platelets on the proliferation of mouse MSC cells. Mol Biol Rep [Internet]. 2011 Apr;38(4):2485-90.

159. Ogino Y, Ayukawa Y, Tsukiyama Y, Koyano K. The effect of platelet-rich plasma on the cellular response of rat bone marrow cells in vitro. Oral Surg Oral Med Oral Pathol Oral Radiol Endod [Internet]. 2005 Sep;100(3):302-7.

160. van den Dolder J, Mooren R, Vloon AP, Stoelinga PJ, Jansen JA. Platelet-rich plasma: Quantification of growth factor levels and the effect on growth and differentiation of rat bone marrow cells. Tissue Eng [Internet]. 2006 Nov;12(11):3067-73.

161. Okada M, Yano K, Namikawa T, Uemura T, Hoshino M, Kazuki K, Takaoka K, Nakamura H. Bone morphogenetic protein-2 retained in synthetic polymer/beta-tricalcium phosphate composite promotes hypertrophy of a vascularized long bone graft in rabbits. Plast Reconstr Surg [Internet]. 2011 Jan;127(1):98-106.

162. Silva GA, Coutinho OP, Ducheyne P, Reis RL. Materials in particulate form for tissue engineering. 2. applications in bone. J Tissue Eng Regen Med [Internet]. 2007 Mar-Apr;1(2):97-109.

163. Kon E, Filardo G, Delcogliano M, Fini M, Salamanna F, Giavaresi G, Martin I, Marcacci M. Platelet autologous growth factors decrease the osteochondral regeneration capability of a collagen-hydroxyapatite scaffold in a sheep model. BMC Musculoskelet Disord [Internet]. 2010 Sep 27;11:220.

164. Weibrich G, Kleis WK, Hafner G, Hitzler WE. Growth factor levels in platelet-rich plasma and correlations with donor age, sex, and platelet count. J Craniomaxillofac Surg [Internet]. 2002 Apr;30(2):97-102.

165. Aghaloo TL, Moy PK, Freymiller EG. Investigation of platelet-rich plasma in rabbit cranial defects: A pilot study. J Oral Maxillofac Surg [Internet]. 2002 Oct;60(10):1176-81.

166. Niemeyer P, Fechner K, Milz S, Richter W, Suedkamp NP, Mehlhorn AT, Pearce S, Kasten P. Comparison of mesenchymal stem cells from bone marrow and adipose tissue

for bone regeneration in a critical size defect of the sheep tibia and the influence of platelet-rich plasma. Biomaterials [Internet]. 2010 May;31(13):3572-9.

167. Goedecke A, Wobus M, Krech M, Munch N, Richter K, Holig K, Bornhauser M. Differential effect of platelet-rich plasma and fetal calf serum on bone marrow-derived human mesenchymal stromal cells expanded in vitro. J Tissue Eng Regen Med [Internet]. 2011 Jan 14

168. Takechi M, Tatehara S, Satomura K, Fujisawa K, Nagayama M. Effect of FGF-2 and melatonin on implant bone healing: A histomorphometric study. J Mater Sci Mater Med [Internet]. 2008 Aug;19(8):2949-52.

169. Zimmermann R, Arnold D, Strasser E, Ringwald J, Schlegel A, Wiltfang J, Eckstein R. Sample preparation technique and white cell content influence the detectable levels of growth factors in platelet concentrates. Vox Sang [Internet]. 2003 Nov;85(4):283-9.

170. Grageda E, Lozada JL, Boyne PJ, Caplanis N, McMillan PJ. Bone formation in the maxillary sinus by using platelet-rich plasma: An experimental study in sheep. J Oral Implantol [Internet]. 2005;31(1):2-17.

171. Lawson JH. The clinical use and immunologic impact of thrombin in surgery. Semin Thromb Hemost [Internet]. 2006 Apr;32 Suppl 1:98-110.

172. Alsousou J, Thompson M, Hulley P, Noble A, Willett K. The biology of platelet-rich plasma and its application in trauma and orthopaedic surgery: A review of the literature. J Bone Joint Surg Br [Internet]. 2009 Aug;91(8):987-96.

173. Bonewald LF, Harris SE, Rosser J, Dallas MR, Dallas SL, Camacho NP, Boyan B, Boskey A. Von kossa staining alone is not sufficient to confirm that mineralization in vitro represents bone formation. Calcif Tissue Int [Internet]. 2003 May;72(5):537-47.

174. Wang YH, Liu Y, Maye P, Rowe DW. Examination of mineralized nodule formation in living osteoblastic cultures using fluorescent dyes. Biotechnol Prog [Internet]. 2006 Nov-Dec;22(6):1697-701.

175. Grayson WL, Bhumiratana S, Grace Chao PH, Hung CT, Vunjak-Novakovic G. Spatial regulation of human mesenchymal stem cell differentiation in engineered osteochondral constructs: Effects of pre-differentiation, soluble factors and medium perfusion. Osteoarthritis Cartilage [Internet]. 2010 May;18(5):714-23.

176. Meinel L, Karageorgiou V, Fajardo R, Snyder B, Shinde-Patil V, Zichner L, Kaplan D, Langer R, Vunjak-Novakovic G. Bone tissue engineering using human mesenchymal stem cells: Effects of scaffold material and medium flow. Ann Biomed Eng [Internet]. 2004 Jan;32(1):112-22.

177. Mao JJ, Giannobile WV, Helms JA, Hollister SJ, Krebsbach PH, Longaker MT, Shi S. Craniofacial tissue engineering by stem cells. J Dent Res [Internet]. 2006 Nov;85(11):966-79.

178. Hannemann P, Gottgens KW, van Wely BJ, Kolkman KA, Werre AJ, Poeze M, Brink PR. Pulsed electromagnetic fields in the treatment of fresh scaphoid fractures. A multicenter, prospective, double blind, placebo controlled, randomized trial. BMC Musculoskelet Disord [Internet]. 2011 May 6;12:90.

179. Walker NA, Denegar CR, Preische J. Low-intensity pulsed ultrasound and pulsed electromagnetic field in the treatment of tibial fractures: A systematic review. J Athl Train [Internet]. 2007 Oct-Dec;42(4):530-5.

180. St John TA, Vaccaro AR, Sah AP, Schaefer M, Berta SC, Albert T, Hilibrand A. Physical and monetary costs associated with autogenous bone graft harvesting. Am J Orthop (Belle Mead NJ) [Internet]. 2003 Jan;32(1):18-23.

APPENDIX

Unmodified Calcium Aluminate – Day 7; n =3

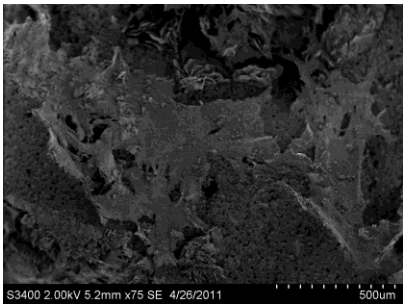

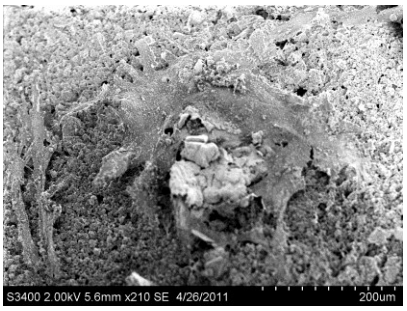

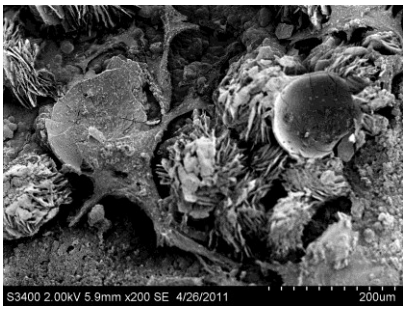

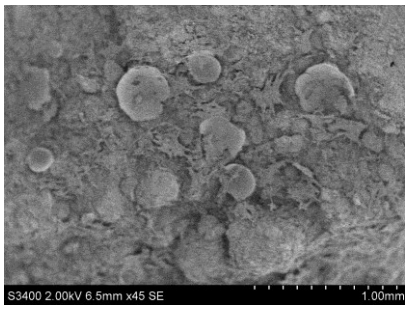

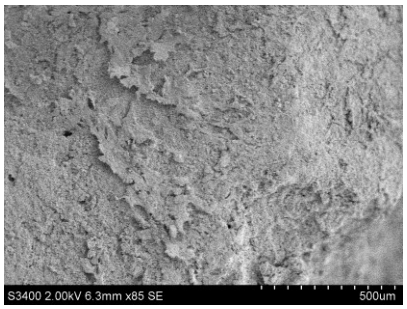

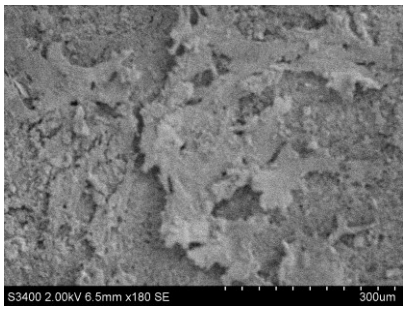

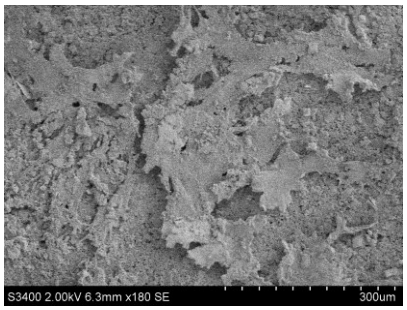

Unmodified Calcium Aluminate – Day 14; n =3

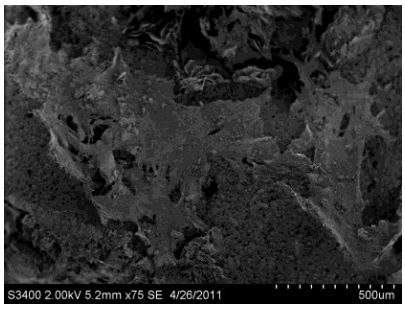

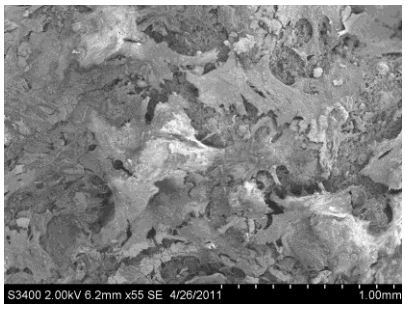

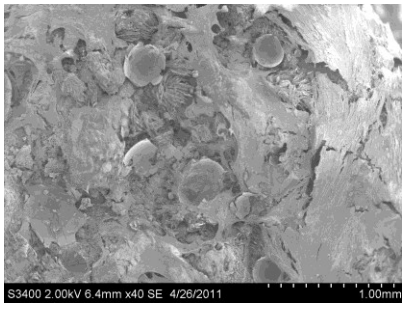

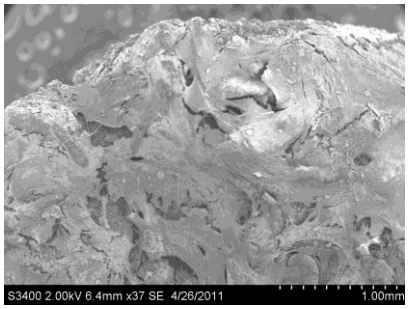

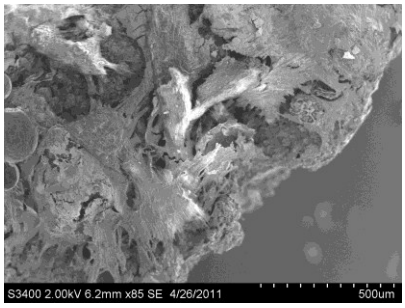

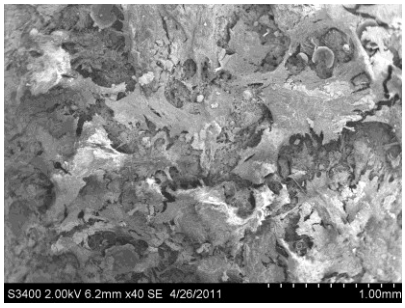

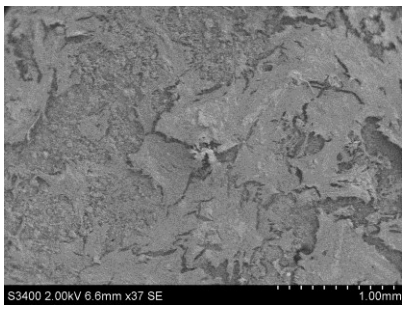

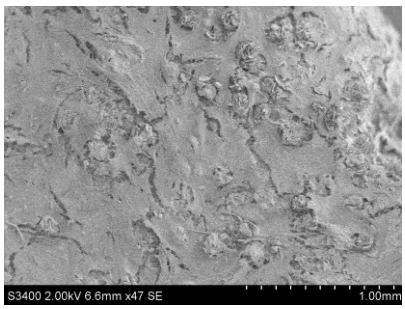

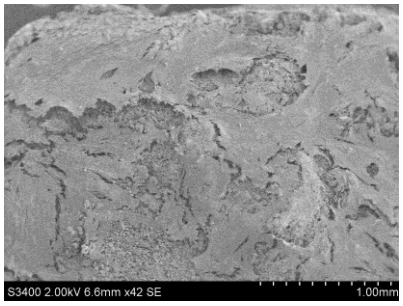

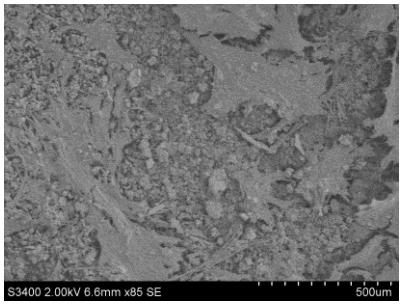

Modified Calcium Aluminate (CA-Mel) – Day 7; n =3

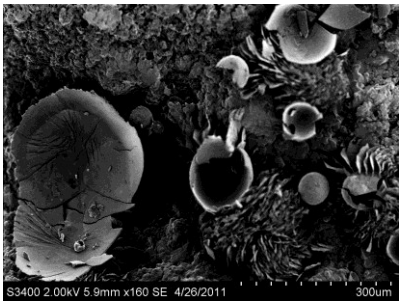

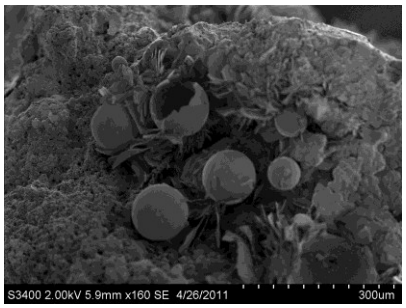

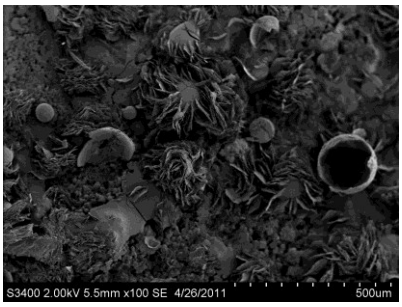

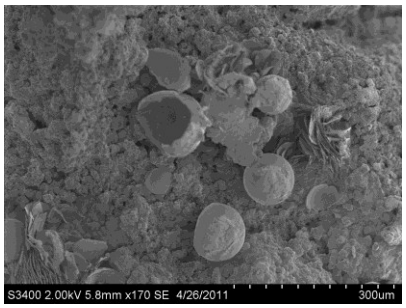

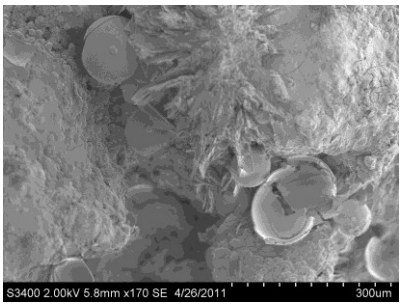

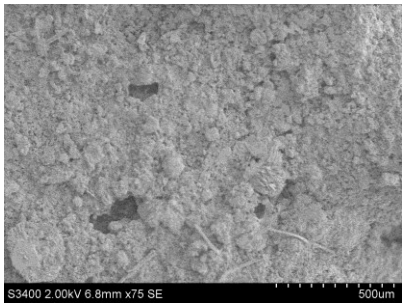

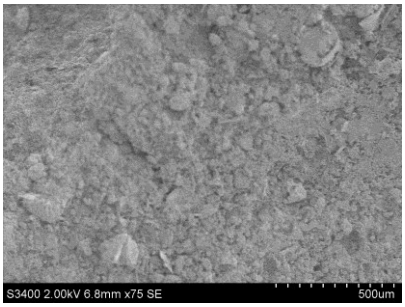

Modified Calcium Aluminate (CA-Mel) – Day 14; n =3